Dynamics and Sensitivity Analysis of a Class of High Speed Aircraft

by

Patrick V. HAGELAUER

Ingénieur de L' Ecole Nationale Supérieure D' Ingénieurs

de Constructions Aéronautiques

(1990)

Submitted to the Department of Aeronautics and Astronautics in

Partial Fulfillment of the Requirements for the Degree of

MASTER OF SCIENCE

in Aeronautics and Astronautics

at the

Massachusetts Institute of Technology

September 1993

Signature of Author _____

Department of Aeronautics and Astronautics

August 6, 1993

Approved by _____

Professor Rudrapatna V. Ramnath

Thesis supervisor, Department of Aeronautics and Astronautics

Accepted by _____

Professor Harold Y. Wachman

Chairman, Department of Graduate Committee

Dynamics and Sensitivity Analysis of a Class of High Speed Aircraft

by

Patrick V. HAGELAUER

Submitted to the Department of Aeronautics and Astronautics on August 5, 1993,

in partial fulfillment of the requirements for the Master of Science in

Aeronautics and Astronautics

Abstract

This thesis presents applications of a particular perturbation method, known as the Generalized Multiple Scales (GMS) theory, to the study of high speed aircraft dynamics.

The GMS theory is first used to approximate the solutions of the fourth order longitudinal and lateral dynamics of a generic hypersonic vehicle flown along a Space Shuttle reentry trajectory. Sensitivity of the vehicle dynamics to first and second order stability derivative variations is assessed through an analytical approach made possible by the simple form of the asymptotic approximations derived through the GMS method. Using state augmentation, optimal control methods are then applied to reduce sensitivity of the vehicle's longitudinal dynamics to first order variations of a particular stability derivative during the reentry.

The dynamics of the SR-71 and the stability of the aircraft along a prescribed trajectory are also investigated. A stability parameter derived through GMS theory is used to predict the stability of the aircraft when it flies from supersonic to subsonic speeds along the trajectory.

Finally, GMS asymptotic approximations are used to define extended handling quality criteria for vehicles with very large flight envelopes. Unlike typical handling quality specifications, these are defined in terms of variable system response and are believed to give a better evaluation of the vehicle's true performance level.

Thesis Supervisor: Rudrapatna V. Ramnath

Title: Adjunct Professor of Aeronautics and Astronautics

Acknowledgments

I would like to express my deep appreciation to Professor Rudrapatna Ramnath for his guidance throughout the course of this study. His original ideas in the field of aircraft dynamics and control made this work particularly interesting. I also very much enjoyed our discussions about tennis and his scientific approach to the sport.

I am also very grateful to Professor R.J. Hansman and the ASL lab who gave me the opportunity to discover MIT and live this exciting two and a half year experience in the United States.

A big thank you to Professor Vander Velde and Valavani for being so helpful in my thesis and course work and to Liz Zoto for her kindness.

Finally, I would like to acknowledge Vimanic Systems for partial support of this work.

Contents

List of Figures

List of Tables

CHAPTER 1

Introduction

1.1 HIGH SPEED VEHICLES

Over the last few years, there has been an increasing interest in the field of hypersonic vehicles. These are defined as the class of flight vehicles to fly at speeds in excess of Mach 6. After the technological efforts of the eighties to achieve a Space Shuttle, the present interest has shifted to reusable hypersonic vehicles that would takeoff horizontally from conventional runways and accelerate to orbital velocity as air-breathing aircraft to reach low-Earth-orbit (LEO). After completing their mission, these vehicles would reenter the Earth's atmosphere and fly to a horizontal landing. There are currently several military and commercial hypersonic vehicles being developed world wide among which the National Aerospace Plane (NASP) designed by NASA.

One particular issue regarding very high speed aircraft, such as supersonic or hypersonic vehicles, is the need for a good understanding of their dynamics along atmospheric trajectories. Continuous variations in speed and density (due to altitude changes for example) renders the dynamics of these aircraft highly time varying. Unlike the dynamics of conventional aircraft which can be efficiently described using linear time invariant (LTI) models, the dynamics of very high speed aircraft can only be accurately described using linear

time varying (LTV) models. However, with the exception of first order systems, there are no known exact solutions to LTV differential

equations. The current approach in dealing with LTV systems is to " freeze " the coefficients over various intervals of time and treat the systems as time invariant over each interval. This method usually yields very inaccurate descriptions of the real system and it appears that substantial improvement would result from treating the system as truly time varying.

1.2 THE GENERALIZED MULTIPLE SCALES THEORY

In order to get an accurate description of high speed aircraft dynamics, time varying systems need to be solved in some manner. One approach is to use perturbation methods to obtain asymptotic approximate solutions. Among these, the Generalized Multiple Scales (GMS) theory developed by Ramnath [6] has proved to be very successful in providing asymptotic approximations to solutions of slowly varying systems. In particular, the longitudinal dynamics of the Space Shuttle [7] as well as the dynamics of a VTOL during transition from hover to cruise [8] were predicted by Ramnath using the GMS theory.

Unlike most approximation methods, which produce solutions in terms of non elementary functions such as Bessel or Mathieu functions, the GMS theory generates approximate solutions in terms of simple mathematical functions. This allows numerous applications along with the study high speed vehicle dynamics. Stability and control issues of vehicles flying through variable flight conditions can be assessed. Sensitivity of vehicle dynamics to parameter variations can be studied. Extended aircraft handling quality criteria for high speed aircraft can be defined through the insight gained by GMS asymptotic approximations.

1.3 THESIS STRUCTURE

Chapter 2 presents the geometric characteristics of the Generic Hypersonic Aerodynamic Model Example (GHAME) vehicle and the optimal shuttle reentry trajectory along which the dynamics of the vehicle are studied.

Fundamental results of the Generalized Multiple Scales (GMS) theory are presented in chapter 3. In particular, the analytical approximations to fourth order linear time varying differential equations obtained using GMS theory are given and compared to exact solutions. Finally, the extension of GMS theory to sensitivity analysis is described.

Chapter 4 and 5 are complete first and second order sensitivity analyses of the lateral and longitudinal dynamics of the GHAME vehicle. The equations of motion are presented and approximate solutions are derived using GMS theory. Sensitivity of the dynamics to first and second order variations in the stability derivatives are assessed through the evaluation of two "sensitivity criteria". These criteria, together, give a good description of the relative sensitivity of the dynamics to stability derivative variations along the reentry trajectory.

An approach to incorporating sensitivity considerations in the design of control systems is described in chapter 6. By augmenting the system, it is shown that classical optimal control techniques can be used to both control the system and reduce its sensitivity to parameter variations. Ultimately, this approach is applied to the longitudinal dynamics of the GHAME vehicle with the objective of reducing their sensitivity to first order variations in one particular stability derivative during a portion of the reentry.

Chapter 7 is a study of the dynamics of the SR-71 along a prescribed trajectory. The GMS theory is used to analyze the stability of the vehicle when it flies from supersonic to subsonic speeds.

Chapter 8 investigates the problem of predicting accurate handling qualities for vehicles with very large flight envelopes such as the GHAME vehicle or the SR-71. By using results from the GMS theory, new aircraft handling quality criteria are defined in terms of variable system response. The criteria are then applied to a generic aircraft flying through variable flight conditions. Finally, the possible display of handling quality information in the cockpit is briefly studied.

The summary of the findings as well as suggestions for future development of the various concepts introduced in this thesis are presented in chapter 9.

CHAPTER 2

GHAME Vehicle and Reentry Trajectory

2.1 GHAME VEHICLE

The recent interest in the development of hypersonic vehicles has led to a need for accurate aerodynamic data in hypersonic flight regime. Much of the existing data is not available to general users. A Generic Hypersonic Aerodynamic Model Example (GHAME) was developed at Dryden Flight Research Facility [1] to provide a simulation model for research and development analysis in the fields of design of control and guidance systems as well as trajectory optimization.

The GHAME data was developed for a flight regime typical of a single stage-to-orbit mission (SSTO) such as the ones that would be encountered by the National Aerospace Plane (NASP). Such missions typically consist of taking off horizontally from a conventional runway and accelerating to orbital velocity as an air-breathing aircraft to reach a low-Earth-orbit (LEO). After completing its mission, the vehicle would reenter the Earth's atmosphere and glide to a horizontal landing.

The model is based upon a combination of flight test data from the Space Shuttle and the X-24C and theoretical data from a swept double delta configuration using modified Newtonian Impact Flow method. The geometric properties of the GHAME vehicle were estimated using simple geometric shapes. The geometry of the simplified vehicle is shown in figure 2.1.

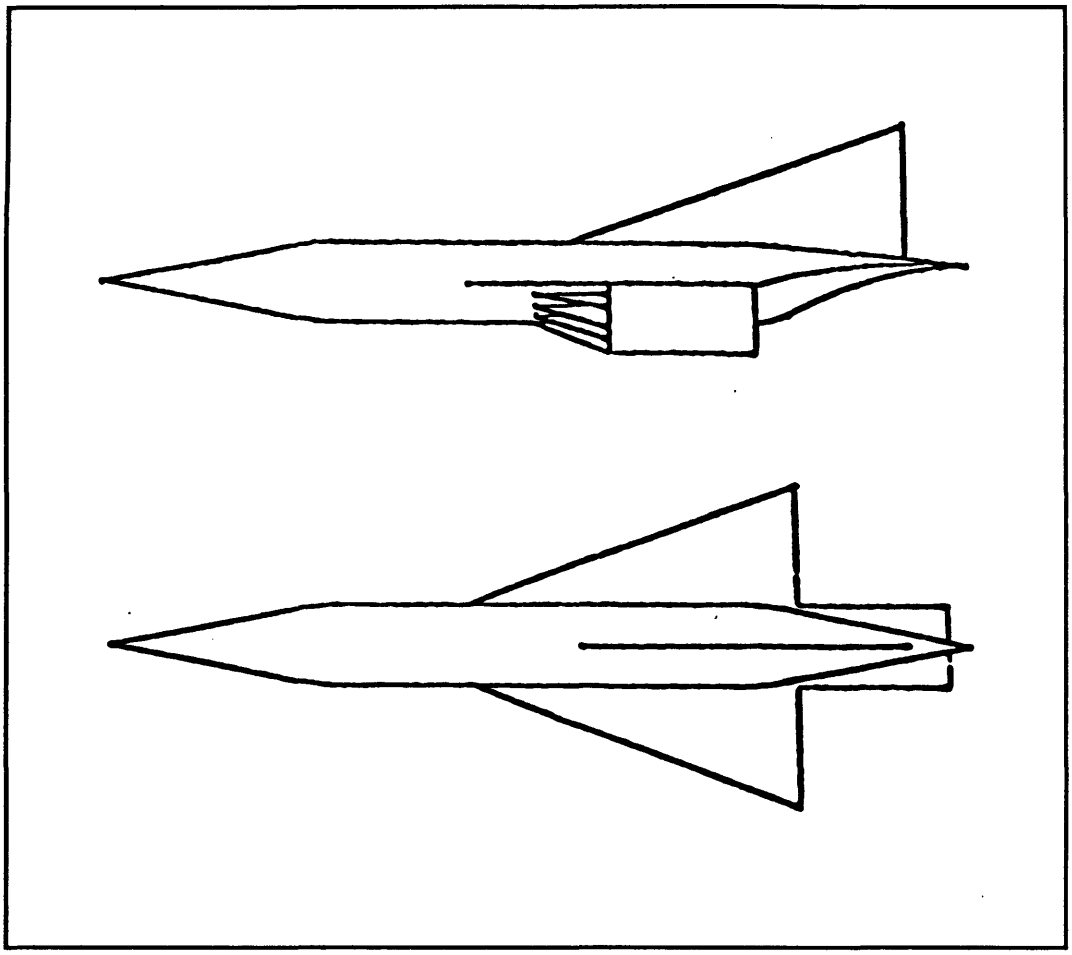

Figure 2.1: GHAME Vehicle

The fuselage was modeled as a cylinder 20 feet in diameter and 120 feet long allowing internal volume requirements for storage of the liquid hydrogen fuel to be met. A pair of 10 degree half cones were attached to this cylinder to complete the fuselage assembly. Both the wings and vertical tail were modeled as thin triangular plates. The engine module is attached around the lower surface of the fuselage.

The geometric properties of the vehicle are summarized in table 2.1:

Length, l	233.4 ft.
Ref. Area, S	6000 $ft.^2$
Ref. Chord, c	75 ft.
Ref. Span, b	80 ft.
Mass, m	120,000 lbs.
I_{xx}	0.87 10^6 slugs $ft.^2$
I_{yy}	14.2 10^6 slugs $ft.^2$
I_{zz}	14.9 10^6 slugs $ft.^2$
I_{xz}	0.28 10^6 slugs $ft.^2$

Table 2.1: Geometric Properties of the GHAME Vehicle

2.2 REENTRY TRAJECTORY

In this study, the dynamics of the GHAME vehicle are studied as it reenters the Earth's atmosphere along a prescribed trajectory. The simulated trajectory is based on the actual trajectory of the Space Shuttle Orbiter 049 which was designed to minimize the thermal-protection-system-weight of the vehicle. The entry starts at the fringe of the atmosphere (~120 km) at approximately Mach 27 and is assumed to end at about 30 km and Mach 3 after which the vehicle initiates a short deceleration to subsonic speeds before beginning approach procedures.

This optimal Shuttle trajectory was studied by Ramnath [7] and is shown on figure 2.2 where angle of attack, velocity altitude and flight path angle are plotted as functions of the non-dimensional variable ξ. This non-dimensional variable defined by Ramnath [7] is the

number of vehicle lengths traversed along the trajectory. The total time of the reentry is approximately 1900 seconds.

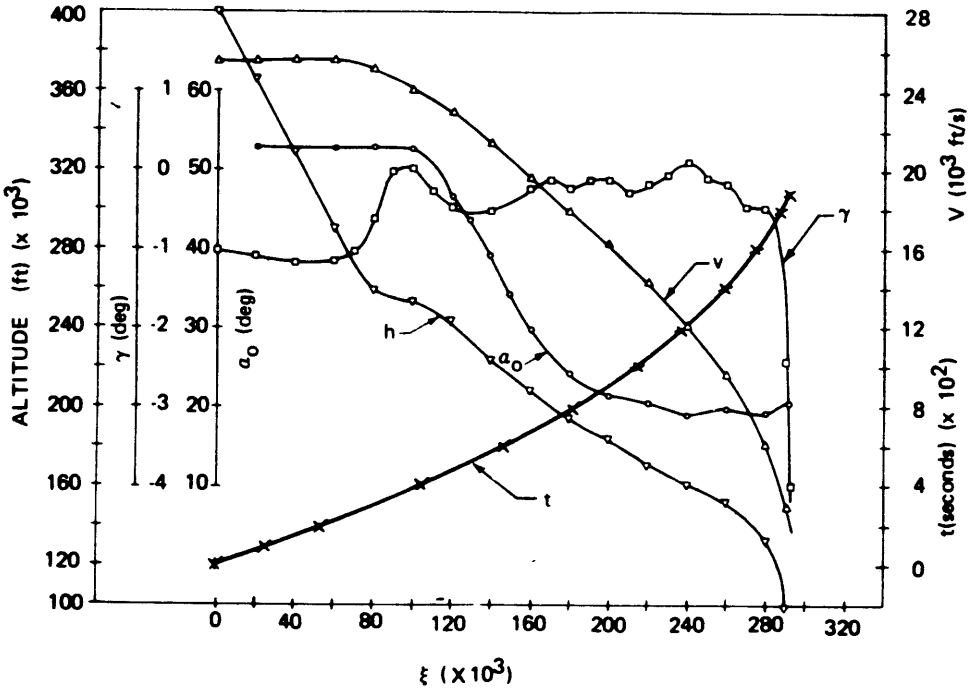

Figure 2.2: Reentry Trajectory

CHAPTER 3

Generalized Multiple Scales Theory

3.1 GENERAL THEORY

The Generalized Multiple Scales (GMS) method formulated by Ramnath [6] is a technique for approximating the solutions for a class of ordinary differential equations with variable coefficients involving a small parameter ε.

While first order linear equations can be solved explicitly in terms of simple analytical functions, higher order equations cannot be handled in the same way. For very particular types of higher order equations, solutions can be expressed in terms of complex mathematical functions such as Bessel or Mathieu functions. However, even these are only available in tabulated tables. The GMS method provides asymptotic approximate solutions to high order linear and nonlinear differential equations with time varying coefficients in closed analytical form in terms of simple mathematical functions such as exponential, sine and cosine functions.

In essence, the GMS method involves extension of the independent variable, t, to a set of independent scales, $\tau_0, \tau_1, \ldots$ replacing the ordinary differential equation by a set of partial differential equations. In this way, the transient response of a dynamical system can be separated into different components, each varying on a different time scale. For a more detailed

description of the Generalized Multiple Scales method and applications, the reader can refer to the work done by Ramnath [6] [7] [8].

3.2 FOURTH ORDER GMS SOLUTION

Following Ramnath [6], a two time scale GMS approximation to the solutions of a fourth order differential equation with time varying coefficients is presented in this section.

The general form of a fourth order differential equation with time varying coefficients can be written as:

$$\frac{d^4y}{dt^4} + \omega_3(t)\frac{d^3y}{dt^3} + \omega_2(t)\frac{d^2y}{dt^2} + \omega_1(t)\frac{dy}{dt} + \omega_0(t) = 0 \qquad (3.1)$$

As shown by Ramnath [7], the GMS solution to this equation is obtained by approximating the motion associated with each of the modes of motion. With the use of two time scales (fast and slow), the GMS method provides an approximation to the amplitude and phase of each of the independent solutions of (3.1).

The modes of motion of (3.1) are characterized by the nature of the roots of the characteristic equation. The characteristic equation of (3.1) has four roots which define four independent modes. Depending on the nature of the modes, the GMS approximation will have different forms.

If a particular mode, m, is represented by a single real root, k(t), then the GMS approximation to the characteristic motion is given by:

$$y_m(t) = \exp\left(\int_{t_0}^{t} k(t)\, dt\right) \tag{3.2}$$

If a mode is represented by a pair of complex conjugate roots, $k(t) = k_r(t) \pm ik_i(t)$, the transient response of the dynamical system associated with the mode can be split into separate components each varying on one of the two time scales. The GMS approximation is then given by:

$$y_m(t) = y_s(t)\, y_f(t) \tag{3.3}$$

where $y_s(t)$ and $y_f(t)$ are referred to as the slow and the fast part of the GMS solution respectively.

The slow part of the solution is then defined as:

$$y_s(t) = \exp\left(\int_{t_0}^{t} \frac{|\dot{k}_r(t)|}{2ik_i(t)}\, dt\right) \tag{3.4}$$

and the fast part of the solution is given by:

$$y_f(t) = \exp\left(\int_{t_0}^{t} k_r(t)\, dt\right)\left[C_1 \sin\left(\int_{t_0}^{t} k_i(t)\, dt\right) + C_2 \cos\left(\int_{t_0}^{t} k_i(t)\, dt\right)\right] \tag{3.5}$$

where C_1 and C_2 are two arbitrary constants, associated with the mode, that are both determined by initial conditions.

The full GMS solution to the fourth order differential equation (3.1) is then obtained by a linear combination of the approximations of the motions of each mode. For example, in a case where the characteristic equation of (3.1) has 2 real roots and one complex conjugate pair, defining three modes, the full solution would be written:

$$y(t) = C_1 y_{m_1}(t) + C_2 y_{m_2}(t) + C_3 y_{m_3}(t) + C_4 y_{m_4}(t) \qquad (3.6)$$

where $y_{m_1}(t)$, $y_{m_2}(t)$, $y_{m_3}(t)$ and $y_{m_4}(t)$ are determined as shown previously, depending on the nature of the associated root (in (3.6), $y_{m_1}(t)$ and $y_{m_2}(t)$ represent the sine and cosine parts of the GMS approximation to the mode associated with the pair of complex conjugate roots).

The previous analysis contains no mention of the small parameter ε. In fact it has been subtly introduced via the slowly varying assertion which allows the dynamics to be split into fast and slow components and then removed from the final result on restriction of the time domain.

In order to simplify the math associated with deriving full GMS solutions, a possible additional approximation consists of considering only the fast part of the solutions. The fast part of the solutions contains all of the frequency and phase information. The slow part acts as a modulation of the amplitude and will be neglected throughout this study.

Figure 3.1 illustrates the accuracy of the full GMS solution when compared to a numerical solution obtained using a fourth order Runge-Kutta integration in the case of a second order differential equation.

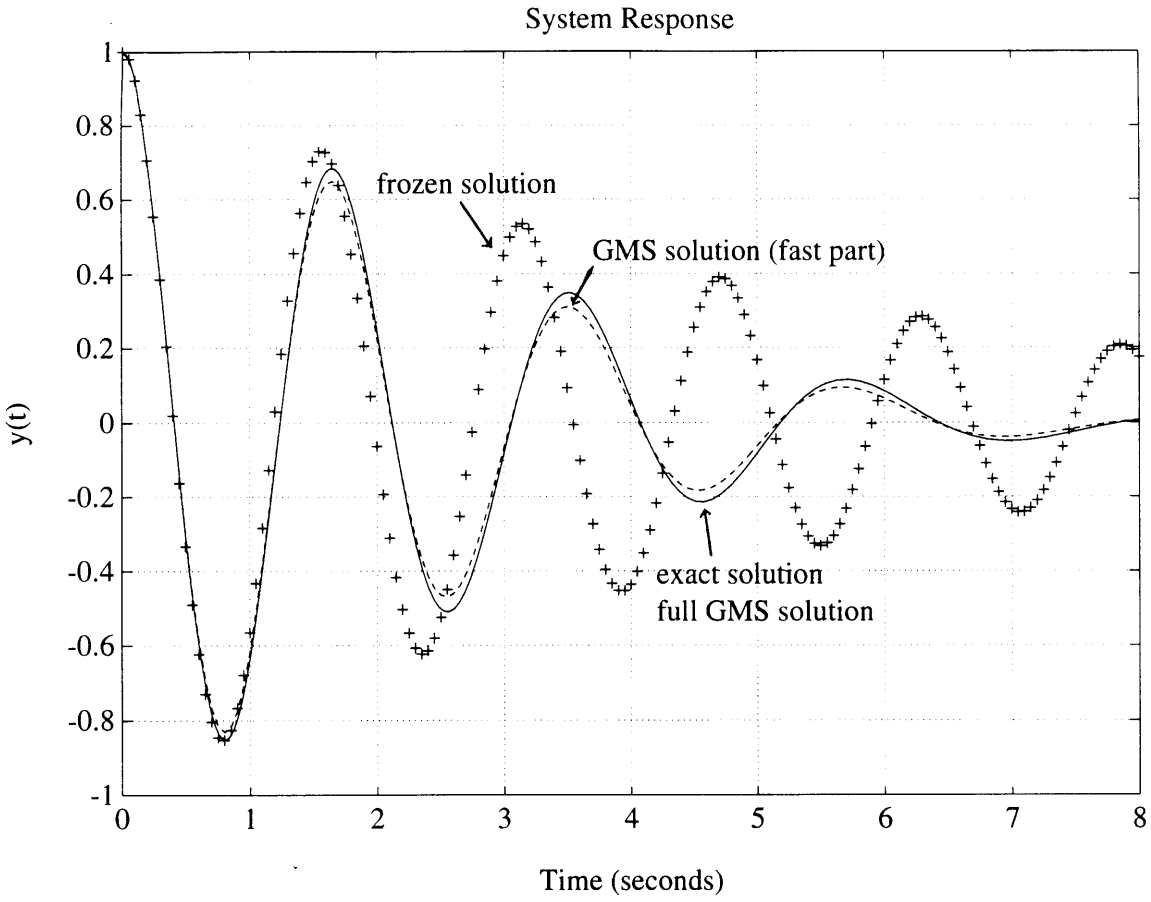

Figure 3.1: GMS vs. Exact Solution

The fast part of the GMS solution is also plotted. The plot shows how the slow part of the solution corrects the amplitude of the fast part which contains all of the frequency and phase information. The widely used "frozen" approximation is also plotted. The results show how the frozen approximation becomes completely invalid after about half a period and the large improvements in accuracy obtained when using a GMS approach.

One big advantage of the GMS method is that it actually provides a complete analytical solution to the fourth order differential equation. Although very tedious, the roots of a fourth order equation can be written in analytical form as follows:

Let

$$p = -\omega_2 \tag{3.7}$$

$$q = \omega_3\omega_1 - 4\omega_0 \tag{3.8}$$

$$r = 4\omega_2\omega_0 - \omega_3^2\omega_0 - \omega_1^2 \tag{3.9}$$

$$a = \frac{1}{3}(3q - p^2) \tag{3.10}$$

$$b = \frac{1}{27}(2p^3 - 9pq + 27r) \tag{3.11}$$

$$A = \left[-\frac{b}{2} + \left(\frac{b^2}{4} + \frac{a^3}{27}\right)^{1/2} \right]^{1/3} \tag{3.12}$$

$$B = -\left[\frac{b}{2} + \left(\frac{b^2}{4} + \frac{a^3}{27}\right)^{1/2} \right]^{1/3} \tag{3.13}$$

$$Y = A + B - \frac{p}{3} \tag{3.14}$$

$$R = \left(\frac{\omega_3^2}{4} - \omega_2 + Y\right)^{1/2} \tag{3.15}$$

$$D = \left(\frac{3}{4}\omega_3^2 - R^2 - 2\omega_2 + \frac{4\omega_3\omega_2 - 8\omega_1 - \omega_3^2}{4R}\right)^{1/2} \tag{3.16}$$

$$E = \left(\frac{3}{4}\omega_3^2 - R^2 - 2\omega_2 - \frac{4\omega_3\omega_2 - 8\omega_1 - \omega_3^2}{4R}\right)^{1/2} \tag{3.17}$$

The roots of the characteristic equation can then be expressed in terms of these new variables. If the characteristic equation has two complex conjugate roots, for example, they would then be given by the expressions:

$$k_1 = k_{1r} \pm i\, k_{1i} \tag{3.18}$$

$$k_2 = k_{2r} \pm i\, k_{2i} \tag{3.19}$$

where

$$k_{1r} = -\frac{\omega_3}{4} - \frac{R}{2} \tag{3.20}$$

$$k_{1i} = \frac{E}{2} \tag{3.21}$$

$$k_{2r} = -\frac{\omega_3}{4} + \frac{R}{2} \tag{3.22}$$

$$k_{2i} = \frac{D}{2} \tag{3.23}$$

Although the full analytical form of the GMS solution is complex, it does provide much more insight into the dynamics of the system than a numerical approach which would typically be adopted for this kind of a problem. The type of information contained in an analytical expression can be very useful, for example, for analyzing the relative influences of different parameters on the dynamics of the system. It would also provide valuable guidelines in designing an adequate control the system.

3.3 GMS SENSITIVITY THEORY

In the study of flight vehicle dynamics, it is often useful to study how certain physical parameters of the aircraft can affect its motion. This problem can be studied in a relatively simple way for conventional aircraft where flight conditions are usually considered to be constant. In that case the equations of motion are time invarying and can be solved explicitly. The sensitivity of the dynamics to variations in certain physical parameters is then simply established by performing partial differentiations with respect to the parameters of interest.

This problem becomes much more complex in the case of a hypersonic vehicle for which flight conditions vary extensively along the reentry trajectory. The equations of motion are time varying and, in addition to the difficulties mentioned earlier in finding exact solutions to these equations, variational principles must be used to establish sensitivity of the dynamics to variations in physical parameters that also vary along the trajectory.

However, Ramnath has shown [8] that, under certain conditions, partial differentiation of solutions of linear time varying systems obtained using the GMS method is a suitable approximation to variational methods. Under those conditions, mainly slowly varying coefficients, vehicle sensitivity to variations of physical parameters can be approximated by treating those parameters as constant.

Consider the general form of a linear time varying system:

$$\dot{Y}(t) = A(t)Y(t) + B(t)U(t) \tag{3.24}$$

As described in the previous sections, if the system is slowly varying, asymptotic solutions $\tilde{Y}(t)$ to equation (3.24) can be derived using the GMS theory. Using the conventional notation, the notion of asymptotic approximations to exact solutions is expressed as:

$$\tilde{Y}(t) \sim Y(t) \qquad \varepsilon \longrightarrow 0 \tag{3.25}$$

where Y(t) is the exact solution of (3.24).

As defined by Ramnath [8], first order sensitivity of $\tilde{Y}(t)$ to changes in a certain parameter, p, is defined by:

$$\tilde{S}_p(t) \triangleq \frac{\partial \tilde{Y}(t)}{\partial p} \tag{3.26}$$

Then under certain conditions, mainly a slowly varying system:

$$\widetilde{S_p}(t) \sim S_p(t) \qquad \varepsilon \longrightarrow 0 \tag{3.27}$$

where $S_p(t)$ is the exact sensitivity derived using variational methods. This means that $\tilde{S}_p(t)$ is in fact an asymptotic approximation of the real sensitivity of the system which is a very powerful and non-trivial result.

In the same way, second order sensitivity to changes in p is obtained by second order partial differentiation of the solutions produced by the GMS method:

$$\tilde{\xi}_p(t) \triangleq \frac{\partial^2 \tilde{Y}(t)}{\partial p^2} \tag{3.28}$$

Therefore, the result proven by Ramnath [8] shows that, under certain circumstances, vehicle sensitivity to variations in physical parameters can be simply approximated by partial differentiation of the asymptotic solutions derived using the GMS method. This result will be used throughout this study to analyze first and second order sensitivity of the dynamics of the GHAME vehicle to variations in the different stability derivatives during its reentry into the Earth's atmosphere.

CHAPTER 4

Sensitivity Analysis of the Lateral Dynamics of the GHAME Vehicle

4.1 EQUATIONS OF MOTION

The general lateral equations of motion of a vehicle in flight are non-linear and time varying. The lateral dynamics of the GHAME vehicle, however, are studied by developing approximate solutions to the equations of motion linearized about a steady flight condition. This approach is justified because of the fact that, in general, solutions to non-linear systems exhibit the same local behavior as the solutions of the linearized systems in the vicinity of the equilibrium.

With the usual notation [5], the linearized equations of motion describing the lateral dynamics of a flight vehicle about a nominal steady flight condition are written in a state space form as:

$$\begin{bmatrix} s-Y_v & V & -g \\ -L_v & -L_r & s^2-L_p s \\ -N_v & s-N_r & -N_p s \end{bmatrix} \begin{bmatrix} \Delta v \\ \Delta r \\ \Delta \phi \end{bmatrix} = \begin{bmatrix} 0 \\ 0 \\ 0 \end{bmatrix} \tag{4.1}$$

or $$A\underline{X} = \underline{0} \tag{4.2}$$

where the parameters L_v, L_r, L_p, N_v, N_r, N_p and Y_v appearing in (4.1) are the lateral-directional stability derivatives of the flight vehicle. The velocity perpendicular to the flight path, v, the yaw rate, r, and the roll angle, ϕ, of the vehicle are the flight parameters and are represented as perturbations about some steady state flight value:

$$v = v_0 + \Delta v \tag{4.3}$$

$$r = r_0 + \Delta r \tag{4.4}$$

$$\phi = \phi_0 + \Delta\phi \tag{4.5}$$

The modes of motion of the lateral dynamics of the flight vehicle are determined from the roots of the characteristic equation, which are also the eigenvalues of the A matrix. The characteristic equation of the system describing the lateral dynamics of the GHAME vehicle is a fourth order equation which can be written as:

$$s^4 + c_3 s^3 + c_2 s^2 + c_1 s + c_0 = 0 \tag{4.6}$$

The coefficients appearing in (4.6) are functions of the stability derivatives and are defined as:

$$c_3 = -L_p - N_r - Y_v \tag{4.7}$$

$$c_2 = VN_v - L_rN_p + Y_vL_p + N_r (L_p + Y_v) \tag{4.8}$$

$$c_1 = Y_v (L_rN_p - N_rL_p) - gL_v + VN_pL_v - VL_pN_v \tag{4.9}$$

$$c_0 = g (L_vN_r - N_vL_r) \tag{4.10}$$

Typically, the lateral dynamics of a flight vehicle has three modes:

1. A relatively lightly damped oscillatory mode, called the "dutch roll".

2. A first order divergent mode of relatively long time constant, called the "spiral" mode.

3. A first order convergent mode of relatively short time constant, called the "roll subsidence" mode.

The typical root locations in the complex plane for the roots representing lateral dynamics are shown in figure 4.1:

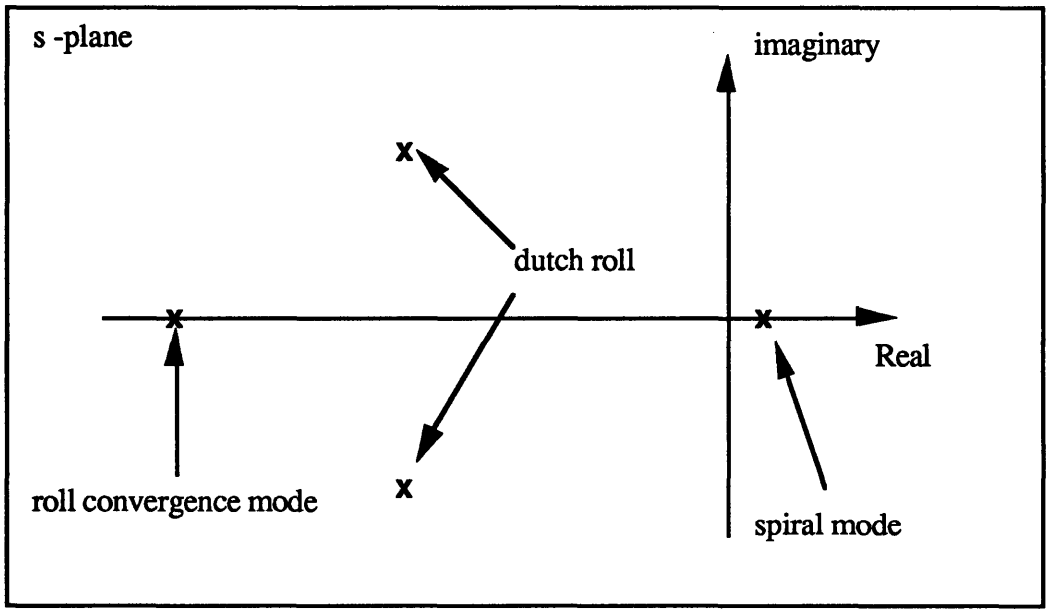

Figure 4.1: Conventional Lateral Directional Root Location

In the case of the GHAME vehicle, flight parameters such as air density and flight velocity change continuously along the reentry trajectory. As a result, the stability derivatives of the vehicle vary with time as the vehicle enters the Earth's atmosphere. Therefore the

roots representing the lateral modes of motion will move in the complex plane as the vehicle flies along the trajectory.

The roots associated with the lateral-directional modes of motions of the GHAME vehicle and their movement with time are shown in figure 4.2. The roots are plotted for up to 1900 seconds into the trajectory. It appears that over that particular phase of the reentry, the GHAME vehicle possesses the three modes of motion that are typical of lateral-directional behavior of a conventional aircraft.

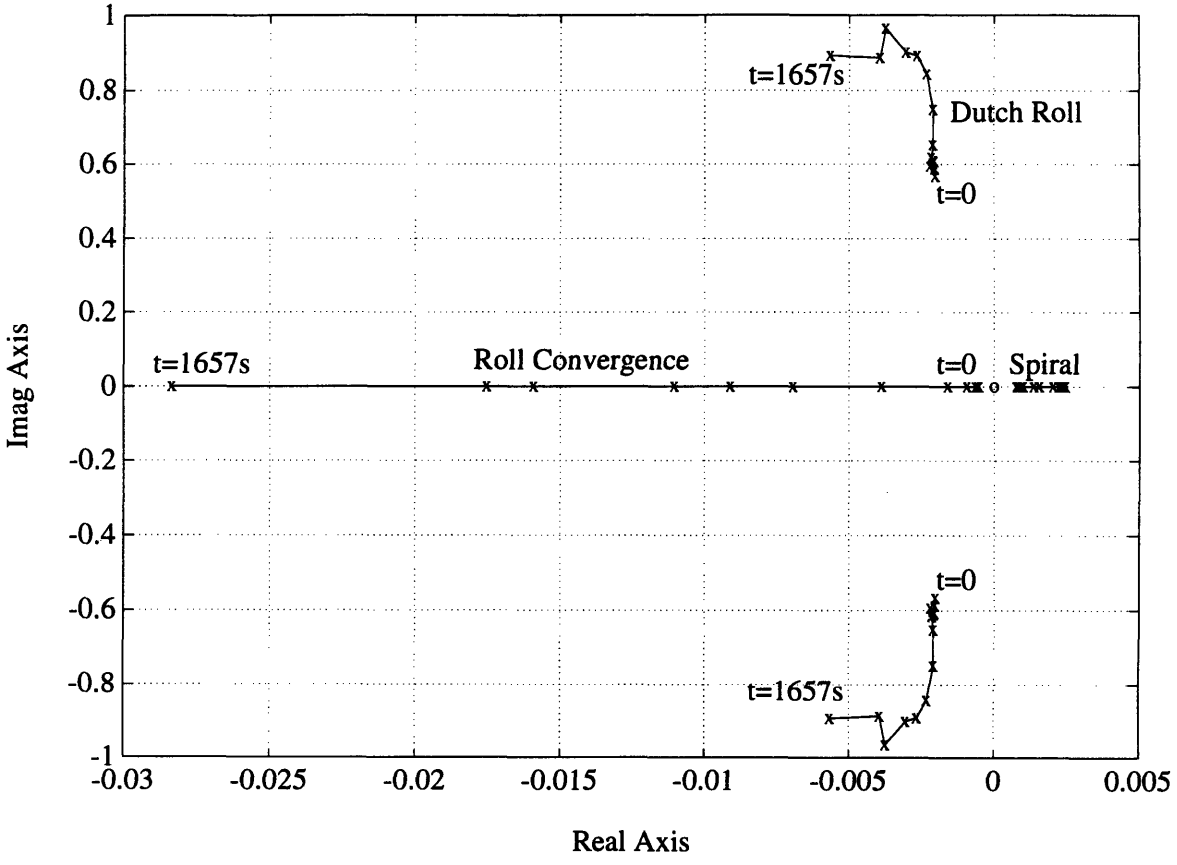

Figure 4.2: Lateral Directional Roots Along the Trajectory

The dutch roll is represented by a pair of complex conjugate roots that remain in the left half plane while the roll convergence and spiral modes are each represented by a real roots that remain in the left and right half plane respectively. As the GHAME vehicle travels further into the atmosphere, the dutch roll mode increases both in frequency and in damping. The roll convergence mode increases significantly in frequency while the spiral mode remains in the same area near the origin. At 1657 seconds into the reentry, were the vehicle is in the lower parts of the atmosphere and flying at low supersonic speeds, the root locations of the lateral directional modes of motion of the GHAME vehicle are similar to the typical root locations of conventional aircraft presented in figure 4.1.

4.2 GMS SOLUTION TO LATERAL DYNAMICS

The lateral-directional dynamical response of the GHAME vehicle is described by a fourth order differential equation:

$$\frac{d^4y}{dt^4} + c_3(t)\frac{d^3y}{dt^3} + c_2(t)\frac{d^2y}{dt^2} + c_1(t)\frac{dy}{dt} + c_0(t) = 0 \qquad (4.11)$$

where y can represent any one of the three flight parameters, v, r or ϕ, since they all exhibit the same basic response. Since the stability derivatives vary along the reentry trajectory, it is clear that this differential equation is time varying. As mentioned in chapter 3, linear time varying (LTV) differential equations can generally not be solved analytically using traditional methods. The GMS method will therefore be used to derive asymptotic approximations to the solutions of (4.11).

In this chapter, we will be studying the lateral dynamics of the GHAME vehicle over a phase of the reentry trajectory. The portion that is considered here corresponds to the first 670

second into the trajectory. In that interval, the vehicle possesses the three typical modes of a conventional aircraft: roll convergence, spiral divergence and dutch roll.

Since the roll convergence and spiral divergence modes are each represented by a single real root, the GMS asymptotic approximations for the respective characteristic motions are given, as shown in chapter 3, by the expressions:

$$y_{rc}(t) = \exp\left(\int_{t_0}^{t} k_{rc}(t)\, dt\right) \tag{4.12}$$

$$y_{sp}(t) = \exp\left(\int_{t_0}^{t} k_{sp}(t)\, dt\right) \tag{4.13}$$

where k_{rc} and k_{sp} are the two real roots of the characteristic equation corresponding to the roll convergence and spiral divergence modes. The dutch roll mode is represented by a pair of complex conjugate roots, therefore the dutch roll response (separated here into a sin-like, dr_1, and a cosine-like, dr_2, dutch roll) is given by:

$$y_{dr1}(t) = \exp\left(\int_{t_0}^{t} \left|\frac{\dot{k}_{drr}(t)}{2ik_{dri}(t)}\right| dt\right) \exp\left(\int_{t_0}^{t} k_{drr}(t)\, dt\right) \sin\left(\int_{t_0}^{t} k_{dri}(t)\, dt\right) \tag{4.14}$$

$$y_{dr2}(t) = \exp\left(\int_{t_0}^{t} \left|\frac{\dot{k}_{drr}(t)}{2ik_{dri}(t)}\right| dt\right) \exp\left(\int_{t_0}^{t} k_{drr}(t)\, dt\right) \cos\left(\int_{t_0}^{t} k_{dri}(t)\, dt\right) \tag{4.15}$$

where $k_{dr} = k_{drr} \pm ik_{dri}$ is the complex conjugate root associated with the dutch roll.

We will make the additional simplification in this study of only considering the fast part of the approximate solutions associated with the dutch roll. By neglecting the slow part, we are losing accuracy in describing the amplitude of the response as illustrated in chapter 3. This approximation, however, considerably simplifies the calculations associated with the sensitivity analysis and was not considered penalizing since the goal of this study consists mainly of validating our approach. The simplified approximation to the dutch roll response will therefore be:

$$y_{dr1}(t) = \exp\left(\int_{t_0}^{t} k_{drr}(t)\,dt\right)\sin\left(\int_{t_0}^{t} k_{dri}(t)\,dt\right) \tag{4.16}$$

$$y_{dr2}(t) = \exp\left(\int_{t_0}^{t} k_{drr}(t)\,dt\right)\cos\left(\int_{t_0}^{t} k_{dri}(t)\,dt\right) \tag{4.17}$$

The full GMS asymptotic approximation to the solutions of the fourth order linear time varying differential equation describing the lateral-directional dynamics of the GHAME vehicle during reentry into the Earth's atmosphere is given by the linear combination of the approximations of the motions of each mode:

$$y(t) = C_1 y_{rc}(t) + C_2 y_{sp}(t) + C_3 y_{dr1}(t) + C_4 y_{dr2}(t) \tag{4.18}$$

where C_1, C_2, C_3 and C_4 are constants that depend on initial conditions.

4.3 FIRST ORDER SENSITIVITY ANALYSIS

4.3.1 Introduction

In this section, we will consider the sensitivity of the lateral-directional dynamics of the GHAME vehicle to variations, along the reentry trajectory, of its lateral stability derivatives. In order to get better insight, the sensitivity of the lateral dynamics to variations in the stability derivatives will be developed by considering the motions associated with each of the modes separately.

The effect of changes in these stability derivatives will be determined by using the GMS sensitivity theory described in chapter 3. True sensitivity will be approximated by partial differentiation of the GMS approximations with respect to the stability derivatives. The validity of this approach for slowly varying systems was demonstrated by Ramnath in the study of the dynamics of a VTOL [8].

First order sensitivity of a particular modal response is therefore simply approximated by partial differentiation of the GMS response associated with that mode with respect to the stability derivatives. As an example, first order sensitivity of the roll convergence mode to variations in the dihedral term, L_v, is simply given by:

$$S^{rc}_{L_v}(t) = \frac{\partial y_{rc}(t)}{\partial L_v} = \exp\left(\int_{t_0}^{t} k_{rc}(t)\,dt\right)\left(\int_{t_0}^{t} \frac{\partial k_{rc}(t)}{\partial L_v}\,dt\right) \qquad (4.19)$$

Once again the GMS solution, defined in chapter 3, provides us with a complete analytical expression for sensitivity. The algebra associated with the different derivations is very tedious and will not be detailed in this study. A good descriptions of the details of these derivations however can be found in [15].

4.3.2 Definition of First Order Sensitivity Criteria

The motivations for a sensitivity analysis are essentially to determine:

1. Which stability derivative variations have the most effect on the dynamics of the GHAME vehicle during the reentry phase.

2. At which point along the reentry trajectory is the vehicle most sensitive to variations in its stability derivatives.

Based on these motivations, two criteria are defined in order to analyze first order sensitivity of the dynamics of the GHAME vehicle to stability derivative variations. These criteria are defined to facilitate comparisons of the magnitudes and time histories of the different sensitivities along the reentry trajectory.

<u>First Order Sensitivity Average Criteria for Lateral Dynamics</u>

The first criterion is defined as the average amplitude of the sensitivity of a particular mode m (dutch roll, spiral or roll convergence) to variations in a particular stability derivatives p (L_v, L_r, L_p, N_v, N_r, N_p or Y_v), over a prescribed phase of the reentry trajectory [0, T] ([0, 670] in this case):

$$S^m_{pav} \triangleq \frac{1}{T}\int_0^T |\, S^m_p(t)\,|\, dt \qquad (4.20)$$

where $S^m_p(t)$ is the first order sensitivity of mode m to variations of the stability derivative p:

$$S^m_p(t) \triangleq \frac{\partial y_m(t)}{\partial p} \qquad (4.21)$$

This first criterion measures the magnitude of sensitivity to variations in the different stability derivatives over the entire phase of the reentry that is studied.

First Order Sensitivity Norm Criteria for Lateral Dynamics

The second criterion can be interpreted as a norm since it combines the effects of the sensitivity of a particular mode to all of the stability derivatives. It is defined, for each particular mode m, as:

$$\left\| S_m(t) \right\| \triangleq \sum_p \left| S_p^m(t) \right| \qquad (4.22)$$

where p are all of the lateral stability derivatives.

This second criterion characterizes the evolution over time of the global sensitivity for each of the vehicle's modes.

4.3.3 Sensitivity of First Order Stability Derivative Variations for Lateral Modes

First order sensitivity of the lateral modes of the GHAME vehicle for variations in the seven lateral stability derivatives (Lv, Nv, Yv, Lp, Np, Lr, Nr) was derived using the GMS sensitivity theory. The following presents the results obtained in this first order sensitivity analysis.

Sensitivity Averages

The sensitivity averages of the three lateral-directional modes for the different lateral stability derivatives are summarized in the three charts presented on page 36.

These charts show that the lateral modes of the GHAME vehicle are more sensitive to variations in the directional derivative N_v than to any other stability derivative. Although N_v has a strong influence on all three modes, it mostly affects the dutch roll and spiral modes. In that sense the vehicle behaves in the same way as a conventional aircraft. The directional stability term is very much dependent on vertical tail size. The vertical tail size of the GHAME vehicle will therefore have great implications on the lateral dynamics characteristics during reentry.

Variations of the dihedral term, L_v, also have a significant effect on the lateral modes of the vehicle. Its influence on roll convergence and spiral modes is nearly as important as that of the directional stability term. L_v also has a significant effect on dutch roll, several orders of magnitude smaller however than that of N_v. There again, the strong sensitivity of the lateral dynamics to changes in the dihedral term is similar to the behavior of a conventional aircraft for which L_v plays an important role in lateral stability and control.

Variations of the yaw damping term, N_r, and adverse yaw term, N_p, have similar affects on lateral dynamics of the GHAME vehicle. These effects are several orders of magnitude smaller than the ones of the directional and dihedral terms and can be considered of secondary importance. They still contribute, however, especially to the characterization of the roll convergence and spiral modes.

Variations in L_r and in the roll damping term, L_p, have similar effects on lateral dynamics of the GHAME vehicle. Changes in L_r and L_p mainly affect the roll convergence and spiral modes but are, however, of secondary importance compared to the influence of N_v and L_v. On the other hand, they have nearly have no influence on dutch roll. This behavior is also consistent with that of a conventional aircraft.

The charts also show that changes in the cross-wind-force term, Y_v, do not have a significant effect on the lateral dynamics of the GHAME vehicle during its reentry.

ROLL CONVERGENCE

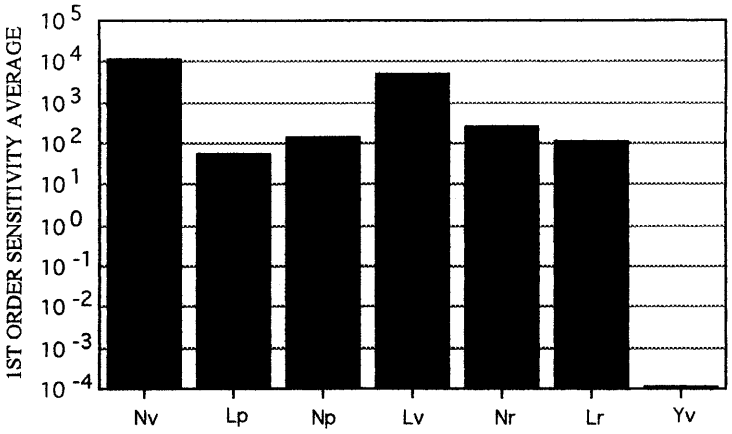

SPIRAL

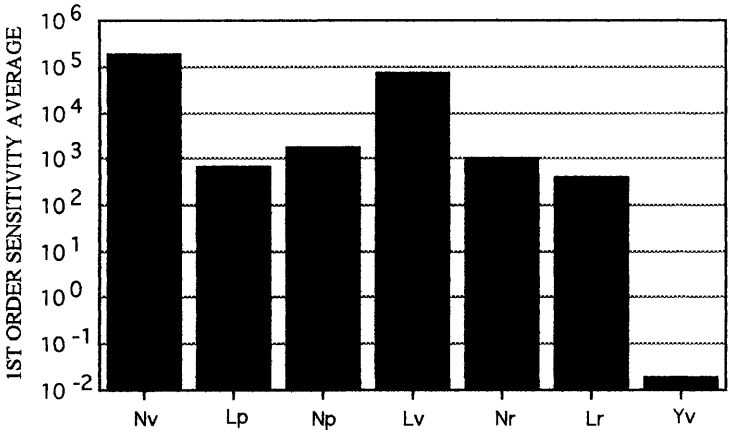

DUTCH ROLL

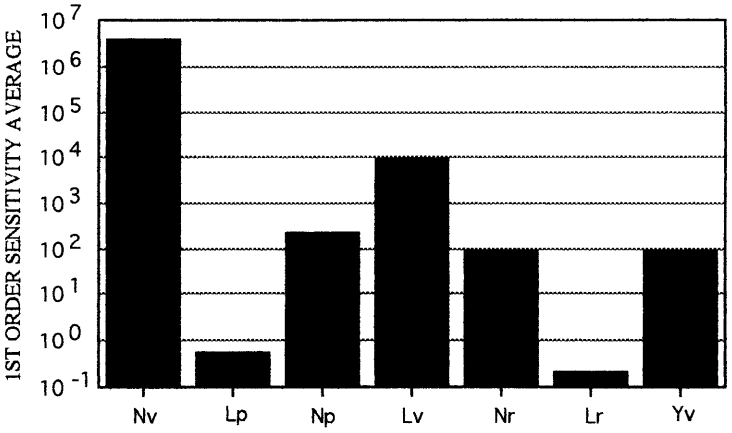

Sensitivity Norm

The plots on page 38 present the evolution over time of what was defined as the sensitivity norm of each of the lateral modes. The sensitivity norm characterizes the evolution over time of the combined sensitivities for a particular mode. Compared to sensitivity averages, this criterion gives insight on the amplitude of the global sensitivity of the vehicle to stability variations at different times along the reentry trajectory.

The first thing to be noticed is that the sensitivity norm of the roll convergence and dutch roll modes reach a maximum at some point of the phase of reentry trajectory we are concerned with. The sensitivity norm of the spiral mode on the other hand grows unbounded. This first observation is consistent with the fact that the spiral mode of the GHAME vehicle is unstable where as both dutch roll and roll convergence modes are stable.

Dutch roll is the mode which is globally most sensitive to stability derivative variations. Furthermore, the oscillatory nature of the dutch roll remains present in the time history of sensitivity. This defines a band in which the global sensitivity varies along the trajectory. This band is bounded at all times and reaches a maximum at about 400 seconds into the trajectory. Because the influence of variations in the directional stability derivative, N_v, is several orders of magnitude larger than that of any other one of the stability derivatives, the sensitivity norm is mostly influenced by the time history of sensitivity of the dutch roll to changes in N_v.

The sensitivity norm of the roll convergence mode remains the smallest of the three modes in amplitude. It grows nearly linearly until about 600 seconds into the trajectory were it reaches its maximum.

The sensitivity norm of the spiral mode has a large value and grows unbounded over the trajectory. Its magnitude would become predominant if the dynamics of the vehicle were to be studied over a larger period of time.

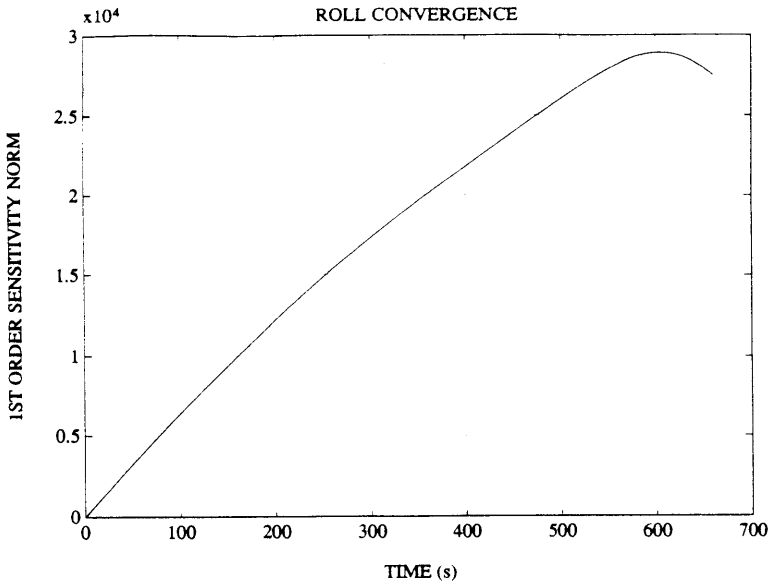
ROLL CONVERGENCE
x10^4
1ST ORDER SENSITIVITY NORM
TIME (s)
0
0.5
1
1.5
2
2.5
3
0
100
200
300
400
500
600
700

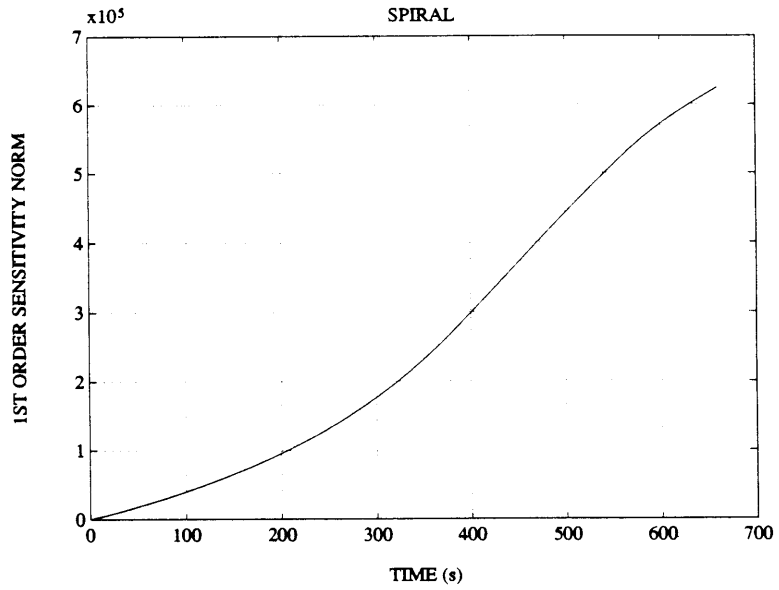
SPIRAL
x10^5
1ST ORDER SENSITIVITY NORM
TIME (s)
0
1
2
3
4
5
6
7
0
100
200
300
400
500
600
700

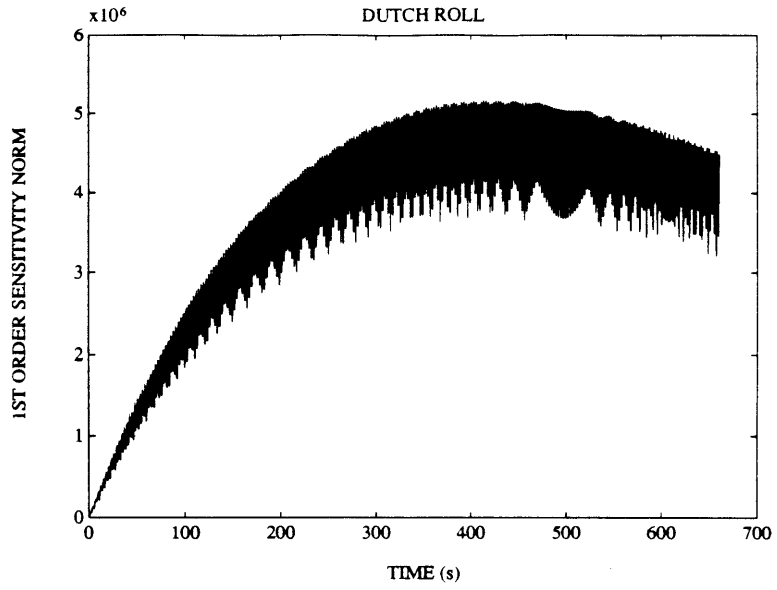
DUTCH ROLL
x10^6
1ST ORDER SENSITIVITY NORM
TIME (s)
0
1
2
3
4
5
6
0
100
200
300
400
500
600
700

4.4 SECOND ORDER SENSITIVITY ANALYSIS

4.4.1 Introduction

In this section, we will consider the second order sensitivity of the lateral-directional dynamics of the GHAME vehicle to variations in the lateral-directional stability derivatives. As for first order , the second order sensitivity analysis is performed on each modal response individually in order to get more insight about the way in which the dynamics of the vehicle are affected by stability derivative variations during the reentry.

Again, true second order sensitivity is approximated by second order partial differentiation of the GMS asymptotic approximations with respect to the stability derivatives. This approach was justified in chapter 3 as a result of the GMS sensitivity theory developed by Ramnath [8]. As an example, second order sensitivity of the roll convergence mode to variations in the directional derivative, N_V, is given by:

$$\xi^{rc}_{N_v}(t) \triangleq \frac{\partial^2 y_{rc}(t)}{\partial N_v^2} = \exp\left(\int_{t_0}^{t} k_{rc}(t)\,dt\right)\left[\left(\int_{t_0}^{t} \frac{\partial^2 k_{rc}(t)}{\partial N_v^2}\,dt\right) + \left(\int_{t_0}^{t} \frac{\partial k_{rc}(t)}{\partial N_v}\,dt\right)^2\right] \qquad (4.16)$$

4.4.2 Definition of Second Order Sensitivity Criteria

As for the first order sensitivity analysis, two equivalent criteria are used to analyze second order sensitivity.

Second Order Sensitivity Average Criteria for Lateral Dynamics

The first criterion is very similar to the one defined for first order sensitivity. It characterizes the average amplitude of second order sensitivity of a particular mode m with respect to one of the stability derivatives p, over a prescribed phase of the reentry trajectory [0,T]:

$$\xi^{m}_{p_{av}} \triangleq \frac{1}{T}\int_{0}^{T}\left|\xi^{m}_{p}(t)\right| dt \tag{4.17}$$

where $\xi^{m}_{p}(t)$ is the second order sensitivity of the mode m to variations of the stability derivative p obtained through the GMS sensitivity theory:

$$\xi^{m}_{p}(t) \triangleq \frac{\partial^2 y_m(t)}{\partial p^2} \tag{4.19}$$

Second Order Sensitivity Norm Criteria for Lateral Dynamics

The second criterion can, as for the first order criteria, be considered as a norm and characterizes the evolution over time of a global second order sensitivity for a particular mode m:

$$\left|\left|\xi_m(t)\right|\right| \triangleq \sum_{p}\left|\xi^{m}_{p}(t)\right| \tag{4.20}$$

where p are all of the stability derivatives.

4.4.3 Second Order Sensitivity to Stability Derivative Variations for Lateral Modes

As for the first order sensitivity analysis, second order sensitivity of each lateral mode of the GHAME vehicle during the initial 670 seconds into the trajectory are derived using the GMS sensitivity theory. The following presents the results obtained through the numerical simulations.

Sensitivity Averages

Sensitivity averages of the three modes to second order variations of the lateral stability derivatives are summarized in the three charts presented on page 42.

These charts show that the lateral modes of the GHAME vehicle are most sensitive to second order variations in the directional stability term N_V. The dutch roll and at a lesser degree the spiral mode are both orders of magnitude more sensitive to second order variations in N_V than in any other stability derivative. This, in conjunction with the very high sensitivity of the lateral modes to first order variations in N_V, emphasizes the critical importance of vertical tail size on the lateral dynamics of the GHAME vehicle during the reentry phase and more particularly on the dutch roll and spiral modes.

Second order variations in the dihedral term, L_V, also has a very important influence on the lateral dynamics. Except for its significant influence on roll convergence, its effects are however offset by the much larger sensitivity of the vehicle to second order variations in N_V.

Second order variations in all of the other lateral stability derivatives have effects that are several orders of magnitude smaller than that of the directional and dihedral terms.

Sensitivity Norm

The set of plots presented on page 43 present the evolution over time of the second order sensitivity norm of each mode.

ROLL CONVERGENCE

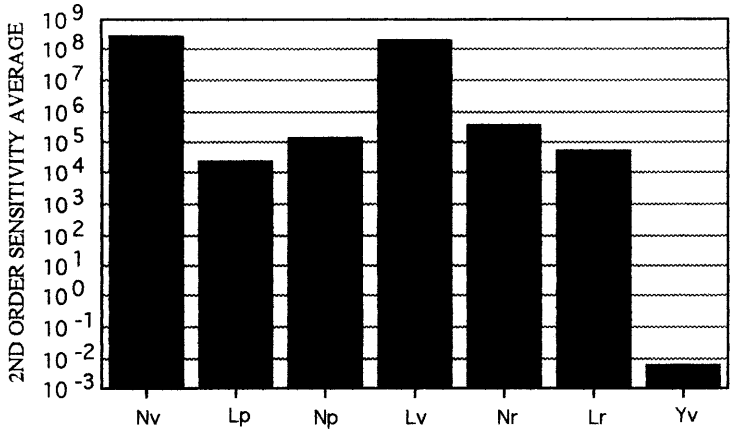

SPIRAL

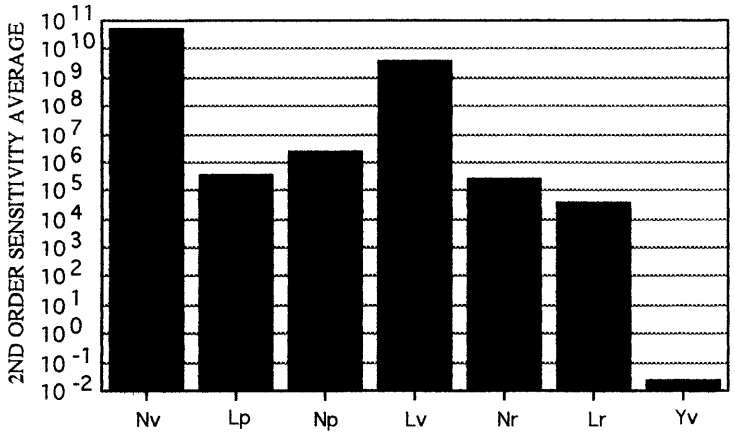

DUTCH ROLL

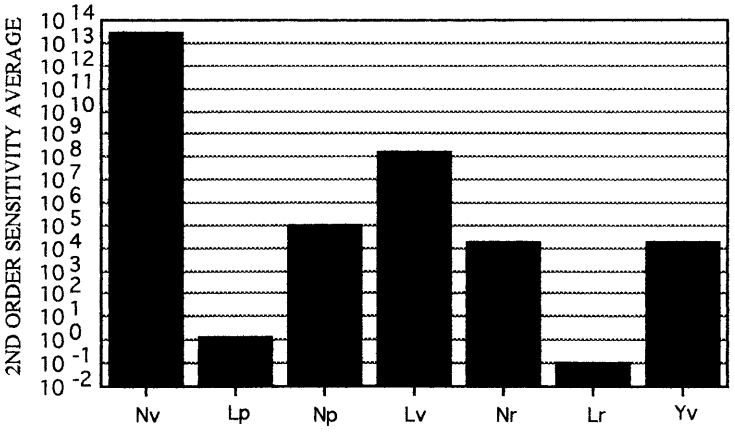

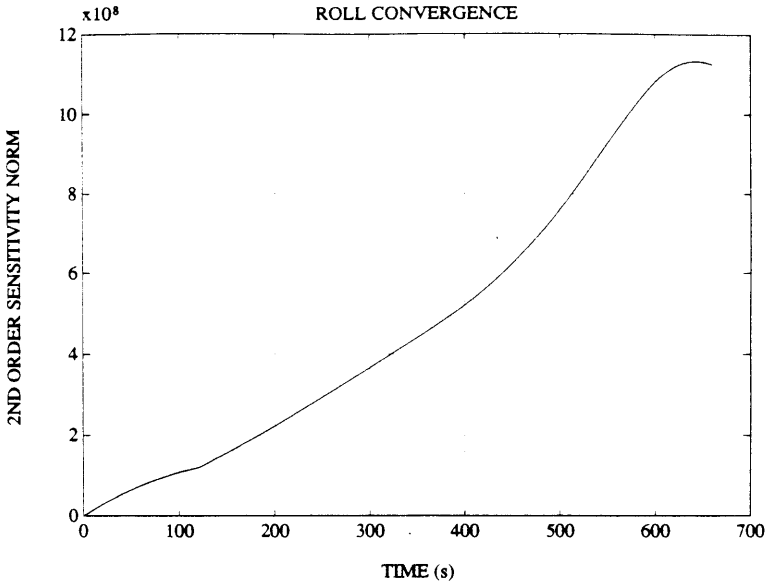
x10^8
ROLL CONVERGENCE
2ND ORDER SENSITIVITY NORM
TIME (s)

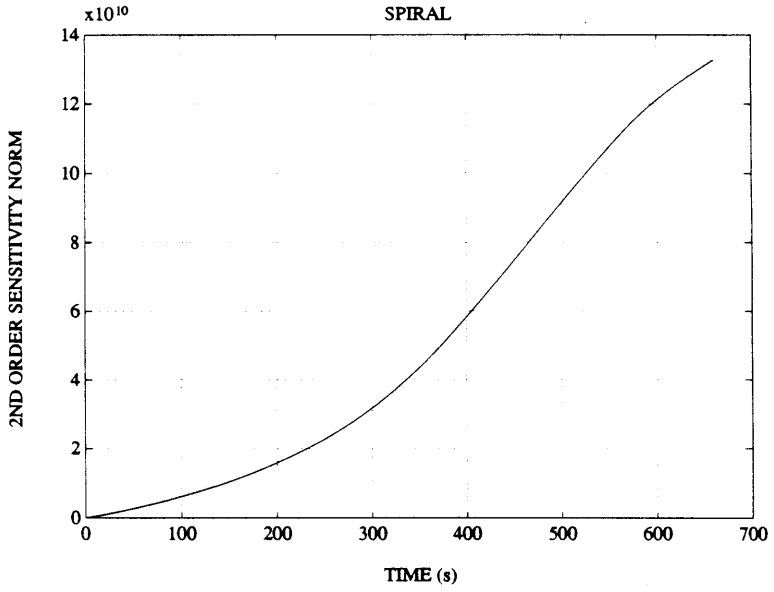
x10^10
SPIRAL
2ND ORDER SENSITIVITY NORM
TIME (s)

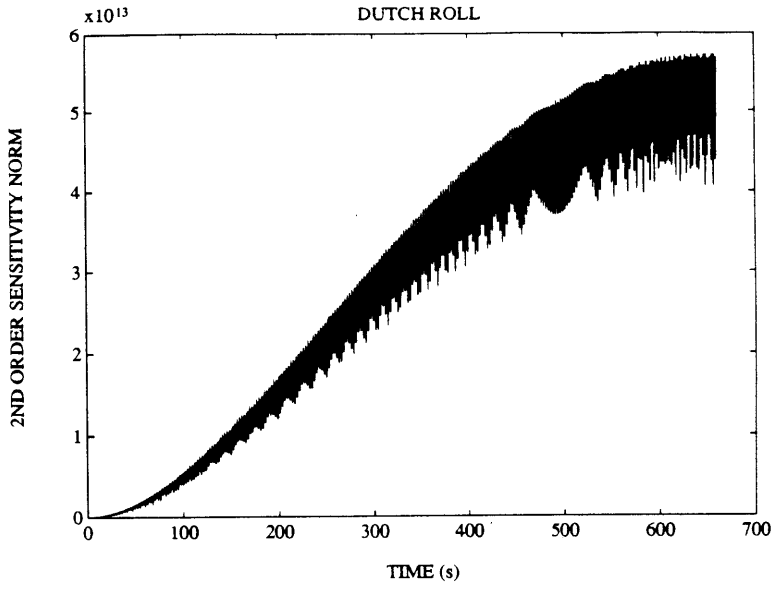
x10^13
DUTCH ROLL
2ND ORDER SENSITIVITY NORM
TIME (s)

Over this particular phase of the reentry, the dutch roll mode is globally far more sensitive to second order variations in lateral stability derivatives than the spiral or roll convergence modes.

As for first order, the sensitivity norm of the roll convergence and dutch roll modes reach a maximum at some point of the reentry trajectory we are considering. The sensitivity norm of the spiral mode here again grows unbounded. It is interesting however to notice that, unlike in the first order case, the global second order sensitivity of all three modes reaches a maximum at approximately the same point corresponding to approximately 650 seconds into the trajectory. This could have severe consequences on the design of good control laws at that point of the reentry.

CHAPTER 5

Sensitivity Analysis of the Longitudinal Dynamics of the GHAME Vehicle

5.1 EQUATIONS OF MOTION

The linearized equations of motion describing the longitudinal dynamics of a flight vehicle about a nominal steady flight condition are written in a state space form [5] as:

$$\begin{bmatrix} s+D_v & D_\alpha - g & g \\ L_v / V_0 & s+L_\alpha / V_0 & -s \\ -M_v & -M_\alpha & s(s-M_q) \end{bmatrix} \begin{bmatrix} \Delta v \\ \Delta\alpha \\ \Delta\theta \end{bmatrix} = \begin{bmatrix} 0 \\ 0 \\ 0 \end{bmatrix} \qquad (5.1)$$

$$\text{or} \qquad A\underline{X} = \underline{0} \qquad (5.2)$$

where the parameters D_v, D_α, L_v, L_α, M_v, M_α and M_q appearing in the equations above are the longitudinal stability derivatives of the vehicle. The velocity perpendicular to the flight path, v, the angle of attack, α, and the pitch angle, q, of the vehicle are the flight parameters and are represented as perturbations about some steady state flight value:

$$v = v_0 + \Delta v$$

$$\alpha = \alpha_0 + \Delta\alpha$$

$$q = q_0 + \Delta q$$

The longitudinal modes of the flight vehicle are determined by the nature of the eigenvalues of the A matrix in equation (5.2). The characteristic equation of the system representing the longitudinal dynamics of the aircraft is a fourth order equation that can be written as:

$$s^4 + c_3 s^3 + c_2 s^2 + c_1 s + c_0 = 0 \qquad (5.3)$$

where the coefficients in (5.3) are defined in terms of the longitudinal stability derivatives as:

$$c_3 = L_\alpha/V_0 - M_q + D_v$$

$$c_2 = (D_v - M_q)(L_\alpha/V_0) - D_v M_q - M_\alpha + (g - D_\alpha)(L_v/V_0)$$

$$c_1 = M_v D_\alpha - M_\alpha D_v - D_v M_q (L_\alpha/V_0) + (D_\alpha M_q - g)(L_v/V_0)$$

$$c_0 = g(M_v (L_\alpha/V_0) - M_\alpha (L_v/V_0))$$

Typically, the longitudinal dynamics of a flight vehicle has two distinct modes:

1. A relatively well damped, high frequency oscillatory mode, called the "short period".

2. A lightly damped relatively low frequency oscillatory mode, called the "phugoid".

The typical locations in the complex plane of the roots representing flight vehicle longitudinal dynamics are shown on figure 5.1.

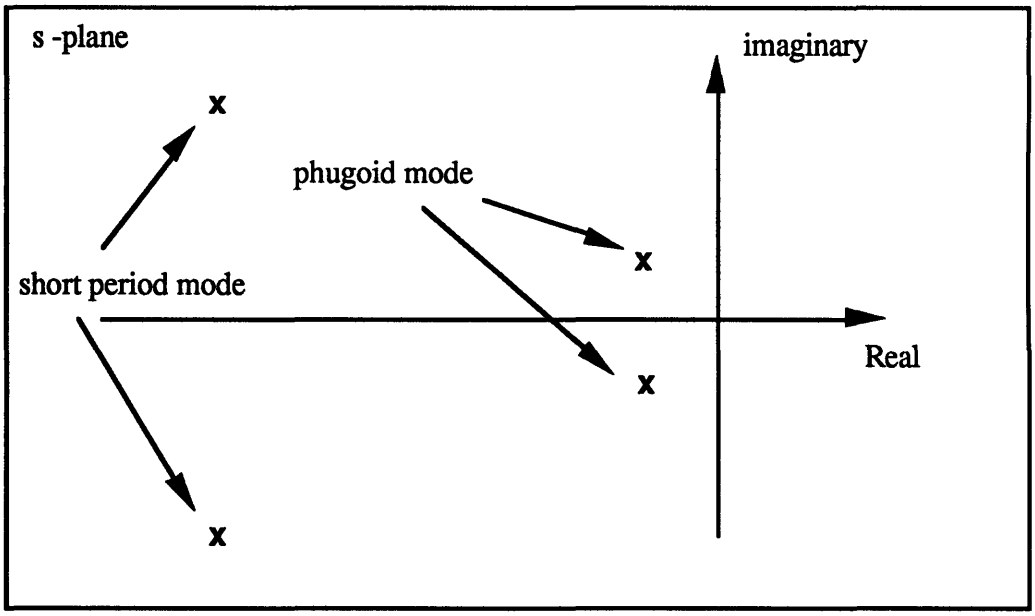

Figure 5.1: Typical Longitudinal Root Location

As for the lateral-directional dynamics, the continuous changes in flight parameters such as air density and flight velocity along the reentry trajectory results in stability derivative variations as the GHAME vehicle enters the Earth's atmosphere. The roots representing the longitudinal modes of motion will therefore move in the complex plane as the vehicle flies along the trajectory.

The roots associated with the longitudinal modes of motions of the GHAME vehicle and their movement with time are shown in figure 5.2. The roots are plotted for up to 1657 seconds into the trajectory. Figure 5.2 clearly shows the complex conjugate pair of roots representing the short period mode and their movement as the vehicle travels into the Earth's atmosphere. As the GHAME vehicle progresses further into the atmosphere, both the frequency and damping of the short period mode increase. However, due to the differences in frequency scales on which the phugoid and short period occur, the root locations and movement of the roots representing the phugoid mode are not visible on figure 5.2.

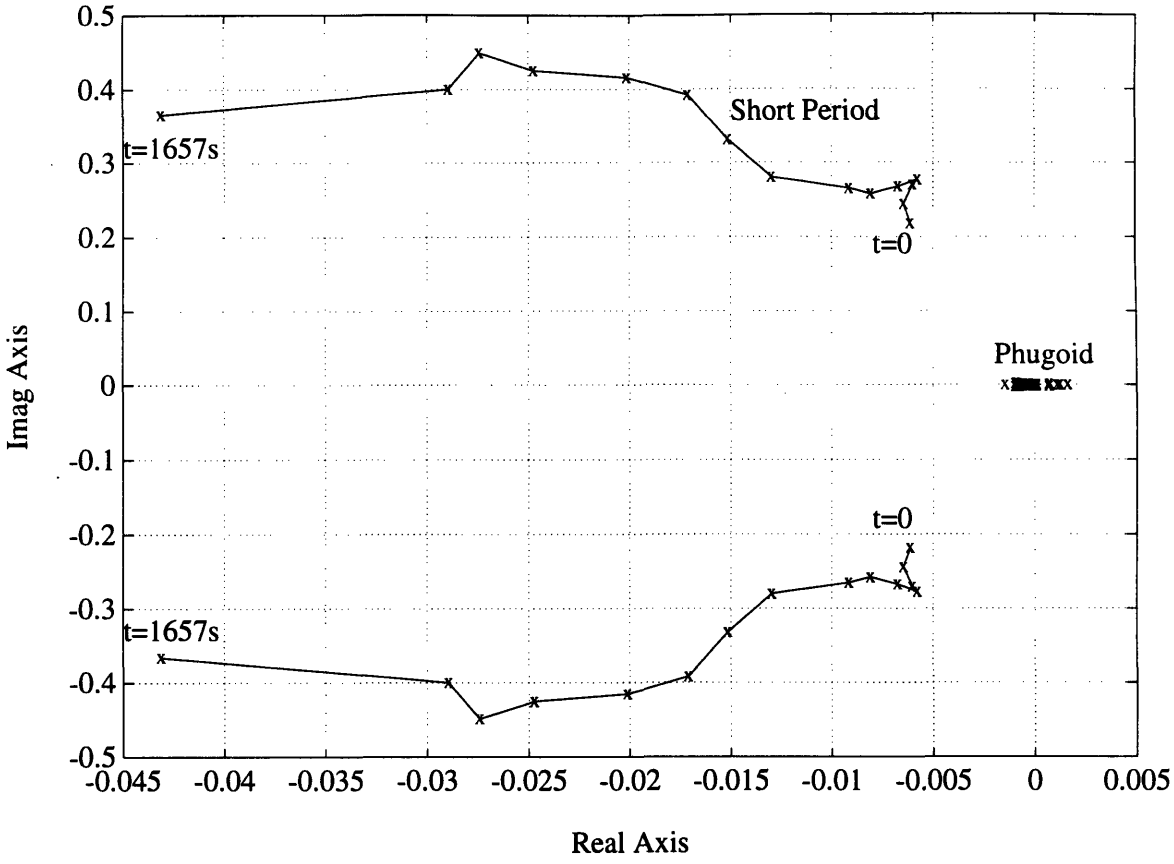

Figure 5.2: Longitudinal Roots Along the Trajectory

The movement of the phugoid roots along the trajectory are detailed on the magnified view presented on figure 5.3. It appears clearly that the phugoid mode does not behave in a conventional manner along during the reentry. At the beginning of the reentry, the phugoid mode is represented by a pair of complex conjugate roots in the right half plane defining a slow and lightly damped unstable mode. As the vehicle progresses into the atmosphere, the phugoid roots move into the left half plane and then back into the right half plane. At about 390 seconds into the trajectory, the complex conjugate pair separates into two real roots that both move towards the origin, one of which remains in the left half plane the other in the right half plane. During that particular phase of the reentry, the GHAME vehicle does not behave in a conventional way and possesses a degenerated phugoid mode. At approximately 600 seconds into the trajectory, the two real roots join to form, once again, a pair of complex

conjugate roots that remain in the left half plane until the end of that portion of the reentry at 1657 seconds. Over that last phase, the vehicle is flying at lower Mach numbers and in the lower portion of the atmosphere and has a behavior that is typical of a conventional aircraft.

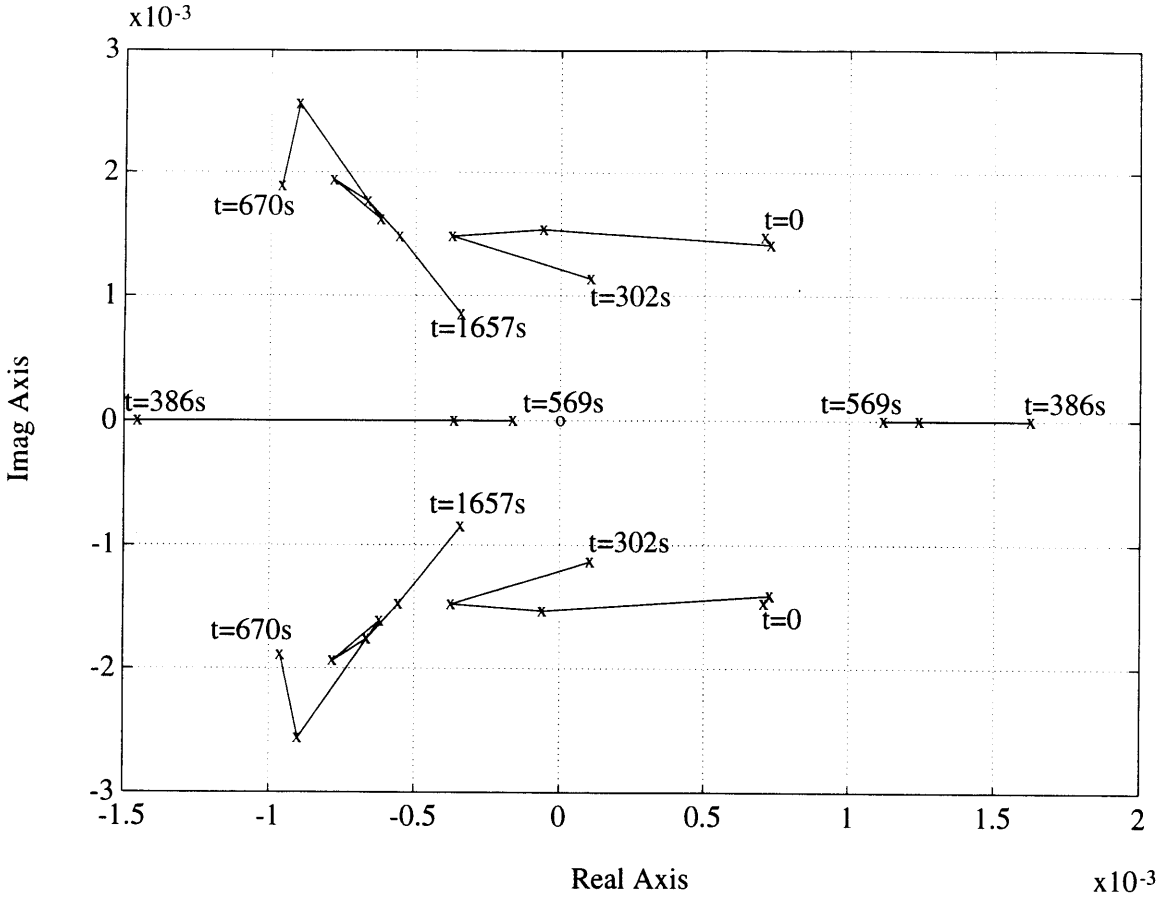

Figure 5.3: Phugoid Roots Along the Trajectory

5.2 GMS SOLUTION TO LONGITUDINAL DYNAMICS

The longitudinal response of the GHAME vehicle is characterized by a fourth order differential equation:

$$\frac{d^4y}{dt^4} + c_3(t)\frac{d^3y}{dt^3} + c_2(t)\frac{d^2y}{dt^2} + c_1(t)\frac{dy}{dt} + c_0(t) = 0 \qquad (5.4)$$

where y can represent any one of the three flight parameters, velocity perpendicular to the flight path, v, angle of attack, α, or pitch angle, q, as they all exhibit the same response. Since the stability derivatives vary along the reentry trajectory, it is clear that this differential equation is time varying. As for the lateral-directional dynamics, the GMS method described in chapter 3 is used to derive asymptotic approximate solutions to (5.4).

The peculiar behavior of the phugoid mode roots require great rigor and a careful use of the Generalized Multiple Scales method to study the GHAME vehicle's longitudinal dynamics. The points at which the phugoid roots change from real roots to a pair of complex conjugate roots and vice versa is known as a " turning point " and represents a change in the nature of the dynamic response, associated with the mode, from an non-oscillatory to an oscillatory behavior. With regards to the GMS approximations, these turning points present additional mathematical difficulties that can be dealt with in a number of different ways. However, for simplification purposes, these problems will be avoided in this study by restricting the study of the GHAME vehicle's longitudinal dynamics to the first 300 seconds along the trajectory where the phugoid is represented by a pair of complex conjugate roots.

Since both the phugoid and short period modes are represented by a pair of complex conjugate roots, $k_p = k_{pr} \pm i k_{pi}$ and $k_{sp} = k_{spr} \pm i\, k_{spi}$ respectively, the fast part of the GMS approximation for the characteristic motions are given, as shown in chapter 3, by the expressions:

$$y_p(t) = \exp\left(\int_{t_0}^{t} k_{pr}(t)\, dt\right)\left[C_1 \sin\left(\int_{t_0}^{t} k_{pi}(t)\, dt\right) + C_2 \cos\left(\int_{t_0}^{t} k_{pi}(t)\, dt\right)\right] \qquad (5.5)$$

$$y_{sp}(t) = \exp\left(\int_{t_0}^{t} k_{spr}(t)\, dt\right)\left[C_3 \sin\left(\int_{t_0}^{t} k_{spi}(t)\, dt\right) + C_4 \cos\left(\int_{t_0}^{t} k_{spi}(t)\, dt\right)\right] \qquad (5.6)$$

where C_1, C_2, C_3 and C_4 are constants that depend on initial conditions.

The full GMS asymptotic approximation to the solutions of the fourth order linear time varying differential equation (5.4) describing the longitudinal dynamics of the GHAME vehicle during its reentry is given by:

$$y(t) = C_1 y_{p1}(t) + C_2 y_{p2}(t) + C_3 y_{sp1}(t) + C_4 y_{sp2}(t) \qquad (5.7)$$

where y_{p1} and y_{sp1} are the sin and y_{p2}, y_{sp2} the cosine parts of the solutions presented in (5.5) and (5.6).

5.3 FIRST ORDER SENSITIVITY ANALYSIS

5.3.1 Introduction

As for the study of first order sensitivity of the lateral modes, the average sensitivity and sensitivity norm criteria will be used to analyze first order sensitivity of the longitudinal modes of the GHAME vehicle.

As a reminder these criteria are:

<u>First Order Sensitivity Average Criteria for Longitudinal Dynamics</u>

The sensitivity average of a particular mode m (phugoid or short period) to variations in one of the longitudinal stability derivatives p, over a prescribed phase of the reentry trajectory [0,T] ([0, 300] in this case):

$$S^m_{p_{av}} \triangleq \frac{1}{T}\int_0^T \left| S^m_p(t) \right| dt \tag{5.9}$$

$$\text{where} \quad S^m_p(t) \triangleq \frac{\partial y_m(t)}{\partial p} \tag{5.10}$$

First Order Sensitivity Norm Criteria for Longitudinal Dynamics

The sensitivity norm of mode m, characterizing the evolution over time of the global sensitivity of the dynamics to first order variations in vehicle stability derivatives:

$$|| S_m(t) || \triangleq \sum_p \left| S^m_p(t) \right| \tag{5.11}$$

where p are the different longitudinal stability derivatives.

5.3.2 Sensitivity to First Order Stability Derivative Variations for Longitudinal Modes

First order sensitivity of the longitudinal modes of the GHAME vehicle for variations in the seven longitudinal stability derivatives (Dv, Lv/V0, Mv, Dα, Lα/V0, Mα, Mq) over the first 300 seconds of the reentry was derived using the GMS sensitivity theory. Over that particular portion of the trajectory, the GHAME vehicle exhibits the two modes of motion that typically characterize the longitudinal dynamics of flight vehicles.

The following presents the results obtained in the first order sensitivity analysis of the longitudinal dynamics of the GHAME vehicle.

Sensitivity Averages

The sensitivity averages of the phugoid and short period modes with respect to longitudinal stability derivatives are summarized in the charts presented on page 54.

These charts show that changes in the lift velocity derivative, L_V/V_0, and speed stability derivative, M_V, have the most influence on the longitudinal modes of the GHAME vehicle. For the short period, and to a even larger extent the phugoid, variations in these two stability derivatives have effects that are several orders of magnitude larger than that of any other stability derivative.

Variations in the lift velocity derivative, L_V/V_0, are the ones that have the most effect on the phugoid mode. L_V/V_0 also significantly affects the short period. Its contribution to the short period however is offset by the influence of M_V. This is consistent with the fact that, for a conventional aircraft, the lift velocity derivative will mainly affect the phugoid mode. Furthermore the important effect of changes in this parameter are also consistent with the fact that the GHAME vehicle flies at very high Mach numbers along the reentry trajectory and that L_V/V_0 is generally very sensitive to Mach number effects.

Variations in the speed stability term, M_V, are those that have the largest effect on the short period mode. In fact the speed stability term affects both modes about equally. However its influence is predominant in the short period mode but several orders of magnitude smaller than that of L_V/V_0 in the phugoid mode. The important effect of changes in the speed stability term are consistent with the high Mach numbers at which is flown the GHAME vehicle and the typical sensitivity of this parameter to Mach number effects. The predominant influence of M_V on the short period is also consistent with the behavior of a conventional aircraft.

Variations in the drag damping, D_V, the vertical damping, L_α/V_0, the static stability, M_α, and the pitch damping, M_q, terms have only secondary effects on the longitudinal modes of

PHUGOID

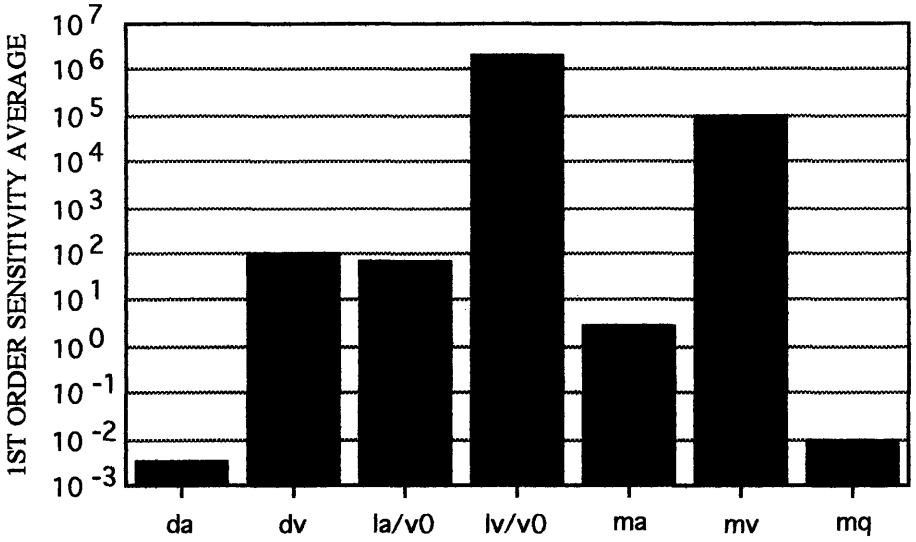

SHORT PERIOD

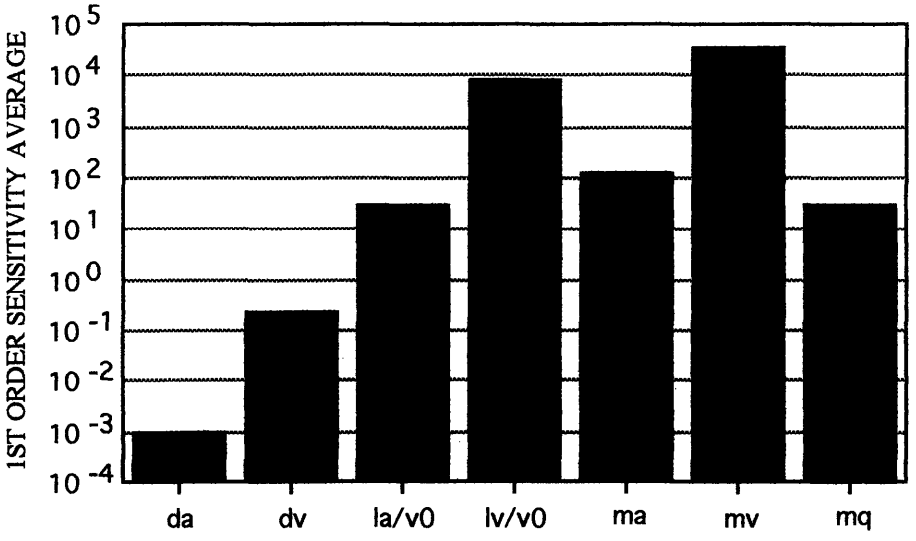

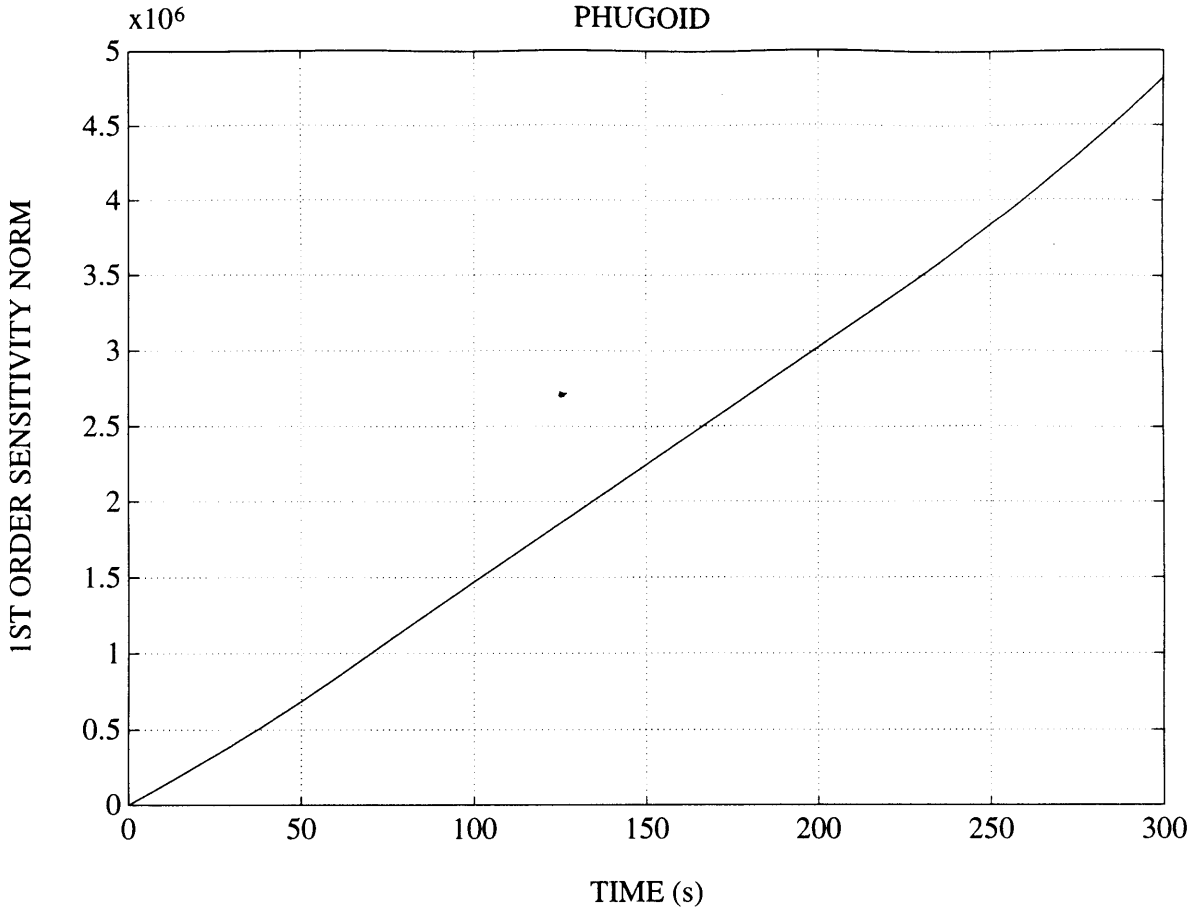
PHUGOID
x10^6
1ST ORDER SENSITIVITY NORM
TIME (s)
0
0.5
1
1.5
2
2.5
3
3.5
4
4.5
5
0
50
100
150
200
250
300

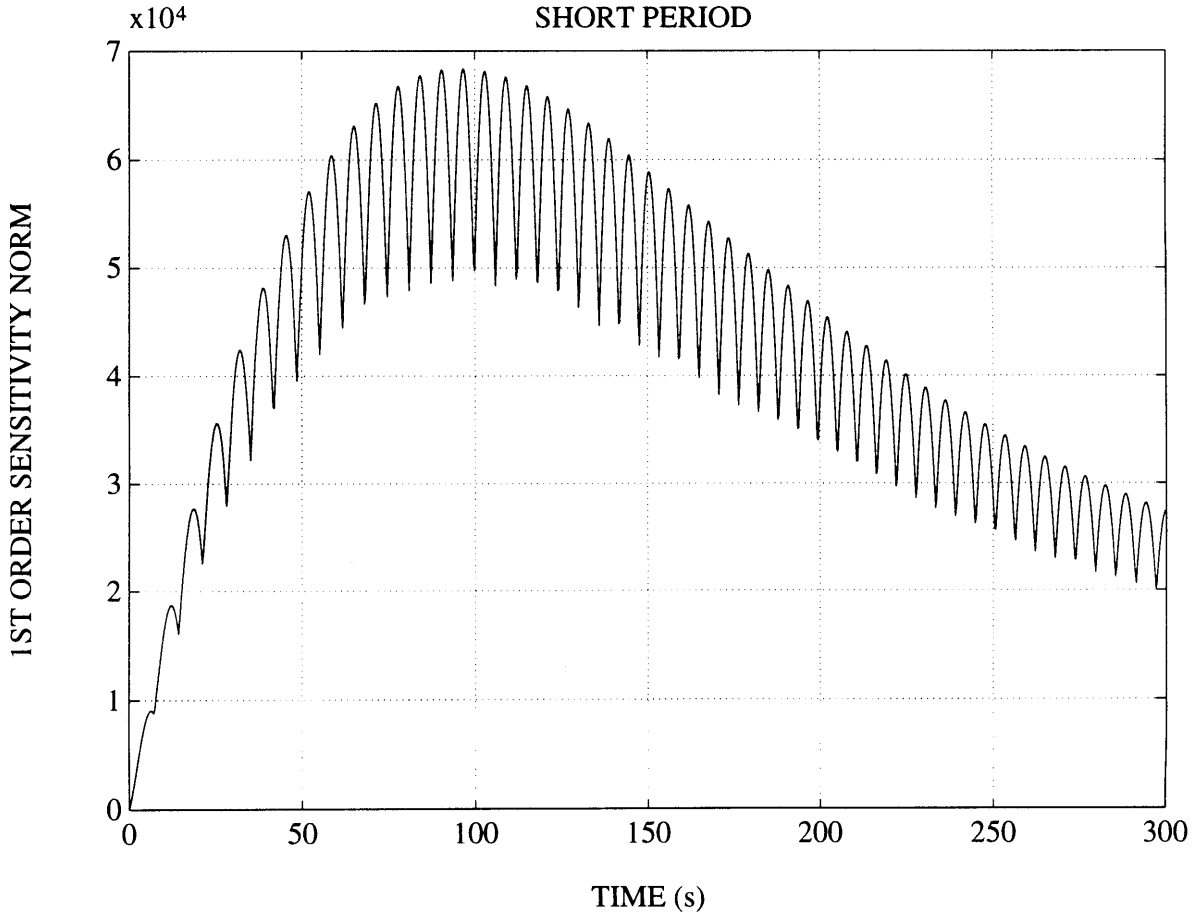
SHORT PERIOD
x10^4
1ST ORDER SENSITIVITY NORM
TIME (s)
0
1
2
3
4
5
6
7
0
50
100
150
200
250
300

the GHAME vehicle. Changes in these terms do however influence the longitudinal dynamics of the GHAME in the same way as they would a conventional aircraft: M_q and M_α mainly affect the short period mode and M_V mostly influences the phugoid mode.

As for a conventional aircraft, variations in D_α have a minor effect on the longitudinal dynamics of the GHAME vehicle during its reentry.

Sensitivity Norm

The sensitivity norm plots of the two longitudinal modes are presented on the plots page 55.

The oscillatory and stable nature of the short period translate into a bounded and oscillating sensitivity norm. The global sensitivity of the short period of the GHAME vehicle reaches a maximum at about 100 seconds into the trajectory after what it tends to decrease until the end of the observation at 300 seconds into the reentry trajectory.

On that portion of the reentry trajectory, the phugoid mode is globally more sensitive to stability derivative variations than the short period mode. The oscillatory nature of the phugoid should also translate into an oscillating sensitivity norm. However, because of the large time constant and very light damping of the phugoid in the initial phase of the reentry, these observations are not possible on a time history of only 300 seconds.

5.4 SECOND ORDER SENSITIVITY ANALYSIS

5.4.1 Introduction

As for the study of second order sensitivity of the lateral modes of the GHAME vehicle, the average sensitivity and sensitivity norm criteria will be used to analyze second order sensitivity of the longitudinal modes. These criteria are defined as:

Second Order Sensitivity Average Criteria for Longitudinal Dynamics

Second order sensitivity average of mode m (phugoid or short period) for variations in one of the longitudinal stability derivatives over [0,T]:

$$\xi^{m}_{p_{av}} \triangleq \frac{1}{T}\int_{0}^{T}\left|\xi^{m}_{p}(t)\right| dt \tag{5.14}$$

where $\xi^{m}_{p}(t)$ is the second order sensitivity of the mode m to variations of the stability derivative p:

$$\xi^{m}_{p}(t) \triangleq \frac{\partial^2 y_m(t)}{\partial p^2} \tag{5.15}$$

Second Order Sensitivity Norm Criteria for Longitudinal Dynamics

The sensitivity norm characterizes the evolution over time of a combined second order sensitivity for a particular mode m:

$$\left|\left|\xi_{m}(t)\right|\right| \triangleq \sum_{p}\left|\xi^{m}_{p}(t)\right| \tag{5.16}$$

where p are all of the stability derivatives.

5.4.2 Second Order Stability Derivative Variations for Longitudinal Modes

As for the first order, second order sensitivity of the longitudinal modes to variations in the different longitudinal stability derivatives was derived using the GMS sensitivity theory

and plotted for up to 300 seconds into the trajectory. The results of this analysis are presented in the following.

Sensitivity Averages

Sensitivity averages of the phugoid and short period to second order variations of the longitudinal stability derivatives are summarized on the plots presented on page 59.

These charts show that the longitudinal modes of the GHAME vehicle are, by far, most sensitive to second order variations in the lift derivative, L_V/V_0, and speed stability, M_V, terms. The phugoid is predominantly affected by second order variations in L_V/V_0 whereas the short period is most influenced by variations in M_V. This also illustrates the critical importance of Mach number effects on the longitudinal dynamics of the vehicle since they have a big influence on both of these stability derivatives.

For both modes, the effects of second order variations of the other longitudinal stability derivatives are several orders of magnitude smaller and can be considered of secondary importance.

These results, with the ones obtained for first order sensitivity, illustrate the important influence of variations of the lift derivative and speed stability terms during the reentry of the GHAME vehicle into the Earth's atmosphere. Large sensitivity of the dynamics to parameter variations such as the ones observed for these two parameters can create severe problems in accurately modeling the longitudinal dynamics and in designing efficient control systems for the vehicle.

Sensitivity Norm

The set of plots on page 60 present the evolution over time of the second order sensitivity norm of the phugoid and short period modes.

PHUGOID

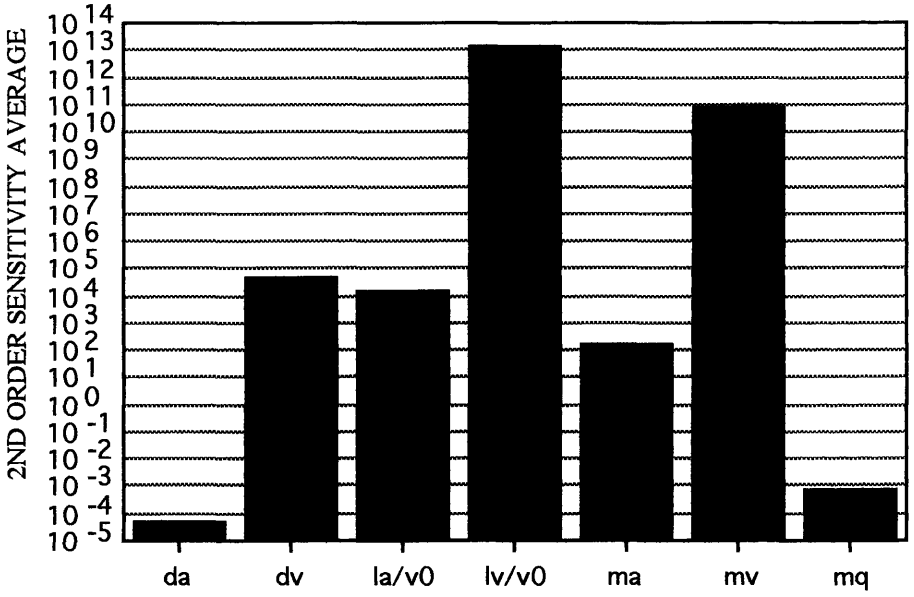

SHORT PERIOD

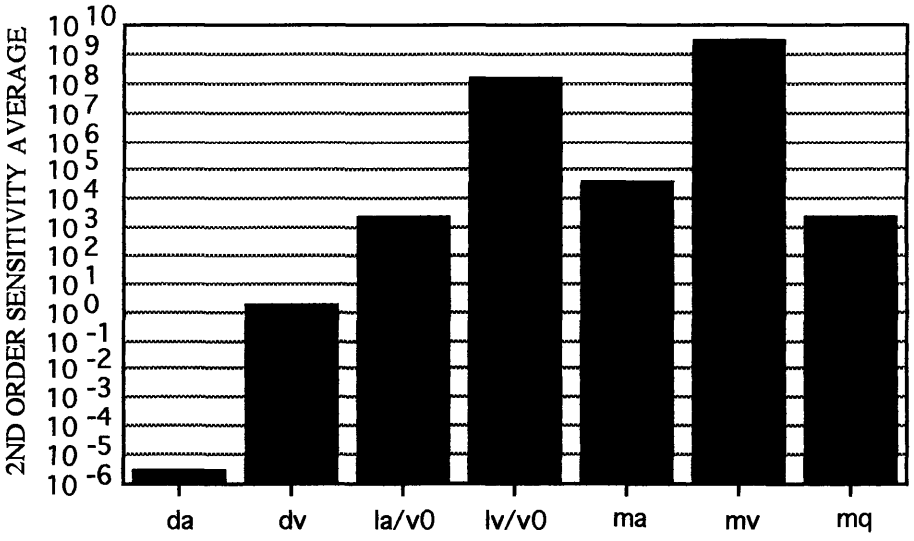

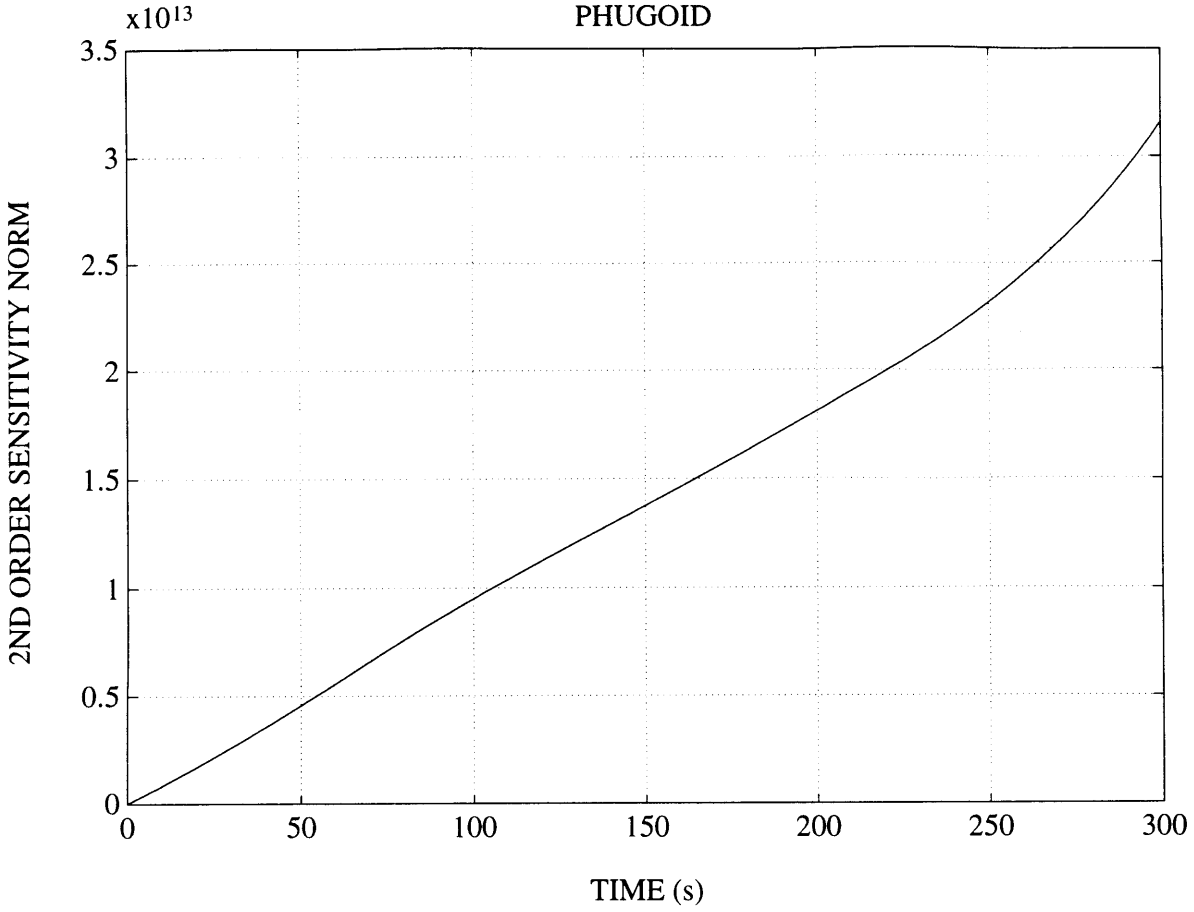
PHUGOID
x10^13
2ND ORDER SENSITIVITY NORM
TIME (s)
0
0.5
1
1.5
2
2.5
3
3.5
0
50
100
150
200
250
300

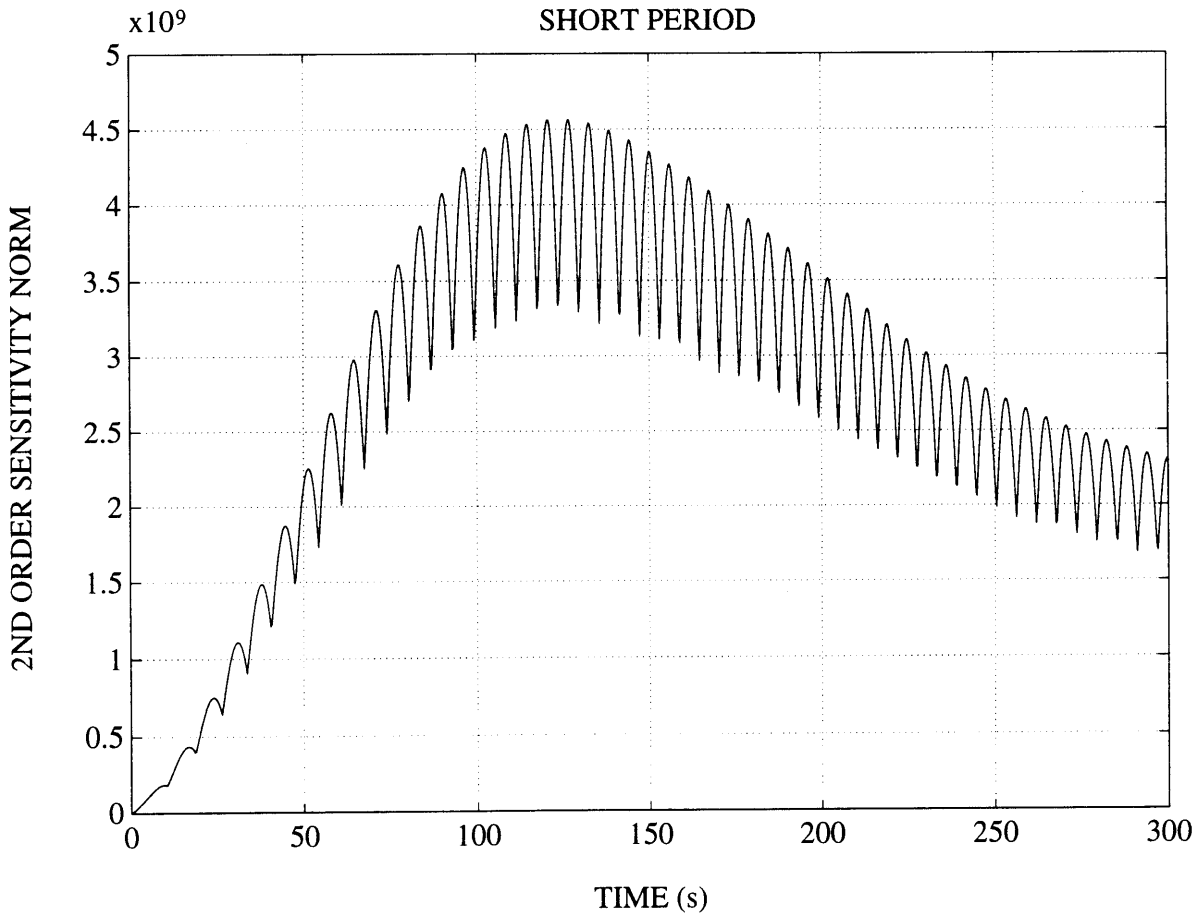
SHORT PERIOD
x10^9
2ND ORDER SENSITIVITY NORM
TIME (s)
0
0.5
1
1.5
2
2.5
3
3.5
4
4.5
5
0
50
100
150
200
250
300

Over the first 300 seconds of the reentry, the phugoid is globally far more sensitive than the short period to second order variations in the longitudinal stability derivatives.

As for first order, second order sensitivity of the phugoid grows unbounded over the first 300 seconds of the reentry whereas second order sensitivity of the short period reaches a maximum at approximately 125 seconds into the trajectory after which it decreases until the end of the observation. Therefore the phugoid mode becomes increasingly more sensitive to second order variations of the stability derivatives than the short period.

These results, in conjunction with the first order results, show that the critical phase of the trajectory for the short period corresponds to the time frame between 50 and 150 seconds into the trajectory were both first and second order sensitivity are at there peak. For the phugoid, both the first and second order sensitivity norms grow with time making that mode increasingly more sensitive to stability derivative variations as the vehicle flies along the trajectory

CHAPTER 6

Optimal Control with Sensitivity Considerations

6.1 INTRODUCTION

As mentioned in the previous chapters, large sensitivity of a system to parameter variations is usually undesirable and can create severe problems in the design of reliable control systems. In this section, a continuous time linear quadratic regulator is derived using optimal control theory to illustrate how sensitivity considerations can be included in the design of a control system in order to reduce the effects of system sensitivity.

At the end of this chapter, these principles are applied to the longitudinal dynamics of the GHAME vehicle in an attempt to reduce their naturally large sensitivity to first order variations in the lift velocity derivative L_V/V_0 along the reentry trajectory.

6.2 CLASSICAL OPTIMAL CONTROL PROBLEM

In the classical optimal control problem, we consider a linear time varying system:

$$\dot{X} = A(t)X + B(t)u \tag{6.1}$$

and an associated quadratic performance index:

$$J = \frac{1}{2} X(T)^T S(T) X(T) + \frac{1}{2} \int_0^T \left[X(t)^T Q X(t) + u(t)^T R u(t) \right] dt \qquad (6.2)$$

where S(T), Q and R are symmetric weighting matrices such that:

$$S(T) \geq 0$$

$$Q \geq 0$$

$$R > 0$$

The necessary conditions yield the following equations for the state and costate known as the two point boundary problem:

$$\begin{bmatrix} \dot{X} \\ \dot{\lambda} \end{bmatrix} = \begin{bmatrix} A & -BR^{-1}B^T \\ -Q & -A^T \end{bmatrix} \begin{bmatrix} X \\ \lambda \end{bmatrix} \qquad (6.3)$$

with

$$X(0) = X_0$$

$$\lambda(T) = S(T)\, X(T)$$

In this study, we are considering a fixed final time and free final state optimal control problem. The optimal control law can be derived using the sweep method. We assume that X(t) and $\lambda(t)$ satisfy a linear relation for all $t \in [0, T]$:

$$\lambda(t) = S(t)X(t) \qquad (6.4)$$

where S(t) is an unknown function solution of the matrix Riccati equation:

$$-\dot{S} = A^T S + SA - SBR^{-1}B^T S + Q \qquad t \leq T \tag{6.5}$$

with final condition S(T).

S(t) is derived by solving the Riccati equation backward in time. The continuous time linear quadratic regulator is then given by:

$$u(t) = -R^{-1}B^T S(t) \tag{6.6}$$

6.3 OPTIMAL CONTROL WITH SENSITIVITY CONSIDERATIONS

We define $X_p \triangleq \frac{\partial X}{\partial p}$, the sensitivity of the state vector X with respect to a parameter p. If X satisfies equation (6.1), and if the A matrix also depends on p, then X_p satisfies the differential equation:

$$\dot{X}_p = \frac{\partial \dot{X}}{\partial p} = AX_p + A_p X + Bu_p \tag{6.7}$$

where

$$A_p = \frac{\partial A}{\partial p} \tag{6.8}$$

$$u_p = \frac{\partial u}{\partial p} \tag{6.9}$$

Next, we define w such that:

$$\dot{u}_p = w \tag{6.10}$$

We then define the augmented state vector:

$$\mathbf{X} = \begin{bmatrix} \mathbf{X} \\ \mathbf{X}_p \\ \mathbf{u}_p \end{bmatrix} \tag{6.11}$$

By combining (6.1), (6.7) and (6.10) in a matrix form, we can see that the augmented vector satisfies the following first order matrix differential equation:

$$\begin{bmatrix} \dot{\mathbf{X}} \\ \dot{\mathbf{X}}_p \\ \dot{\mathbf{u}}_p \end{bmatrix} = \begin{bmatrix} \mathbf{A} & 0 & 0 \\ \mathbf{A}_p & \mathbf{A} & \mathbf{B} \\ 0 & 0 & 0 \end{bmatrix} \begin{bmatrix} \mathbf{X} \\ \mathbf{X}_p \\ \mathbf{u}_p \end{bmatrix} + \begin{bmatrix} \mathbf{B} & 0 \\ 0 & 0 \\ 0 & 1 \end{bmatrix} \begin{bmatrix} \mathbf{u} \\ \mathbf{w} \end{bmatrix} \tag{6.12}$$

$$\text{or} \quad \dot{\mathbf{X}} = \mathbf{F}\mathbf{X} + \mathbf{G}\mathbf{u} \tag{6.13}$$

From the formulation in (6.13), we can define a new optimal control problem in the classical form, having added however the possibility of placing a penalty on the sensitivity of the different states to first order variations in p.

The quadratic performance index associated with the augmented system (6.13) is:

$$\mathbf{J} = \frac{1}{2}\mathbf{X}(\mathrm{T})^{\mathrm{T}}\,\mathbf{S}(\mathrm{T})\,\mathbf{X}(\mathrm{T}) + \frac{1}{2}\int_0^{\mathrm{T}} \left[\mathbf{X}(\mathrm{t})^{\mathrm{T}}\,\mathbf{Q}\,\mathbf{X}(\mathrm{t}) + \mathbf{u}(\mathrm{t})^{\mathrm{T}}\,\mathbf{R}\,\mathbf{u}(\mathrm{t})\right] \mathrm{dt} \tag{6.14}$$

where

$$\mathbf{S}(\mathrm{T}) \geq 0$$

$$\mathbf{Q} \geq 0$$

$$\mathbf{R} > 0$$

are the new penalty matrices.

We are again considering a fixed final time problem with no constraints on the final states. The solution is therefore derived using the sweep method presented in the previous section. We first define the function S(t) for all $t \in [0, T]$:

$$\lambda(t) = \mathbf{S}(t)\mathbf{X}(t) \tag{6.15}$$

S(t) is solution of the matrix Riccati equation:

$$-\dot{\mathbf{S}} = \mathbf{F}^T\mathbf{S} + \mathbf{S}\mathbf{F} - \mathbf{S}\mathbf{G}\mathbf{R}^{-1}\mathbf{G}^T\mathbf{S} + \mathbf{Q} \tag{6.16}$$

with final condition S(T).

The optimal control law is then given by:

$$\mathbf{u}(t) = -\mathbf{R}^{-1}\mathbf{G}^T\mathbf{S}(t) \tag{6.17}$$

The expression in (6.17) can then be used to yield the closed loop dynamics of the system for the optimal control problem defined in (6.13) and (6.14). The closed loop response is dependent on the choice of the values in S(T), **Q** and **R** which are all three design parameters that need to de selected in order to solve this linear quadratic regulator problem.

6.4 APPLICATION TO THE LONGITUDINAL DYNAMICS OF THE GHAME VEHICLE

6.4.1 The Optimal Regulator Problem

As described in chapter 5, the longitudinal equations of motion of the GHAME vehicle are linearized about a nominal reentry trajectory. The state vector chosen to define the dynamics of the vehicle during the reentry phase is:

$$X = \begin{bmatrix} \Delta v \\ \Delta \alpha \\ \Delta q \\ \Delta \theta \end{bmatrix} \tag{6.18}$$

where Δv = velocity perpendicular to flight path perturbation

$\Delta \alpha$ = angle of attack perturbation

Δq = pitch rate perturbation

$\Delta \theta$ = pitch angle perturbation

We also define:

$\Delta \delta_e$ = elevator deflection around trim point

The linearized longitudinal equations of motion around the nominal trajectory are then given by:

$$\dot{X} = \begin{bmatrix} -Dv & -(D\alpha - g) & 0 & -g \\ -\frac{Lv}{V0} & -\frac{L\alpha}{V0} & 1 & 0 \\ Mv & M\alpha & Mq & 0 \\ 0 & 0 & 1 & 0 \end{bmatrix} X + \begin{bmatrix} 0 \\ 0 \\ M\delta \\ 0 \end{bmatrix} \Delta \delta e \tag{6.19}$$

where the parameters appearing in the 4 x4 matrix are the longitudinal stability derivatives defined in chapter 5 and $M\delta$ is the control effectiveness of the vehicle's elevator.

The stability derivatives appearing in the equations of motion (6.19) vary with time as a result of variations in air density and flight velocity along the trajectory. As shown in the previous chapter, the longitudinal dynamics of the GHAME vehicle can be very sensitive to these variations. This can create serious problems in controlling the vehicle during its reentry into the Earth's atmosphere.

Among the different stability derivatives, the longitudinal dynamics appeared to be most sensitive to first order variations in the lift velocity term L_V/V_0. Therefore, it would be of great interest to define a control law which reduces the sensitivity of the dynamics to variations in that specific stability derivative along the trajectory. This can be done by following the steps described in section 6.2.

The perturbed longitudinal dynamics of the GHAME vehicle in (6.19) are in the classical time varying form presented at the beginning of this chapter:

$$\dot{X} = A(t)X + B(t)u \tag{6.20}$$

Since we are interested in designing a control law that reduces the sensitivity of the states to first order variations in the lift velocity derivative L_V/V_0, we will define:

$$A_p = \frac{\partial A}{\partial (L_V / V_0)} = \begin{bmatrix} 0 & 0 & 0 & 0 \\ -1 & 0 & 0 & 0 \\ 0 & 0 & 0 & 0 \\ 0 & 0 & 0 & 0 \end{bmatrix} \tag{6.21}$$

as in (6.8).

The optimal control law incorporating sensitivity considerations is then determined by selecting values for the different weighting matrices and going through the different steps presented in section 6.3.

6.4.2 Results of the Optimal Control Problem

The following section illustrates the effectiveness of a linear quadratic regulator in reducing the GHAME vehicle's sensitivity to first order variations in L_V/V_0. As in chapter 5,

the model of the longitudinal dynamics of the aircraft, shown in (6.19), is studied over the first 300 seconds of the reentry into the Earth's atmosphere. Therefore, for this particular application, T that appears in (6.14) is defined by T = 300.

The control laws will be designed to regulate the states associated with the longitudinal dynamics of the GHAME vehicle when the system is placed at an initial position defined by:

$$X_0 = \begin{bmatrix} 150 \\ 0 \\ 0 \\ 0 \end{bmatrix} \tag{6.22}$$

Furthermore, there exists certain constraints imposed on elevator deflection. These are summarized in (6.23).

$$-30 \text{ deg} \leq \delta_e \leq 30 \text{ deg} \tag{6.23}$$

The weighting matrices that appear in (6.14) can be broken into submatrices that correspond to the penalties on the states themselves and submatrices that correspond to the penalties placed on state sensitivity.

$$S(T) = \begin{bmatrix} S(T)_1 & 0 \\ 0 & S(T)_2 \end{bmatrix} \qquad Q = \begin{bmatrix} Q_1 & 0 \\ 0 & Q_2 \end{bmatrix} \qquad R = \begin{bmatrix} R_1 & 0 \\ 0 & R_2 \end{bmatrix} \tag{6.24}$$

where the different submatrices are defined by:

$S(T)_1$ = 4 x 4 matrix representing penalties associated with the states final conditions.

$S(T)_2$ = 4 x 4 matrix representing penalties associated with states sensitivity final conditions.

Q_1 = 4 x 4 matrix representing penalties associated with the states.

Q_2 = 4 x 4 matrix representing penalties associated with states sensitivity.

R_1 = 1 x1 matrix representing penalties associated with the control u.

R_2 = 1 x 1 matrix representing penalties associated with w.

Next, the time histories of the control, the states and sensitivities of these states for different values of the weighting matrices are presented.

Case 1:

In the first case, the weighting matrices are selected such that there is no penalty imposed on state sensitivity. Therefore optimal control theory is simply used to design a continuous time linear quadratic regulator for the states without sensitivity considerations. The numerical coefficients appearing in the different matrices are defined in table (6.1).

$$Q_1 = \begin{bmatrix} 1 & & & \\ & 1 & & \\ & & 1 & \\ & & & 1 \end{bmatrix} \qquad Q_2 = \begin{bmatrix} 0 & & & \\ & 0 & & \\ & & 0 & \\ & & & 0 \end{bmatrix}$$

$$S(T)_1 = \begin{bmatrix} 1 & & & \\ & 1 & & \\ & & 1 & \\ & & & 1 \end{bmatrix} \qquad S(T)_2 = \begin{bmatrix} 0 & & & \\ & 0 & & \\ & & 0 & \\ & & & 0 \end{bmatrix}$$

$R_1 = 40$ $\qquad$ $R_2 = 1$

Table 6.1: Weighting Matrices for Quadratic Regulator Without Sensitivity Considerations

Solving the linear quadratic regulator problem with these matrices produces the control law presented in figure 6.1.

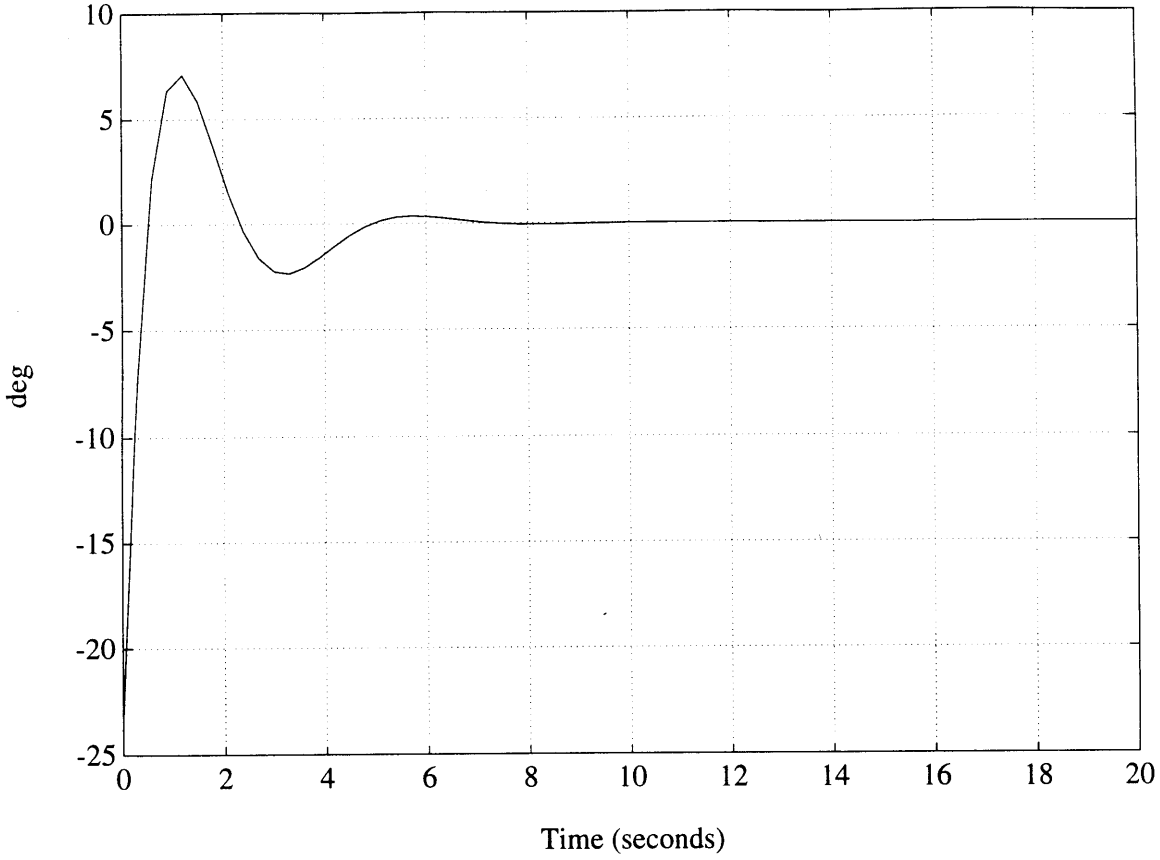

Figure 6.1: Optimal Regulator Without Sensitivity Considerations

The regulator requires large controls for the first few seconds of the response. After approximately 7 seconds, however, elevator deflection has stabilized and remains at its trim value.

The time histories of the states and state sensitivities are presented on page 72. It appears from the top four plots that the different states are driven to zero in less than 10 seconds.

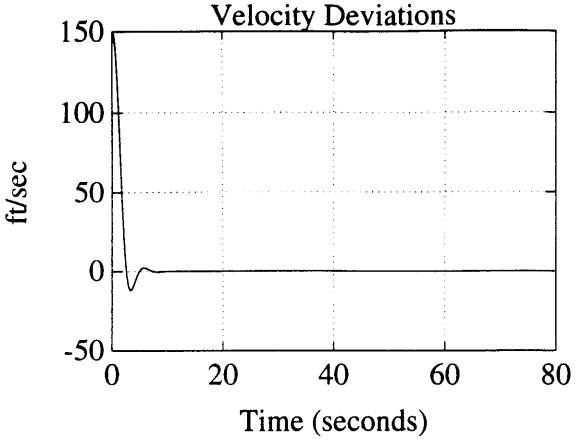
Velocity Deviations
ft/sec
150
100
50
0
-50
0
20
40
60
80
Time (seconds)

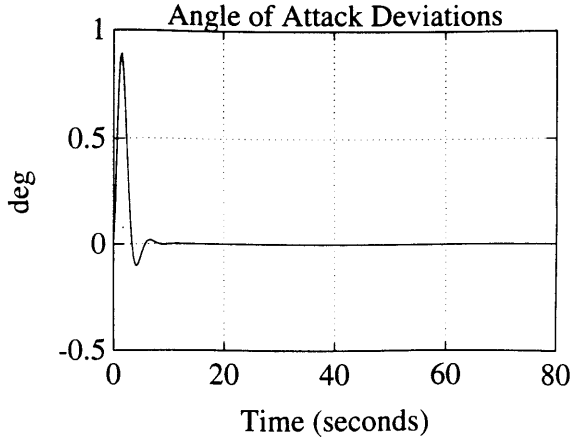
Angle of Attack Deviations
deg
1
0.5
0
-0.5
0
20
40
60
80
Time (seconds)

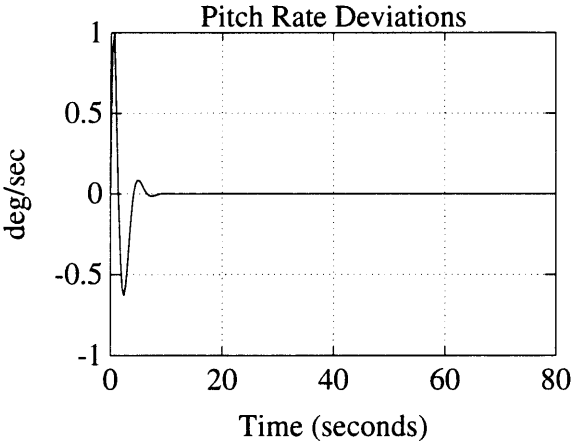
Pitch Rate Deviations
deg/sec
1
0.5
0
-0.5
-1
0
20
40
60
80
Time (seconds)

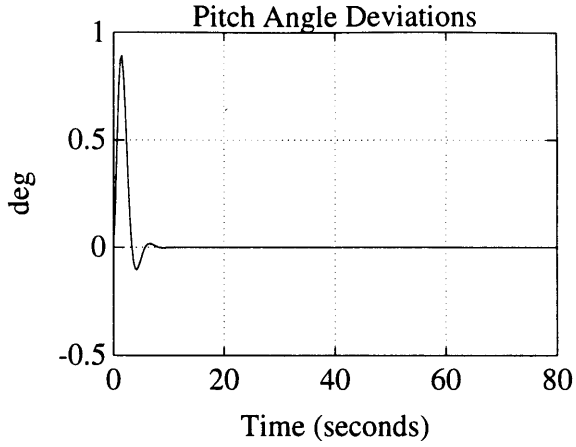
Pitch Angle Deviations
deg
1
0.5
0
-0.5
0
20
40
60
80
Time (seconds)

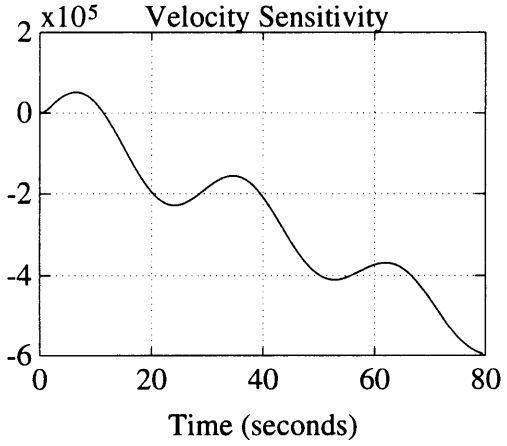
x10^5
Velocity Sensitivity
2
0
-2
-4
-6
0
20
40
60
80
Time (seconds)

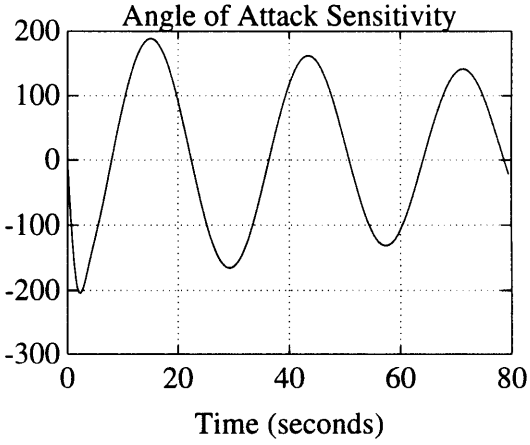
Angle of Attack Sensitivity
200
100
0
-100
-200
-300
0
20
40
60
80
Time (seconds)

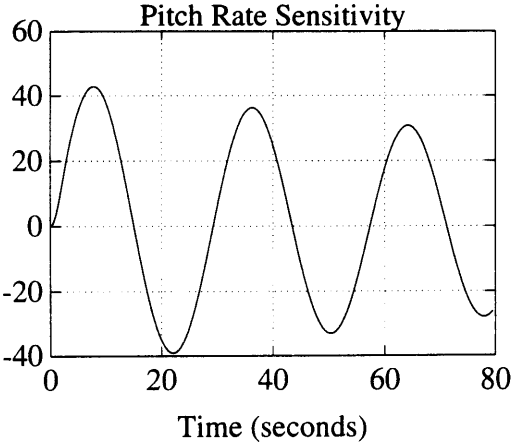
Pitch Rate Sensitivity
60
40
20
0
-20
-40
0
20
40
60
80
Time (seconds)

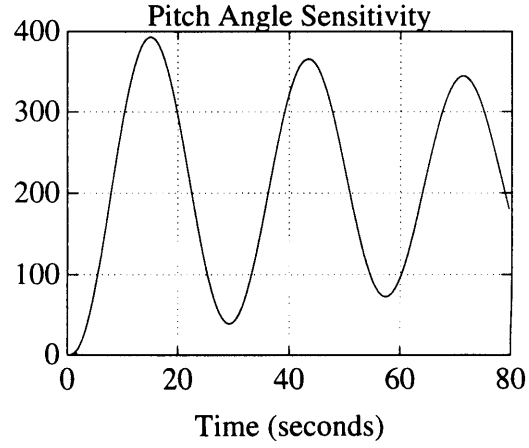
Pitch Angle Sensitivity
400
300
200
100
0
0
20
40
60
80
Time (seconds)

The bottom four plots clearly show that the different states are very sensitive to first order variations in L_V/V_0. Furthermore, the longitudinal dynamics of the GHAME vehicle tend to become more sensitive to L_V/V_0 as the vehicle travels further into the reentry trajectory.

Case 2:

In the second case, the weighting matrices are selected to incorporate slight penalties on state sensitivities. These penalties, however, are limited because of the constraint imposed on elevator deflection in (6.23). The matrices that were selected in this application are defined in table (6.2).

$$Q_1 = \begin{bmatrix} 1 & & & \\ & 1 & & \\ & & 1 & \\ & & & 1 \end{bmatrix} \qquad Q_2 = \begin{bmatrix} 10^{-5} & & & \\ & 10^{-5} & & \\ & & 10^{-5} & \\ & & & 10^{-5} \end{bmatrix}$$

$$S(T)_1 = \begin{bmatrix} 1 & & & \\ & 1 & & \\ & & 1 & \\ & & & 1 \end{bmatrix} \qquad S(T)_2 = \begin{bmatrix} 10^{-5} & & & \\ & 10^{-5} & & \\ & & 10^{-5} & \\ & & & 10^{-5} \end{bmatrix}$$

$$R_1 = 100 \qquad R_2 = 1$$

Table 6.2: Weighting Matrices for Quadratic Regulator With Sensitivity Considerations

Solving the optimal regulator problem with the matrices of table 6.2 yields the control law shown on figure 6.2.

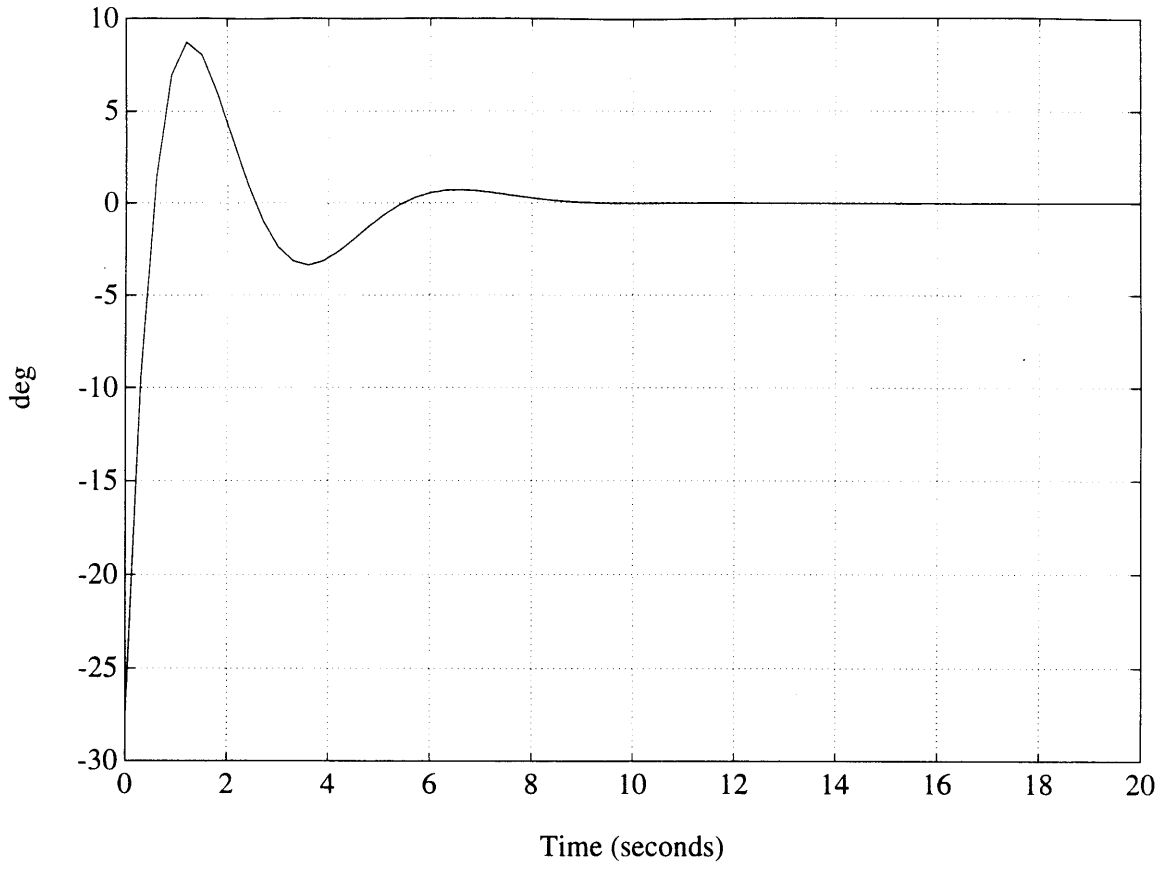

Figure 6.2: Optimal Regulator With Sensitivity Considerations

Once again, very large controls are required during the first few seconds of the time response of the system. In the second case, it takes a little longer (about 9 seconds) before the elevator stabilizes at its trim position. Over all, this regulator requires slightly larger controls than the first one.

The time histories of the states and state sensitivities are presented on page 75. It appears from the top four plots that it takes approximately 20 seconds for the different states to be driven to zero. Therefore the performance of the second regulator in driving the states to zero is not as good as that of the previous regulator.

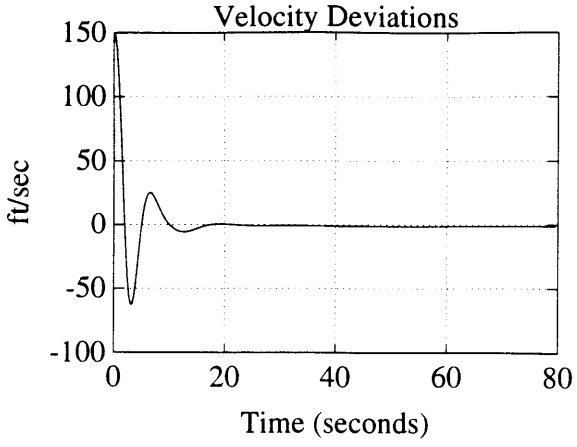
Velocity Deviations
ft/sec
150
100
50
0
-50
-100
0
20
40
60
80
Time (seconds)

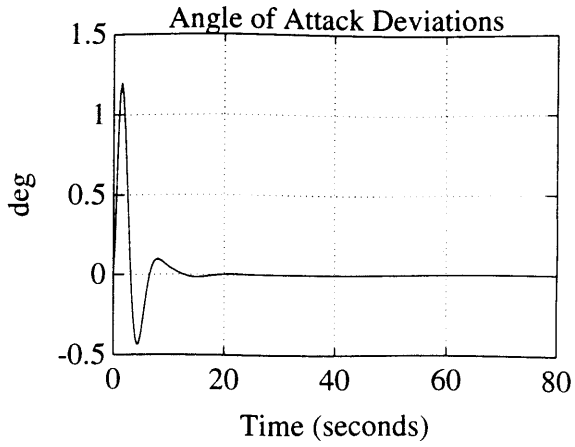
Angle of Attack Deviations
deg
1.5
1
0.5
0
-0.5
0
20
40
60
80
Time (seconds)

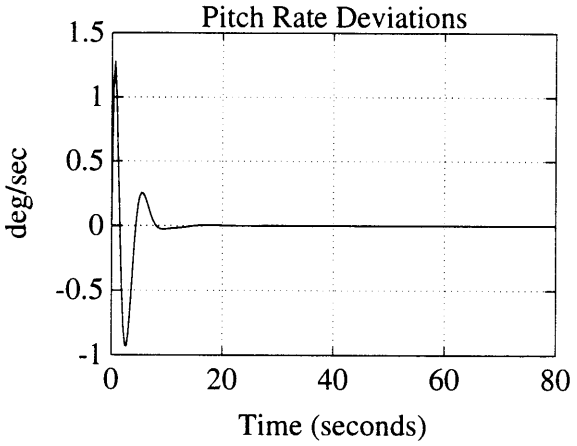
Pitch Rate Deviations
deg/sec
1.5
1
0.5
0
-0.5
-1
0
20
40
60
80
Time (seconds)

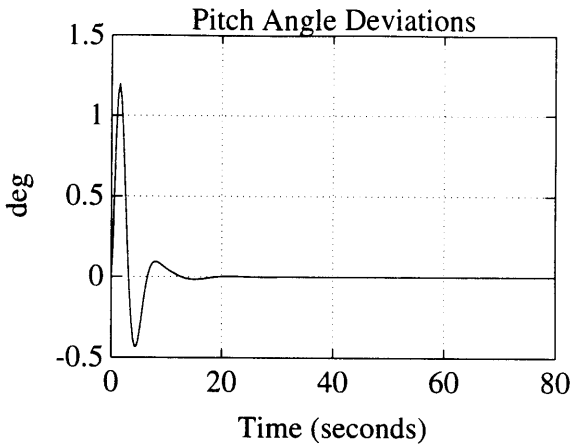
Pitch Angle Deviations
deg
1.5
1
0.5
0
-0.5
0
20
40
60
80
Time (seconds)

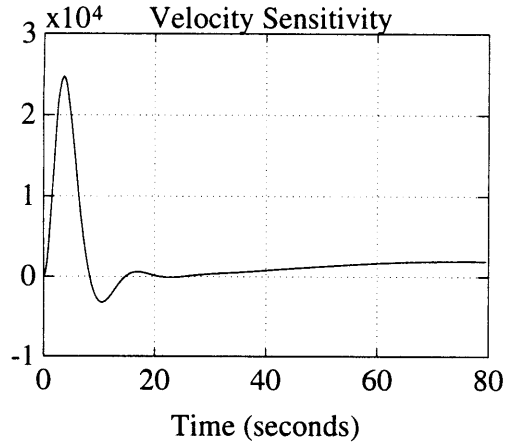
x10^4
Velocity Sensitivity
3
2
1
0
-1
0
20
40
60
80
Time (seconds)

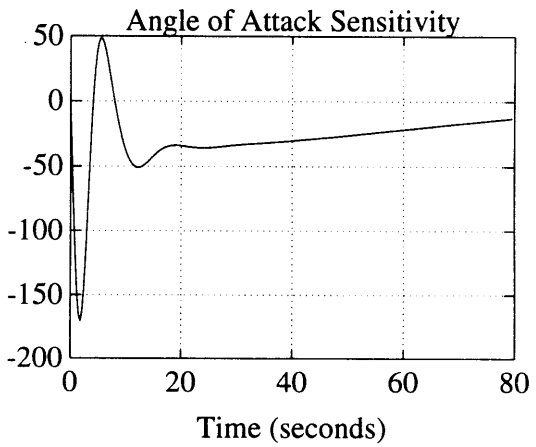
Angle of Attack Sensitivity
50
0
-50
-100
-150
-200
0
20
40
60
80
Time (seconds)

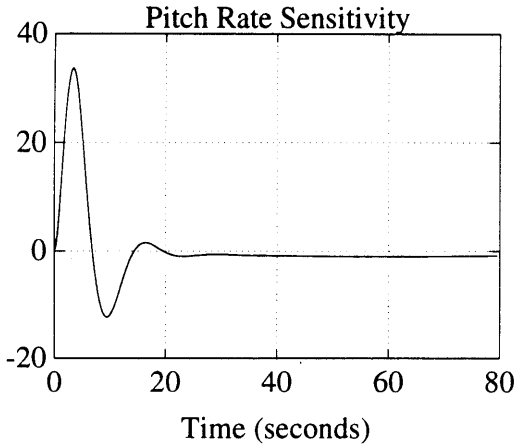
Pitch Rate Sensitivity
40
20
0
-20
0
20
40
60
80
Time (seconds)

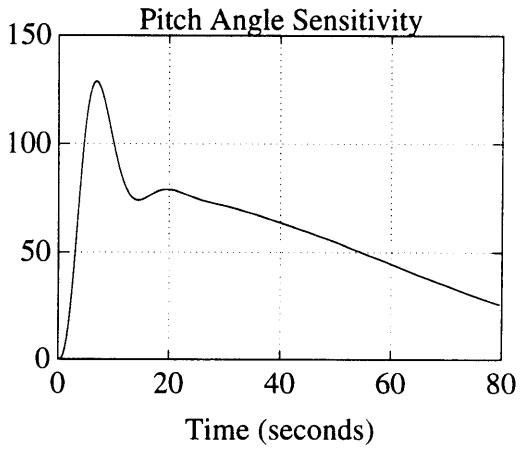
Pitch Angle Sensitivity
150
100
50
0
0
20
40
60
80
Time (seconds)

However, the bottom four plots show the significant improvements achieved in reducing the sensitivity of the different states to first order variations in L_V/V_0. Over the initial part of the trajectory, the sensitivity of the states is roughly reduced by half. As the vehicle flies further into the trajectory, sensitivities of all states decrease and approach zero.

6.4.3 Numerical Implementation of the Solutions

In going through the theoretical steps for solving this optimal control problem, there was no mention of how the different equations are solved in practice. This section describes the algorithm used throughout this study.

In the process of solving the optimal control problem, the matrix Riccati equations (6.5) or (6.16) need to be solved backward in time. Such equations are highly nonlinear differential equation for which there exists no closed form solutions. Deriving the solutions to this type of problem therefore requires the use of a computer.

The algorithm used for solving the continuous time linear quadratic problem presented in this study is the following:

1. Select values for S(T), **Q** and **R**.

2. Transform the Riccati equation (6.16) to be solved backward in time into an equation that can be solved forward in time by making the change of variables t --> (T - t).

3. Solve the new equation forward in time using a fourth order Runge-Kutta method.

4. Determine the optimal control law from (6.17).

5. Solve the system describing the closed loop dynamics of the vehicle from (6.12) for the optimal control using a fourth order Runge Kutta method.

CHAPTER 7

Study of the Dynamics of the SR-71

7.1. DESCRIPTION OF THE SR-71

The airplane is illustrated in the drawing on figure 7.1.

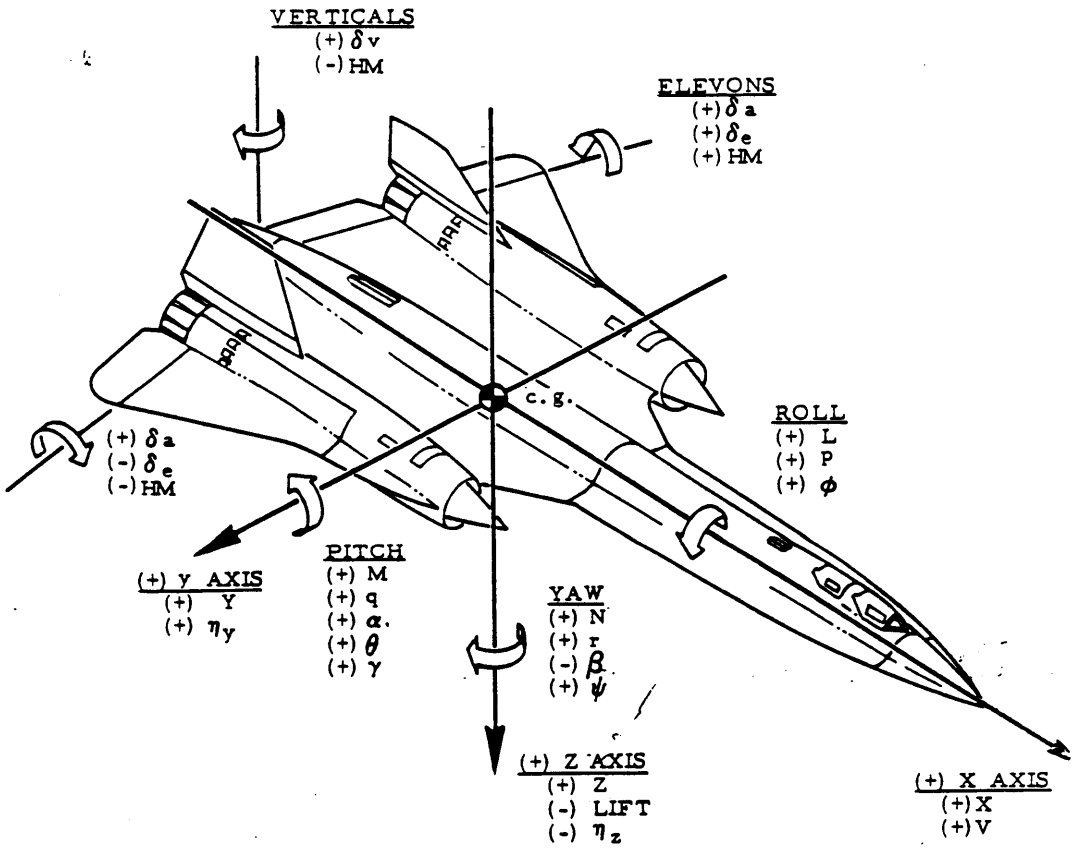

Figure 7.1: The SR-71

The basic dimensions and surface areas that appear in the longitudinal dynamics of the SR-71 are shown in table 7.1.

Weight W	80, 000 lbs.
Wing Area S	1605 ft^2.
Length l	105 ft.
MAC c	37.7 ft.
Span b	56.7 ft.
Moment of Inertia I_y	1.02 10^6 Slug.ft^2.

Table 7.1: Geometric Characteristics of the SR-71

The geometric and aerodynamic data in this study was made available through a Lockheed report on the handling qualities of the SR-71 [14]. The report includes flight simulator data, wind tunnel tests and actual flight test results.

7.2. FLIGHT TRAJECTORY

The dynamics of the SR-71 are examined as it flies along a prescribed trajectory. The trajectory is chosen to analyze the behavior of the aircraft when flight conditions are varying with time.

In this study, the SR-71 is flying from an altitude of 90,000 feet to an altitude of 10,000 feet along a straight line. Along the flight path, the speed of the vehicle decreases linearly

from Mach 3.5 to Mach 0.6. Due to the variations in air density and flight speed, the coefficients of the equations describing the dynamics of the aircraft vary along the trajectory. As for the GHAME vehicle, the dynamics of the aircraft can only be accurately modeled by a linear time varying (LTV) system.

A sketch of the trajectory is presented in figure 7.2.

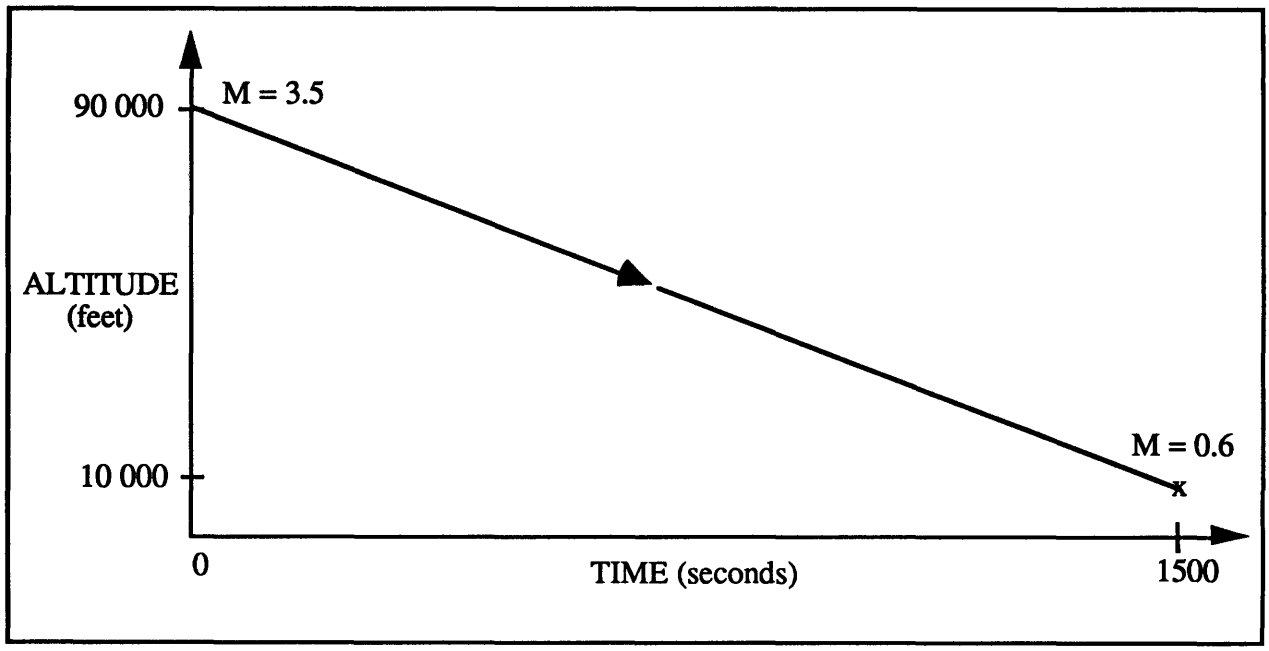

Figure 7.2: SR-71 Flight Trajectory

The Mach number and altitude of the aircraft decrease linearly along the trajectory as:

$$M(t) = -1.933\,10^{-3}t + 3.5 \qquad \text{(in seconds)} \qquad (7.1)$$

$$H(t) = -5.333\,10^{1}t + 90000 \qquad \text{(in feet)} \qquad (7.2)$$

7.3 LONGITUDINAL DYNAMICS OF THE SR-71

7.3.1 Equations of Motion

The longitudinal dynamics of the SR-71 are approximated by the typical linearized longitudinal equations of motion of an aircraft [2].

The longitudinal equations of motion are linearized about the nominal trajectory presented in section 7.2. The state vector chosen to define the dynamics of the vehicle is:

$$X = \begin{bmatrix} \Delta v \\ \Delta \alpha \\ \Delta q \\ \Delta \theta \end{bmatrix} \tag{7.3}$$

where Δv = velocity perpendicular to flight path perturbation

$\Delta \alpha$ = angle of attack perturbation

Δq = pitch rate perturbation

$\Delta \theta$ = pitch angle perturbation

The linearized longitudinal equations of motion around the nominal trajectory are then given by:

$$\dot{X} = \begin{bmatrix} -D_v & -(D_\alpha - g) & 0 & -g \\ -\frac{L_v}{V_0} & -\frac{L_\alpha}{V_0} & 1 & 0 \\ M_v & M_\alpha & M_q & 0 \\ 0 & 0 & 1 & 0 \end{bmatrix} X + \begin{bmatrix} 0 \\ 0 \\ M_\delta \\ 0 \end{bmatrix} \delta_e \tag{7.4}$$

or

$$\dot{X} = AX + Bu \tag{7.5}$$

7.3.2 Longitudinal Stability Derivatives

The stability derivatives that appear in the equations of motion of the aircraft are defined in table 7.2:

$$D_v = \frac{\rho SV}{m}\left[C_D + \frac{M}{2}\frac{\partial C_D}{\partial M}\right] \qquad \frac{L_v}{V_0} = \frac{\rho SV}{m}\left[C_L + \frac{M}{2}\frac{\partial C_L}{\partial M}\right]$$

$$M_v = \frac{\rho SVc}{I_y}\left[C_M + \frac{M}{2}\frac{\partial C_M}{\partial M}\right] \qquad D_\alpha = \frac{\rho SV}{2m}C_{D_\alpha}$$

$$\frac{L_\alpha}{V_0} = \frac{\rho SV}{2m}C_{L_\alpha} \qquad M_\alpha = \frac{\rho SV^2c}{2I_y}C_{M_\alpha}$$

$$M_q = \frac{\rho SVc^2}{4I_y}C_{M_q}$$

Table 7.2: Longitudinal Stability Derivatives

The longitudinal stability derivatives of the SR-71 are approximated by substituting vehicle aerodynamic and geometric data into the equations of table 7.2. The stability derivatives that appear in the equations of motion will vary with time as a result of variations in air density, ρ, and flight velocity, V, along the trajectory. The plots on page 82 present the time histories of the Mach number and stability derivatives when the vehicle flies from high supersonic to subsonic speeds along the prescribed trajectory.

The angle of attack stability parameter, M_α, is an important parameter which determines the static stability of the vehicle. This parameter is negative in the supersonic and transonic region, therefore the aircraft will be statically stable in those regions. At very high

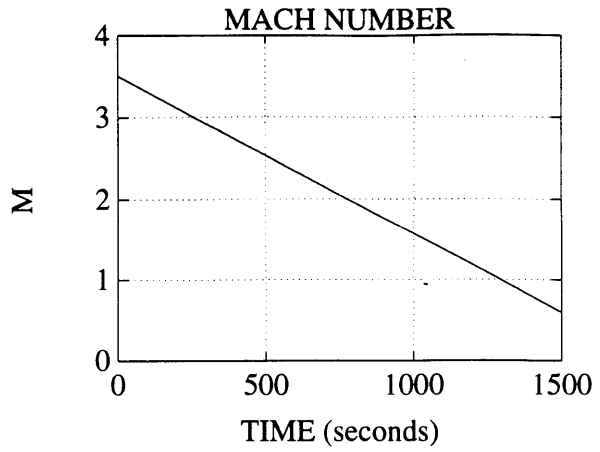
MACH NUMBER
M
TIME (seconds)

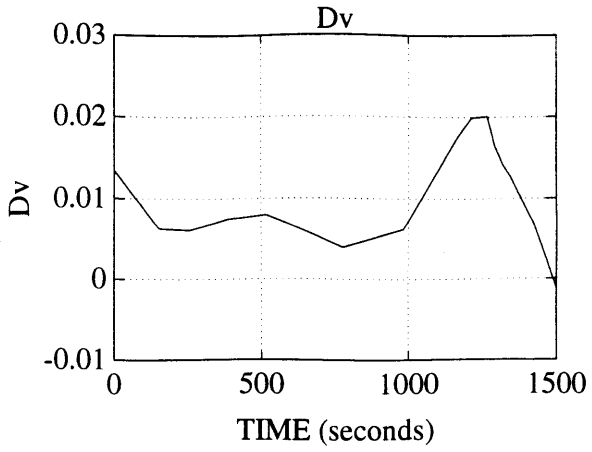
Dv
Dv
TIME (seconds)

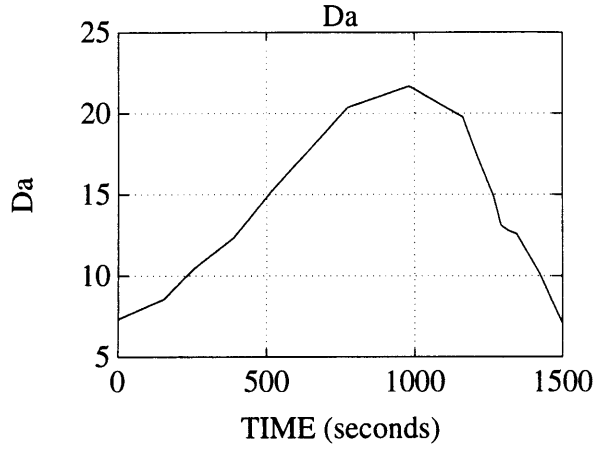
Da
Da
TIME (seconds)

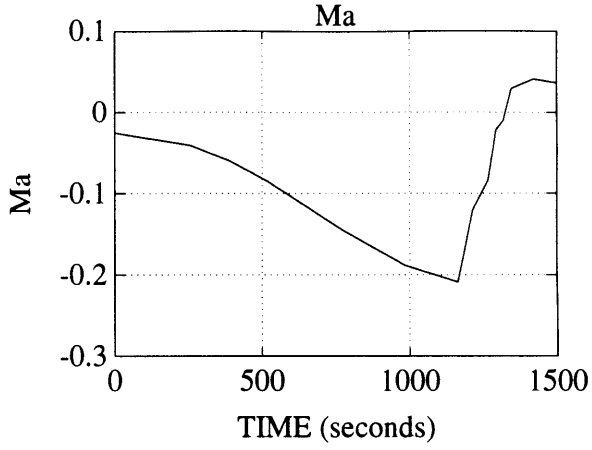
Ma
Ma
TIME (seconds)

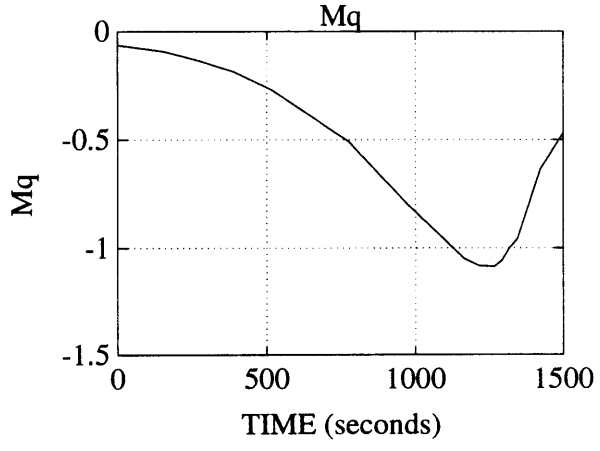
Mq
Mq
TIME (seconds)

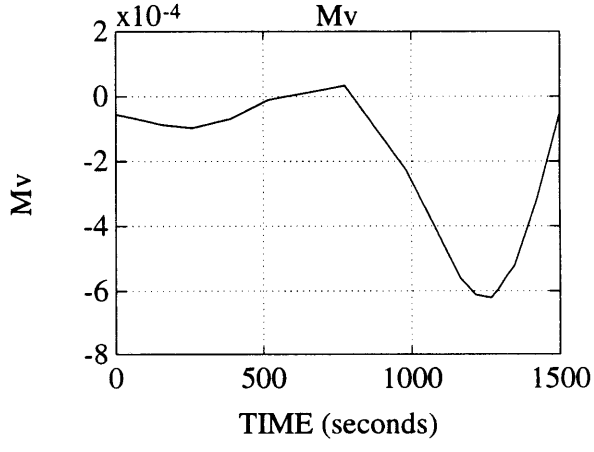
x10-4
Mv
Mv
TIME (seconds)

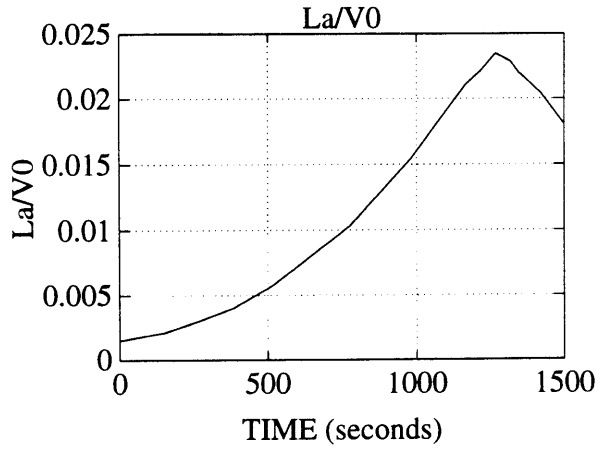
La/V0
La/V0
TIME (seconds)

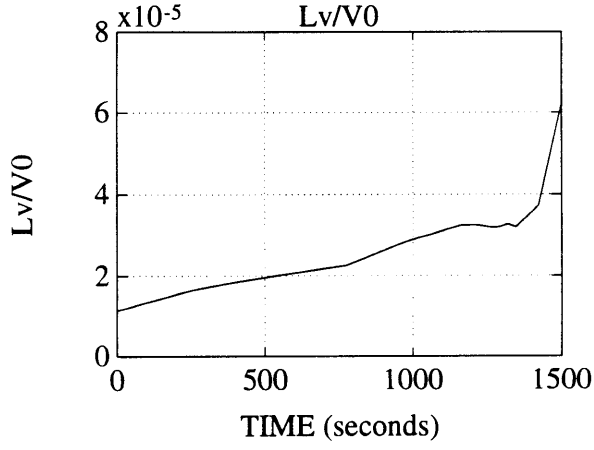
x10-5
Lv/V0
Lv/V0
TIME (seconds)

Mach numbers, however, the airplane only has a low level of positive static stability. In the subsonic region, M_α becomes positive. These result are consistent with the characteristics of the SR-71 described in the report [14] which states that the SR-71 does not possess static stability with respect to angle of attack at subsonic Mach numbers and only low static stability at Mach 3.2. This requires an artificial stability augmentation system to be incorporated in the automatic flight control system of the SR-71 to improve the dynamic response in all flight conditions.

The speed stability derivative, M_V, is another important parameter with regards to the dynamics. If M_V is positive, it has a dynamically destabilizing effect on the aircraft while if it is negative, it has a tendency to statically de stabilize the vehicle. Therefore it is usually desirable to maintain M_V as close to zero as possible. For the SR-71, the speed stability derivative is extremely small in the subsonic and supersonic regions. As the aircraft flies at transonic speeds, however, M_V reaches a significantly smaller negative value.

The third important stability derivative in longitudinal dynamics is the pitch damping parameter, M_q, because it contributes a large portion of the damping of the short period for conventional aircraft. The combination of the simplified model chosen to describe the dynamics of the aircraft with aerodynamic data from multiple sources, required the need for a correcting factor (which was chosen to be 57) on M_q to improve the damping of the short period. This factor is introduced to compensate for other sources of short period damping that might have been neglected in the simplified model of the longitudinal dynamics and enables this model to produce results that are compatible with the flight test results that are presented in the handling qualities report [14]. The plot of the variation of M_q along the trajectory show that the pitch damping is small at high Mach number and reaches a maximum in the transonic region.

The other plots on page 82 show the variations of the remaining stability derivatives along the trajectory which usually have secondary effects on longitudinal dynamics. It is

interesting to notice, however, that in the transonic region, where aircraft dynamics are always unclear, several coefficients reach an extremum. This could lead to an unusual behavior of the aircraft in that region.

7.4 LONGITUDINAL STABILITY OF THE SR-71

7.4.1 Root Locus

The speed and path of the eigenvalues of the A matrix defined in (7.5) determine the nature of the modes of the system. The next two figures present the evolution of the characteristic roots along the trajectory . Figure 7.3 presents the scaled root locus whereas figure 7.4 is a simplified and blown up sketch which gives a better understanding of how the roots are moving in the complex plane.

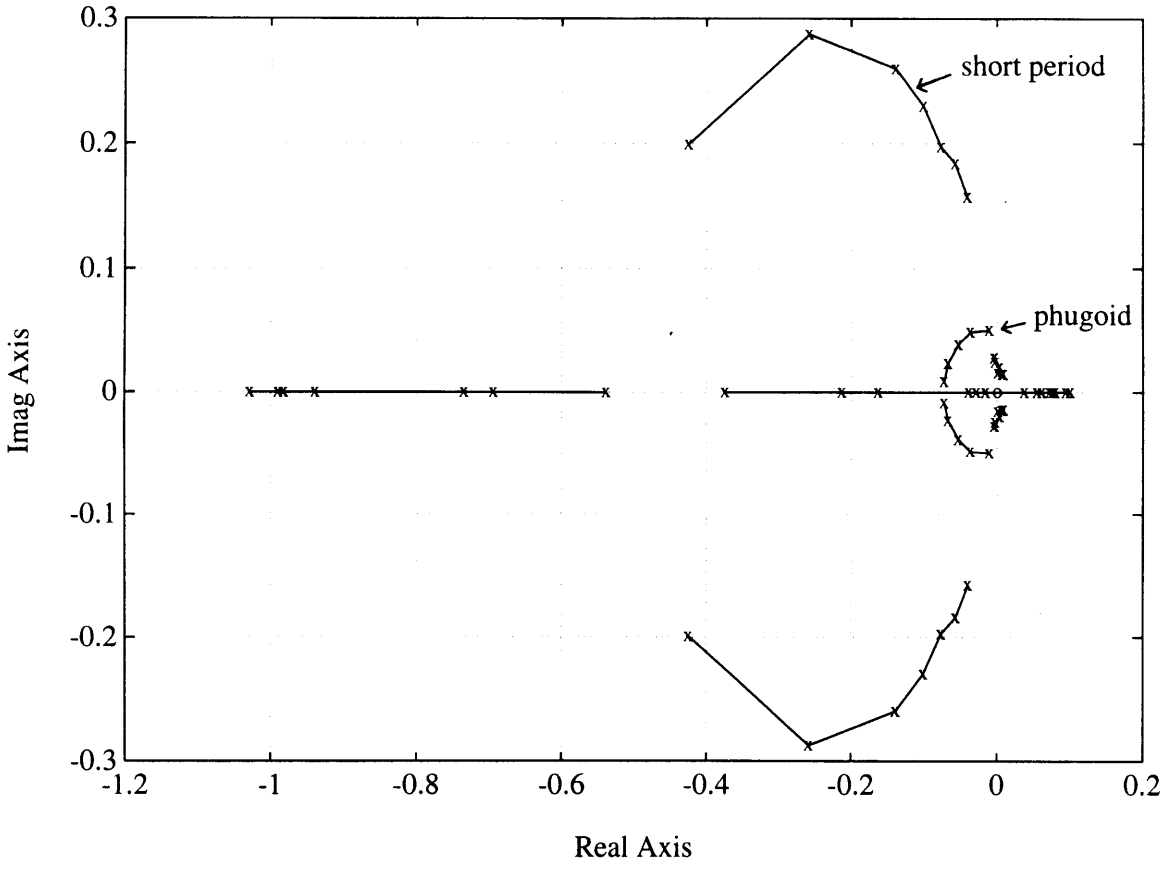

Figure 7.3: Scaled Root Locus

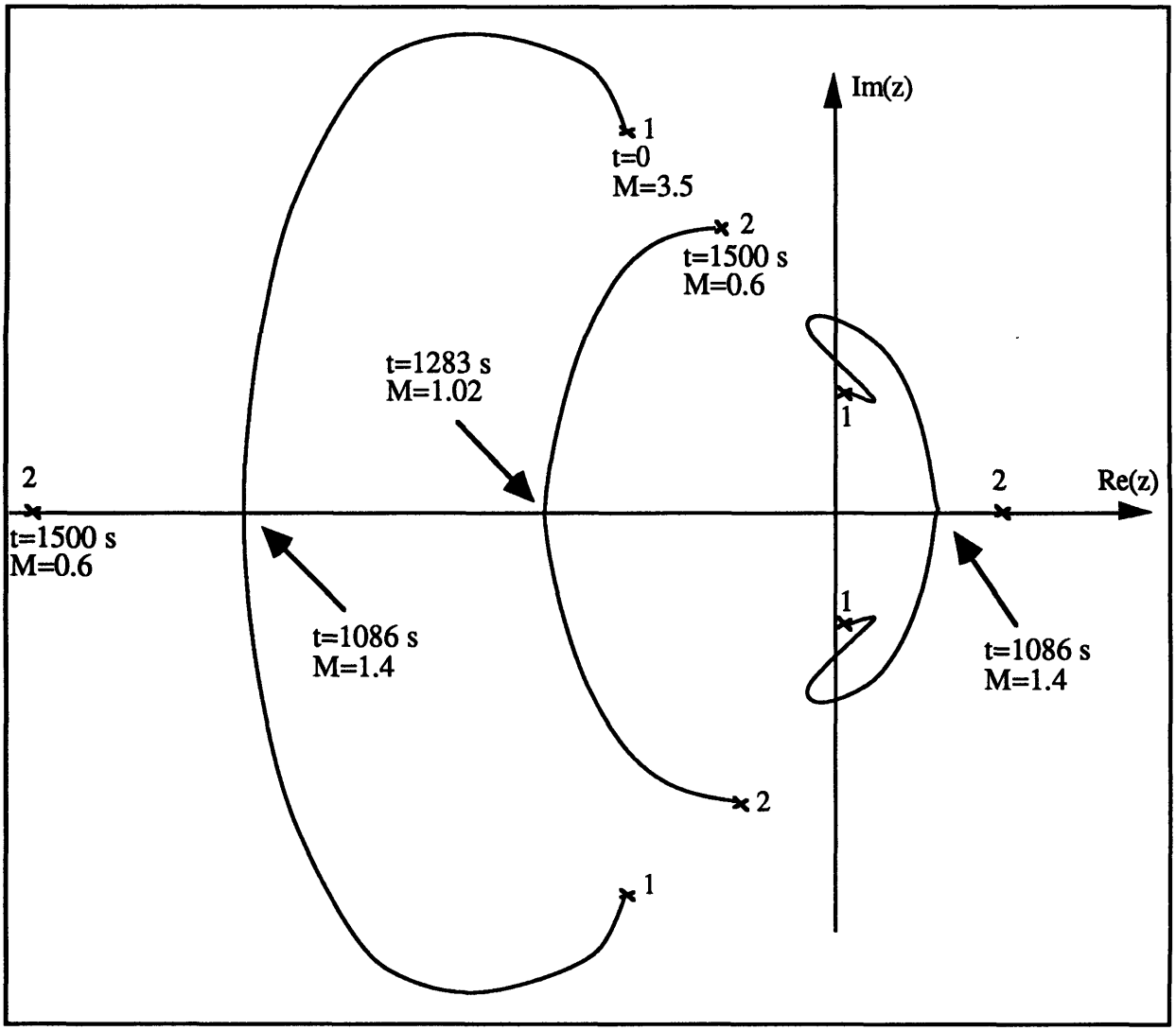

Figure 7.4: Simplified Root Locus

For supersonic speeds, the SR-71 exhibits the two modes, each defined by a pair of complex conjugate roots, of a conventional aircraft:

- A slow and poorly damped mode representing the phugoid.

- A fast and well damped mode representing the short period.

In the supersonic region, the roots of the short period mode remain in the left half plane. The roots of the phugoid, on the other hand, go back and forth about the real axis. The

period of the phugoid mode is so large at those speeds, however, that the pilot can easily compensate for slight instabilities should they occur.

In the transonic region, the dynamics of the aircraft do not exhibit a conventional behavior. The characteristic equation has four real roots, one of which has a positive real parts.

In the subsonic region, the phugoid mode is well defined by a pair of complex conjugate roots that remain in the left half plane, defining a slow and lightly damped mode. The short period mode exists but as two real roots, one of which is in the left half plane while the other is in the right half plane. If the aircraft were to fly in this configuration at constant flight conditions, it would have unacceptable handling qualities. That is why an artificial augmentation system was incorporated to the automatic flight control system.

7.4.2 Stability

Since the system describing the longitudinal dynamics of the SR-71 is a linear time varying system, the stability of the system cannot be simply predicted by examining the location of the characteristic roots as for time invariant systems. In fact, the stability of variable systems is, in general, very difficult to predict.

One simple approach to getting a good indication of the stability of the second order dynamics of the system was developed by Ramnath using the Generalized Multiple Scales method. This approach is used in this section to predict the longitudinal stability of the SR-71 as it flies along the trajectory.

The GMS criterion developed by Ramnath for longitudinal stability of aircraft flying through variable flight conditions is defined by:

$$P = C_{L_\alpha} - C_{D_T} - \sigma C_{m_\alpha} \tag{7.6}$$

where C_{D_T} = Trim Drag.

$$\sigma = \frac{Wl^2}{I_y}$$

If the stability parameter P is greater than zero, the vehicle's second order longitudinal dynamics are stable. If P is negative, the aircraft is longitudinally unstable.

Figure 7.5 shows the evolution over time of the stability parameter P along the trajectory when the SR-71 data is substituted into (7.6).

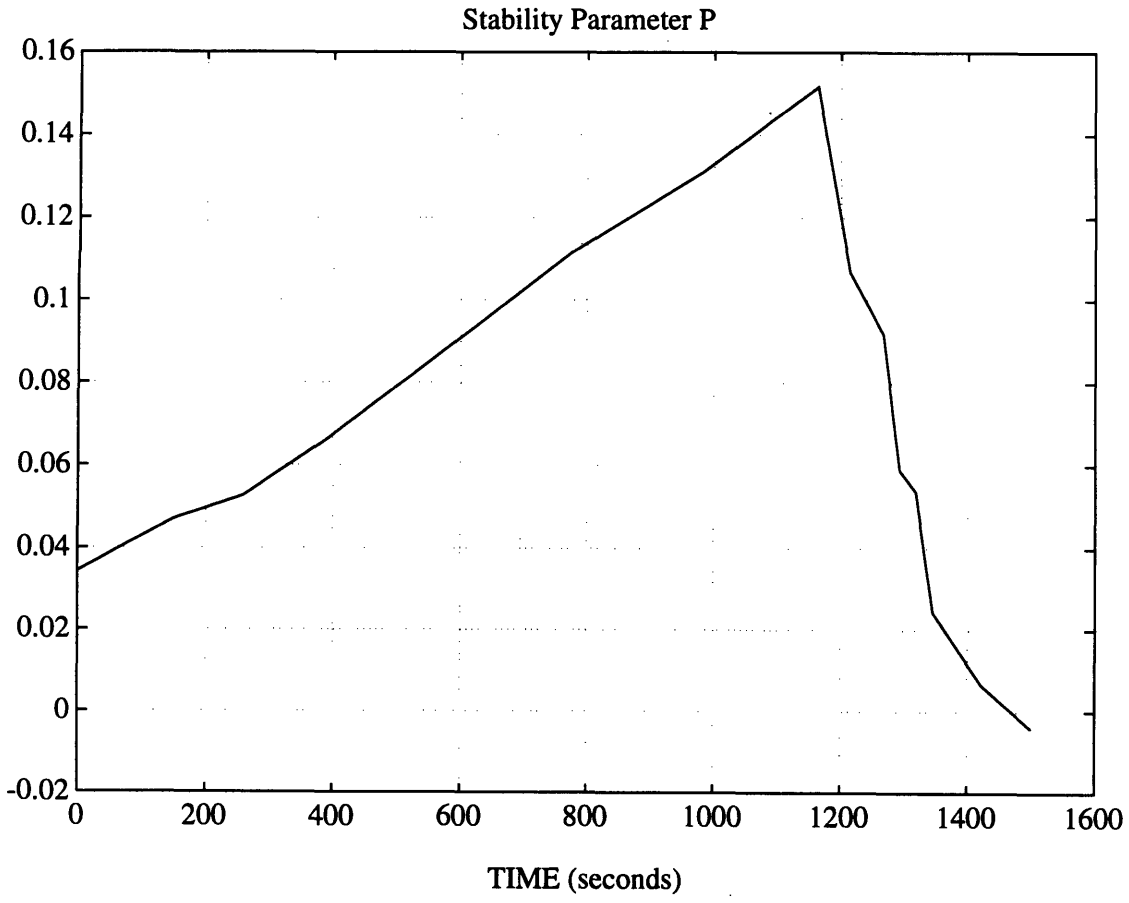

Figure 7.5: Stability Parameter Along the Trajectory

It can be seen from figure 7.5 that the stability parameter is closest to zero at the beginning of the trajectory, when the aircraft is flying at high supersonic speeds, and at the end of the trajectory, when the aircraft is in the transonic and subsonic region. In fact, the parameter becomes negative at about 1460 seconds into the trajectory which means that the second order longitudinal dynamics of the SR-71 are unstable after that point. P grows from the initial point until around 1150 seconds into the trajectory where it reaches its maximum. At that point, the aircraft is flying at low supersonic speeds. From there, the aircraft enters the transonic region and the stability of the aircraft decreases dramatically and becomes unstable. These results, although approximate, are consistent with the actual flight test results of the aircraft that showed that the longitudinal dynamics of the SR-71 are unstable at transonic and subsonic speeds and only lightly stable at high supersonic speeds.

CHAPTER 8

Handling Qualities Through Variable Flight Conditions

8.1 INTRODUCTION

To date, aircraft handling qualities are based on analysis of the dynamic equations of motion at constant flight conditions and parameters used to define the acceptable handling qualities (natural frequency, damping, bandwidth etc.) are derived through classical methods of linear constant coefficient differential equations. These handling quality specifications may or may not suffice for vehicles with very large flight envelopes such as the NASP or the SR-71. It is therefore worthwhile pursuing an analytical treatment of the variable dynamics of the aircraft and to specify handling qualities in terms of variable system response.

It has been recognized for the past few decades that the ability of a pilot to perform precise flight path tasks is a function of the inherent short period dynamic characteristics (ω_{sp} and ζ_{sp}) of the aircraft. Numerous flight and simulator investigations have, therefore, been conducted to determine the short period dynamic characteristics which identify iso-opinion lines of desirable, acceptable and unacceptable longitudinal handling qualities. This study discusses a possible extension of one of these handling quality criterion which would incorporate the time varying nature of the dynamics of high speed aircraft.

8.2 HANDLING QUALITIES

8.2.1 Description of the Levels of Handling Qualities

Flying qualities may be defined as those qualities that govern the ease and precision with which the pilot-vehicle system performs the requirements of the mission. The military Specification levels of flying qualities are defined as follows:

LEVEL 1: Clearly adequate for mission phase.

LEVEL 2: Adequate to accomplish flight phase, but some increase in pilot workload or degraded mission effectiveness exists.

LEVEL 3: Aircraft can be controlled safely, but pilot workload is excessive or mission effectiveness is inadequate.

These levels can be related to the well known Cooper - Harper pilot rating scale as shown in table 8.1.

LEVEL	PILOT RATING
1	Satisfactory 1 - 3.5
2	Unsatisfactory 3.5 - 6.5
3	Unacceptable 6.5 - 9+

Table 8.1: Military Specification Definition of Levels of Handling Qualities

8.2.2 Handling Quality Criteria for Steady State Flight Conditions

The general form of the second order differential equation describing the dynamics of the short period mode of an aircraft in steady state flight conditions is:

$$\ddot{y} + 2\zeta_{sp}\omega_{sp}\dot{y} + \omega_{sp}^{2} y = 0 \tag{8.1}$$

Since the coefficients are time invariant, the behavior of the system can easily be predicted by the location of the two roots of the characteristic equation:

$$s^{2} + 2\zeta_{sp}\omega_{sp} s + \omega_{sp}^{2} = 0 \tag{8.2}$$

The general form of the time response can be written as:

$$y(t) = Ae^{-\zeta_{sp}\omega_{sp}(t-t_0)} \sin\left[\left(\omega_{sp}\sqrt{1-\zeta_{sp}^{2}}\right)(t-t_0)+\phi\right] \tag{8.3}$$

From (8.3) , it appears that the time response of a second order linear time invariant (LTI) system is characterized by the two terms $\zeta_{sp}\omega_{sp}$ and $\omega_{sp}\sqrt{1-\zeta_{sp}^{2}}$. It is therefore justified to assume that the handling qualities of the aircraft can be related to these two quantities.

For the purpose of this study, we will suppose that the different levels of handling qualities can be related to the two quantities defined previously, which together characterize the dynamic response of the short period, in a very simple way. The simplified criterion is described in table 8.2.

LEVEL 1:	$A_{1_{min}} \leq \zeta_{sp}\omega_{sp} \leq A_{1_{max}}$	and	$B_{1_{min}} \leq \omega_{sp}\sqrt{1-\zeta_{sp}^2} \leq B_{1_{max}}$
LEVEL 2:	$A_{2_{min}} \leq \zeta_{sp}\omega_{sp} \leq A_{2_{max}}$	and	$B_{2_{min}} \leq \omega_{sp}\sqrt{1-\zeta_{sp}^2} \leq B_{2_{max}}$
LEVEL 3:	Any other situation		

Table 8.2: Steady State Simplified Handling Quality Criterion

The different bounds ($A_{1_{min}}$, A_{1max}, etc.) are constant coefficients that need to be determined.

This constitutes quite a large assumption compared to regions of handling qualities that have been defined through simulations or flight tests. Although the levels of handling qualities have, in the past, been related to these quantities, these boundaries have usually not been as simple or clearly defined. However, since the goal of this study is to define possible extensions of handling quality criteria to time varying systems, these simplifying assumptions should not invalidate the present approach.

Figure 8.1 graphically summarizes the regions of level 1 and level 2 handling qualities defined in table 8.2.

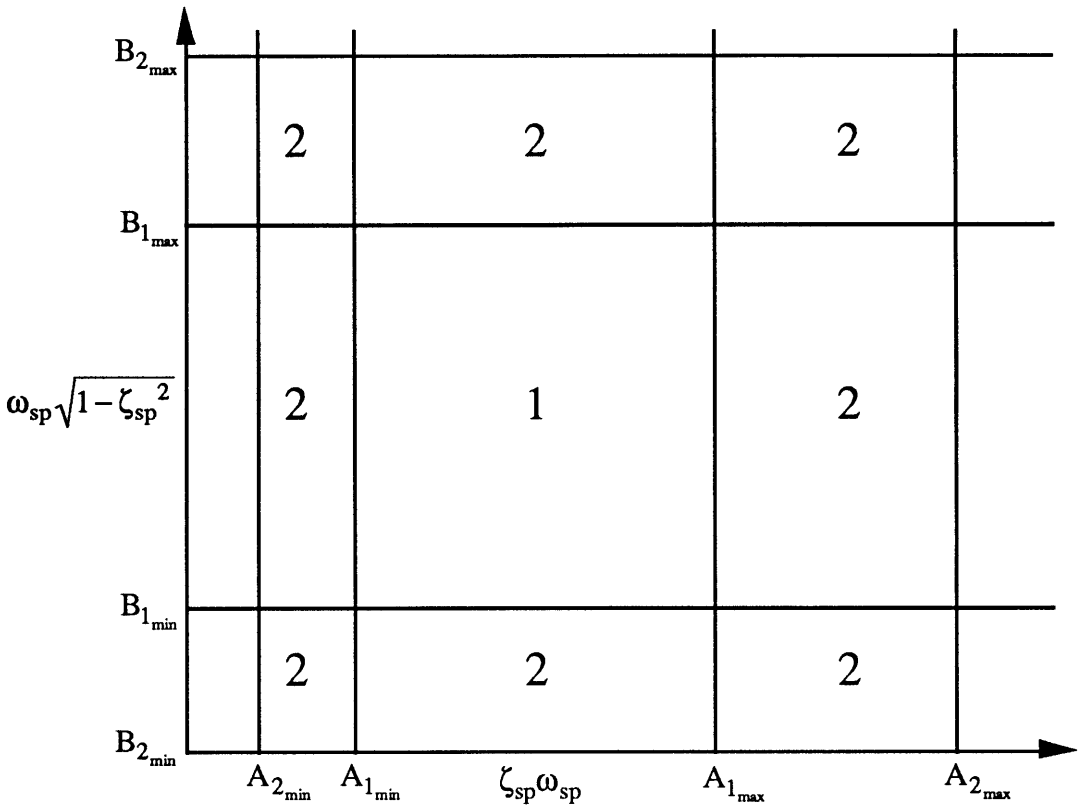

Figure 8.1: Levels of Handling Qualities

8.2.3 Handling Qualities for Aircraft Flying Through Variable Flight Conditions

The general form of the second order time varying differential equation describing the dynamics of the short period mode of an aircraft flying through variable flight conditions is:

$$\ddot{y} + 2\zeta_{sp}(t)\omega_{sp}(t)\dot{y} + \omega_{sp}(t)^2 y = 0 \qquad (8.4)$$

Since $\zeta_{sp}(t)$ and $\omega_{sp}(t)$ vary with time, the characteristic roots do not remain stationary and there path and speed in the complex plane will determine the nature of the

response of the system. Conversely to the LTI case, however, simply determining the location of the roots does not enable straight forward conclusions about the behavior or even the stability of the system.

An interesting example to illustrate this last point is given by Ramnath in [5] by considering the second order time varying differential equation:

$$\ddot{y} - 0.1\dot{y} + e^{0.2t}y = 0$$

This equation has a pair of complex conjugate roots with positive real part. Although the characteristic roots remain in the right half plane, the system is in fact stable.

Linear time varying (LTV) systems, such as the one presented in (8.4), cannot usually be solved analytically. Furthermore, the time response of an LTV system is dependent on the initial time t_0 at which it is excited. This makes it particularly difficult to relate the nature of the time response to characteristics of the system such as frequency or damping. Any extension of handling quality criteria to an LTV system will, therefore, have to incorporated in some way, the time varying nature of the system's response and its dependency on initial time.

The Generalized Multiple Scales method, presented in chapter 3, gives approximate solutions to second order linear time varying differential equations. The characteristic equation associated with (8.4) is:

$$s^2 + 2\zeta_{sp}(t)\omega_{sp}(t)s + \omega_{sp}(t)^2 = 0 \qquad (8.5)$$

The fast part of the complete GMS solution gives the following asymptotic approximation of the system's time response at any time t of the time frame $[t_0, t_f]$ we are interested in:

$$y(t)=Ae^{-\int_{t_0}^{t}\zeta_{sp}(\tau)\omega_{sp}(\tau)\,dt}\sin\left[\left(\int_{t_0}^{t}\omega_{sp}(\tau)\sqrt{1-\zeta_{sp}(\tau)^2}\,d\tau\right)+\Phi\right] \tag{8.6}$$

It is interesting to notice that, if the coefficients are time invariant, this approximation does in fact yield the exact solutions to the second order differential equation which was given in (8.3). Furthermore, the simple analytical form of the asymptotic approximate solution gives good insight of how handling qualities for steady state flight conditions could be extended to variable flight conditions. The fast part of the GMS solution looks a lot like that of the LTI system but involves integrals rather than simple products. Since the use of integrals would capture the time varying nature of the coefficients and include a dependency on initial time, they seems to be good candidates for defining time dependent handling quality criteria.

It is also important to be aware of the fact that for high speed vehicles the handling qualities, as most of the other quantities, are dependent on time. Therefore the idea of aircraft handling qualities has to be extended to handling qualities at a specific time t. A possible extension of the criterion defined in table 8.2 is to determine the handling quality levels of the aircraft at time $t \in [t_0, t_f]$ from the following criterion.

LEVEL 1 (at $t \in [t_0, t_f]$):

$$A_{1_{min}} \leq \frac{1}{T}\int_t^{t+T} \omega_{sp}(\tau)\,\zeta_{sp}(\tau)\,d\tau \leq A_{1_{max}} \text{ and } B_{1_{min}} \leq \frac{1}{T}\int_t^{t+T} \omega_{sp}(\tau)\sqrt{1-\zeta_{sp}(\tau)^2}\,d\tau \leq B_{1_{max}}$$

LEVEL 2 (at $t \in [t_0, t_f]$):

$$A_{2_{min}} \leq \frac{1}{T}\int_t^{t+T} \omega_{sp}(\tau)\,\zeta_{sp}(\tau)\,d\tau \leq A_{2_{max}} \text{ and } B_{2_{min}} \leq \frac{1}{T}\int_t^{t+T} \omega_{sp}(\tau)\sqrt{1-\zeta_{sp}(\tau)^2}\,d\tau \leq B_{2_{max}}$$

LEVEL 3 (at $t \in [t_0, t_f]$):

Any other situation

Table 8.3: Extended Handling Quality Criterion

This new criterion basically says that the average over the interval of time [t, t+T] of each one of the two parameters should satisfy the conditions set, in table 8.2, for the LTI case. It is interesting to notice that if the terms that appear in the integrals are constant, this criterion is in fact the classical handling quality criterion defined in table 8.2. Clearly, the choice of T will influence this criterion.

Choice of the Parameter T

If T is infinitely small, the criterion in table 8.3 is equivalent to:

LEVEL 1 (at $t \in [t_0, t_f]$):

$$A_{1_{min}} \leq \zeta_{sp}(t)\omega_{sp}(t) \leq A_{1_{max}} \qquad \text{and} \qquad B_{1_{min}} \leq \omega_{sp}(t)\sqrt{1-\zeta_{sp}(t)^2} \leq B_{1_{max}}$$

LEVEL 2 (at $t \in [t_0, t_f]$):

$$A_{2_{min}} \leq \zeta_{sp}(t)\omega_{sp}(t) \leq A_{2_{max}} \qquad \text{and} \qquad B_{2_{min}} \leq \omega_{sp}(t)\sqrt{1-\zeta_{sp}(t)^2} \leq B_{2_{max}}$$

In order to get level 1 handling qualities over the entire flight period $[t_0, t_f]$, the conditions defined in table 8.2 for the LTI system would have to hold at every single point in time. This certainly yields a very constraining criterion that will very probably poorly rate certain aircraft responses that are in fact adequate. The consequences of choosing very small values of T are therefore the definition of a very conservative criterion in the sense that it will tend to under rate the handling qualities of the aircraft.

On the other hand, if T is very large, the criterion will carry along a very long time history and will not give a good description of the handling qualities at a the time of interest t.

A good choice of T is probably a value of the order of the time period of the short period mode. For a level 2 rating, the largest acceptable period for the short period mode is typically around 3 seconds. Furthermore, with the typical damping requirements associated with level 2 handling qualities, the short period mode should be properly damped after about 2 full periods. This leads a the choice of T of T = 6 s.

The Extended Handling Quality Criterion

We can now define a time dependent handling quality criterion which is a direct extension of the handling quality criterion defined for constant flight conditions. Over a flight

period $[t_0, t_f]$, the aircraft will have handling quality ratings at time $t \in [t_0, t_f]$ determined by the criterion presented in table 8.4:

LEVEL 1 (at $t \in [t_0, t_f]$):

$$A_{1_{min}} \leq \frac{1}{6}\int_t^{t+6} \omega_{sp}(\tau)\,\zeta_{sp}(\tau)\,d\tau \leq A_{1_{max}} \text{ and } B_{1_{min}} \leq \frac{1}{6}\int_t^{t+6} \omega_{sp}(\tau)\sqrt{1-\zeta_{sp}(\tau)^2}\,d\tau \leq B_{1_{max}}$$

LEVEL 2 (at $t \in [t_0, t_f]$):

$$A_{2_{min}} \leq \frac{1}{6}\int_t^{t+6} \omega_{sp}(\tau)\,\zeta_{sp}(\tau)\,d\tau \leq A_{2_{max}} \text{ and } B_{2_{min}} \leq \frac{1}{6}\int_t^{t+6} \omega_{sp}(\tau)\sqrt{1-\zeta_{sp}(\tau)^2}\,d\tau \leq B_{2_{max}}$$

LEVEL 3 (at $t \in [t_0, t_f]$):

Any other situation

Table 8.4: Handling Qualities for Aircraft Flying Through Variable Flight Conditions

As for the steady state handling quality criterion, this criterion can be represented graphically as shown on figure 8.2.

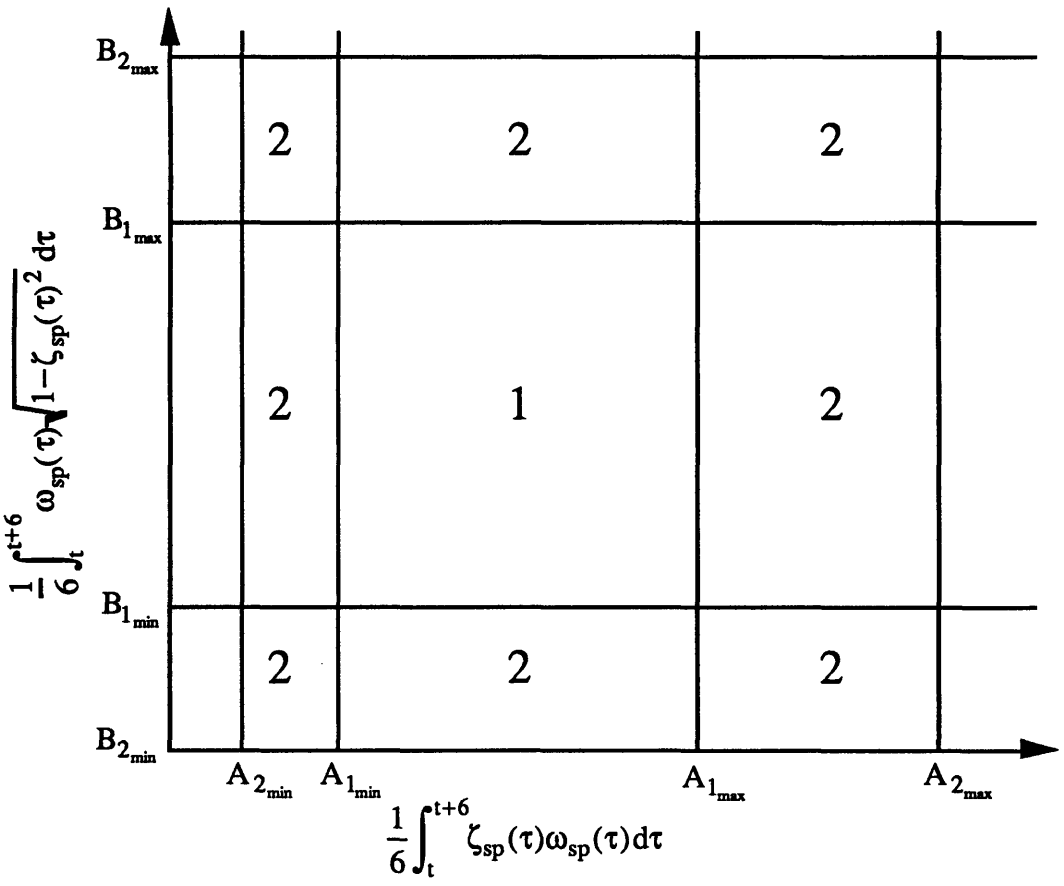

Figure 8.2: Time Dependent Handling Quality Criterion

8.3 TIME - DEPENDENT HANDLING QUALITY CRITERION: APPLICATION

8.3.1 Numerical Values for the Time Dependent Handling Quality Criterion

Typical values of acceptable damping and natural frequencies of short period dynamics for level 1 and level 2 ratings are:

LEVEL 1: $0.4 \le \zeta_{sp} \le 0.9$ and $2.4 \le \omega_{sp} \le 3.8$

LEVEL 2: $0.25 \le \zeta_{sp} \le 1.0$ and $2.0 \le \omega_{sp} \le 5.0$

These values yield the extended handling quality criterion presented in table 8.5.

LEVEL 1 (at $t \in [t_0, t_f]$):

$$0.96 \leq \frac{1}{6}\int_t^{t+6} \omega_{sp}(\tau)\,\zeta_{sp}(\tau)\,d\tau \leq 3.42 \text{ and } 1.05 \leq \frac{1}{6}\int_t^{t+6} \omega_{sp}(\tau)\sqrt{1-\zeta_{sp}(\tau)^2}\,d\tau \leq 3.48$$

LEVEL 2 (at $t \in [t_0, t_f]$):

$$0.50 \leq \frac{1}{6}\int_t^{t+6} \omega_{sp}(\tau)\,\zeta_{sp}(\tau)\,d\tau \leq 5.00 \text{ and } 0 \leq \frac{1}{6}\int_t^{t+6} \omega_{sp}(\tau)\sqrt{1-\zeta_{sp}(\tau)^2}\,d\tau \leq 4.90$$

LEVEL 3 (at $t \in [t_0, t_f]$):

Any other situation

Table 8.5: Application of the Extended Handling Quality Criterion

8.3.2 Application to an Aircraft Flying Through Variable Flight Conditions

As mentioned in section 8.2.3, the time responses of LTV systems cannot be simply predicted by the location of the characteristic roots in the complex plane since they also depend on their path and speed over the time period of interest.

In this section, the effects on the handling quality levels of simple variations in the path and speed of the characteristic roots of the second order system representing the short

period dynamics of a generic aircraft are examined. To accomplish this, we consider systems having same root locations at initial and final time. The path and speed of the roots from the initial point to the final point in the complex plane are varied and the time responses of the systems described by these roots as well as the handling quality levels are compared. Figure 8.3 shows different paths for a typical pair of complex conjugate roots representing the short period mode.

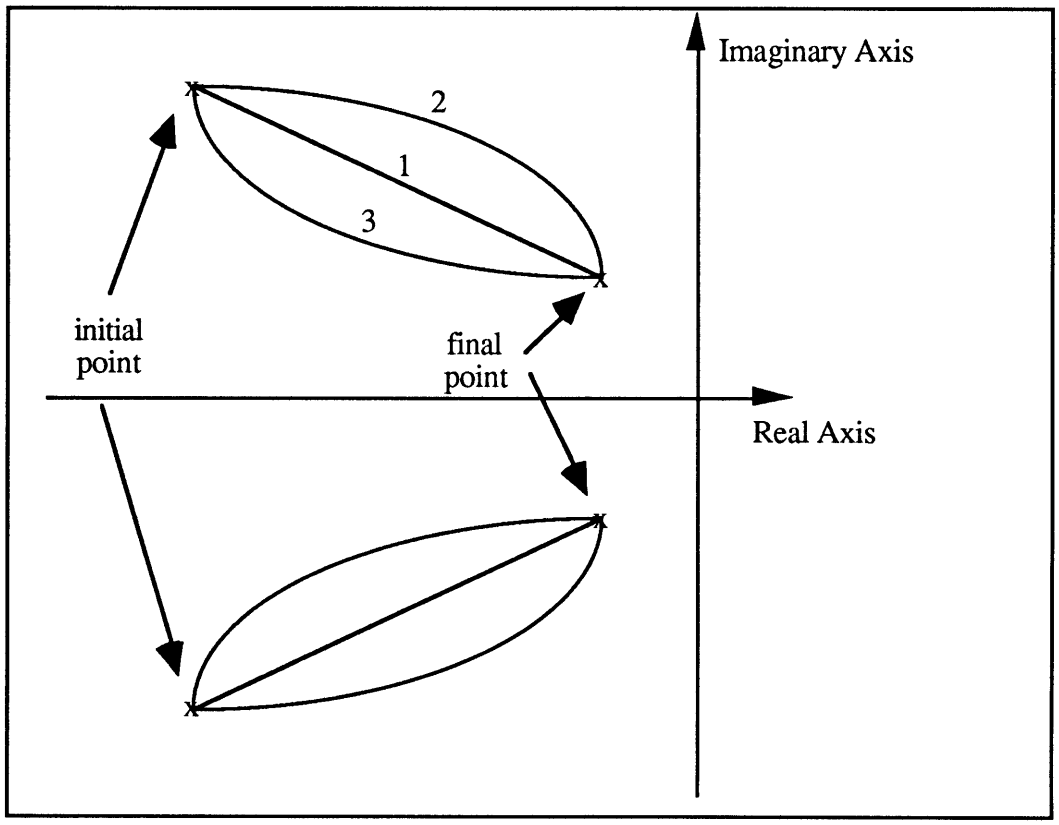

Figure 8.3: Evolution of the Roots in the Complex Plane

Case Study

In the following case study, the aircraft can fly, as shown in figure 8.3, along three different prescribed flight trajectories. To analyze the time history of the handling qualities along these trajectories, the aircraft is flown from a level 1 flight condition to a level 2 flight

condition. The roots of the short period move along three different paths, corresponding to the different trajectories, from the initial point to the final point in a time of 130 seconds. The characteristics of the initial and final points are summarized in table 8.6.

INITIAL POINT:	t = 0	Level 1	$\omega_{sp_1} = 3.5$	$\zeta_{sp_1} = 0.8$
FINAL POINT:	t = 130 s	Level 2	$\omega_{sp_2} = 2.0$	$\zeta_{sp_2} = 0.3$

Table 8.6: Initial and Final Point Characteristics of System Short Period Dynamics

For each one of the three flight trajectory, computer simulations generate plots corresponding to the path of the characteristic roots in the complex plane, the evolution of the levels of handling qualities along the trajectory, the evolution with time of the real and imaginary part of the short period roots and the time response of the system at four different preset points in time.

Trajectory 1: (see plots on page 103)

The first case corresponds to the roots of the short period going from the initial point to the final point along a straight line, as shown on the root locus plot of figure 8.3.The time dependent handling quality criteria is used to determine, at each point in time, the level of handling qualities along the corresponding flight trajectory. As shown on page 103, the aircraft has level 1 handling qualities from the initial time to about 105 seconds into the trajectory and level 2 handling qualities from that point on. The four bottom plots show the time response of the system at four different points along the trajectory. At t = 0 s, 40 s and 80 s, where the aircraft has level 1 handling qualities, the responses are fast and well damped. At t = 120 s, however, the response is a little slow (first period > 3s) which explains the level 2 rating.

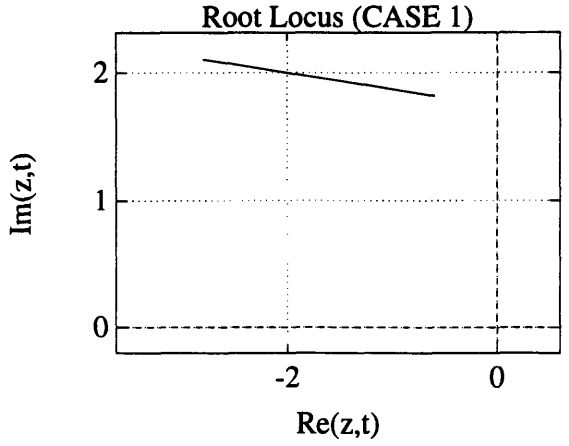
Root Locus (CASE 1)
Im(z,t)
Re(z,t)
2
1
0
-2
0

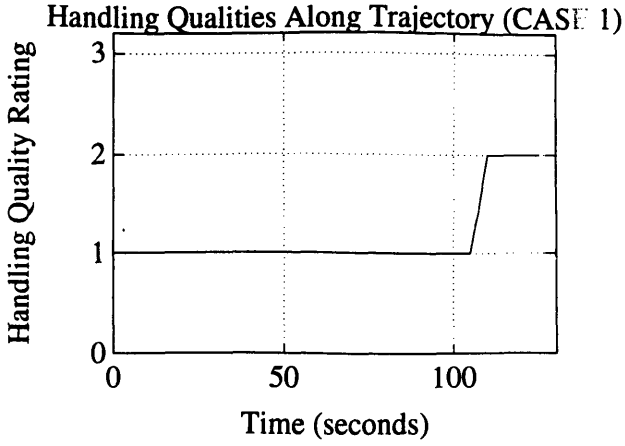
Handling Qualities Along Trajectory (CASE 1)
Handling Quality Rating
Time (seconds)
3
2
1
0
0
50
100

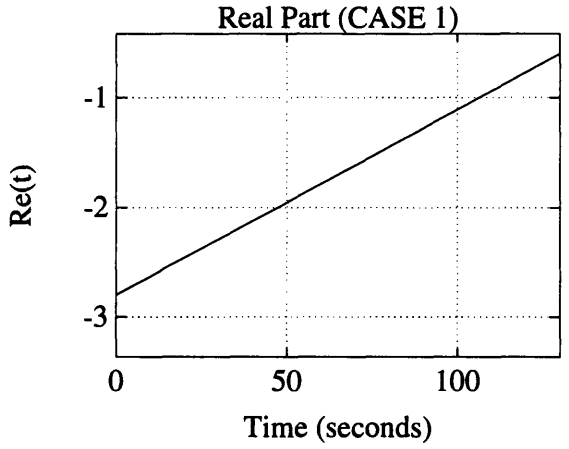
Real Part (CASE 1)
Re(t)
Time (seconds)
-1
-2
-3
0
50
100

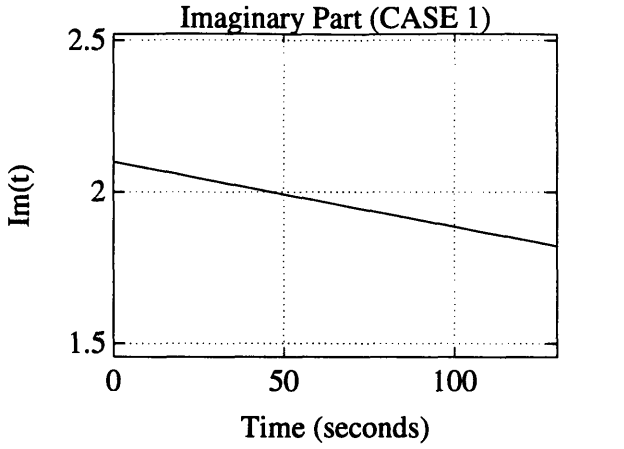
Imaginary Part (CASE 1)
Im(t)
Time (seconds)
2.5
2
1.5
0
50
100

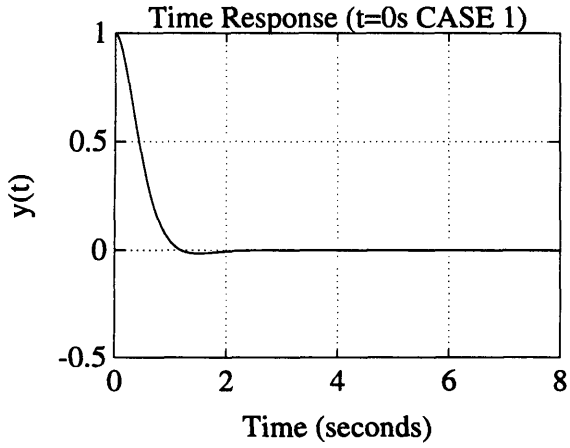
Time Response (t=0s CASE 1)
y(t)
Time (seconds)
1
0.5
0
-0.5
0
2
4
6
8

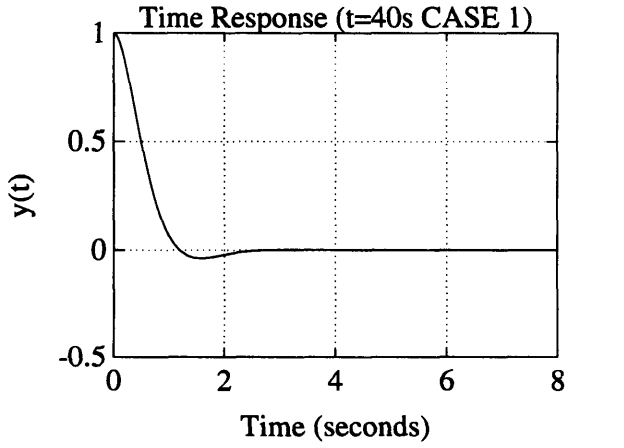
Time Response (t=40s CASE 1)
y(t)
Time (seconds)
1
0.5
0
-0.5
0
2
4
6
8

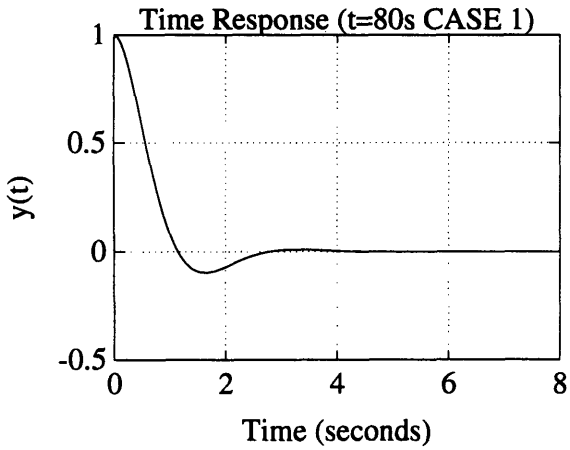
Time Response (t=80s CASE 1)
y(t)
Time (seconds)
1
0.5
0
-0.5
0
2
4
6
8

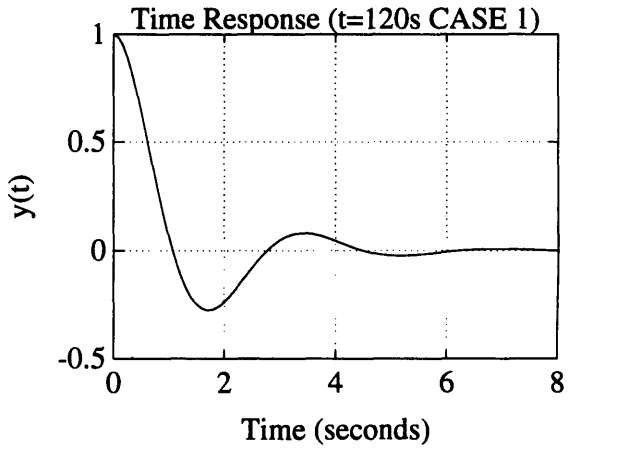
Time Response (t=120s CASE 1)
y(t)
Time (seconds)
1
0.5
0
-0.5
0
2
4
6
8

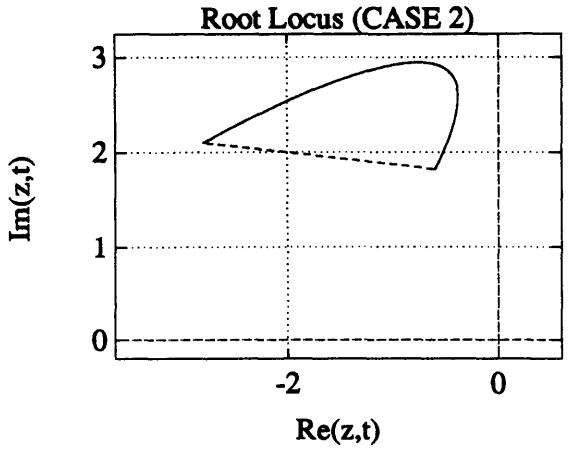
Root Locus (CASE 2)
Im(z,t)
Re(z,t)
3
2
1
0
-2
0

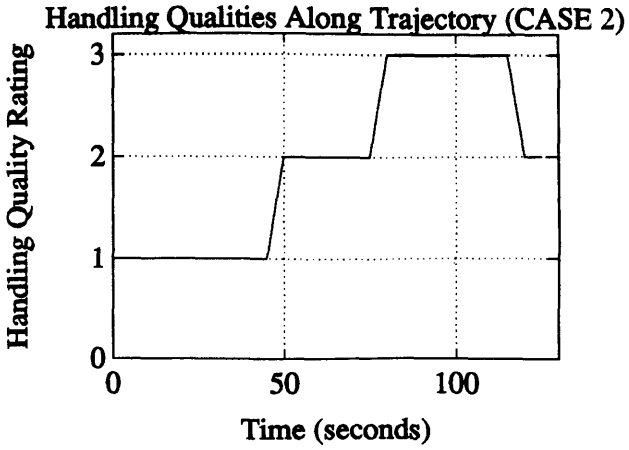
Handling Qualities Along Trajectory (CASE 2)
Handling Quality Rating
Time (seconds)
3
2
1
0
0
50
100

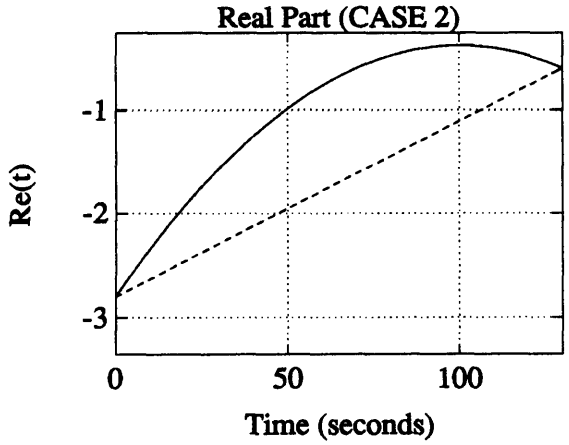
Real Part (CASE 2)
Re(t)
Time (seconds)
-1
-2
-3
0
50
100

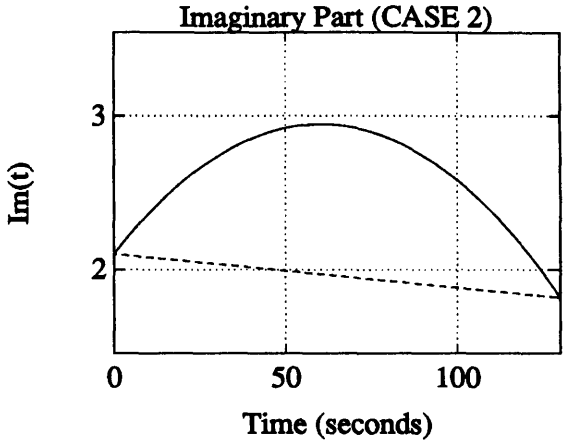
Imaginary Part (CASE 2)
Im(t)
Time (seconds)
3
2
0
50
100

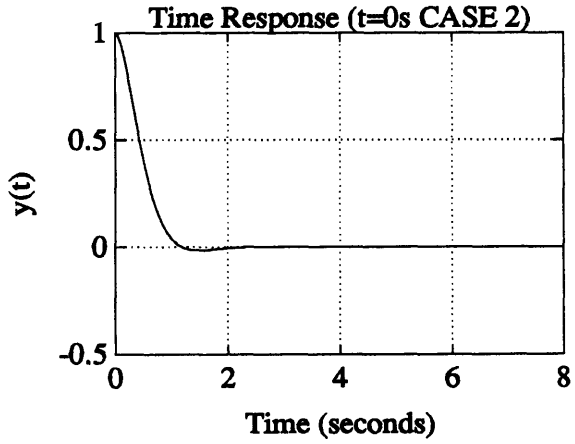
Time Response (t=0s CASE 2)
y(t)
Time (seconds)
1
0.5
0
-0.5
0
2
4
6
8

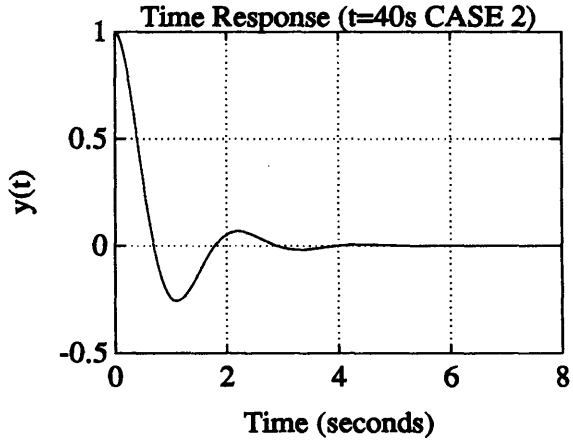
Time Response (t=40s CASE 2)
y(t)
Time (seconds)
1
0.5
0
-0.5
0
2
4
6
8

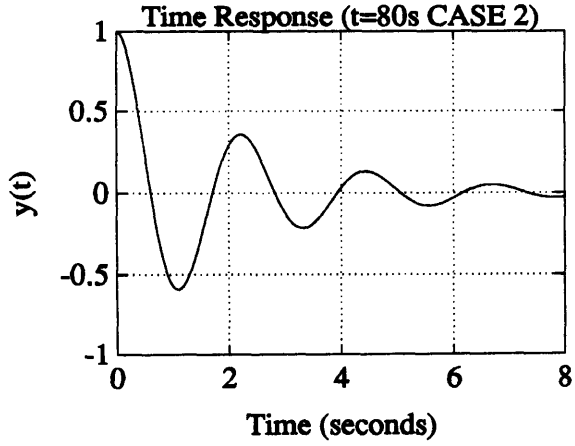
Time Response (t=80s CASE 2)
y(t)
Time (seconds)
1
0.5
0
-0.5
-1
0
2
4
6
8

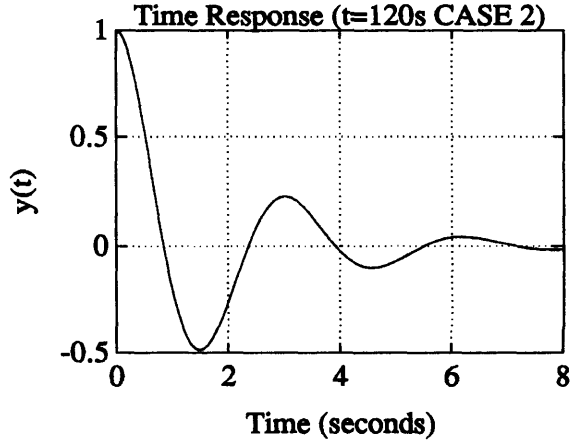
Time Response (t=120s CASE 2)
y(t)
Time (seconds)
1
0.5
0
-0.5
0
2
4
6
8

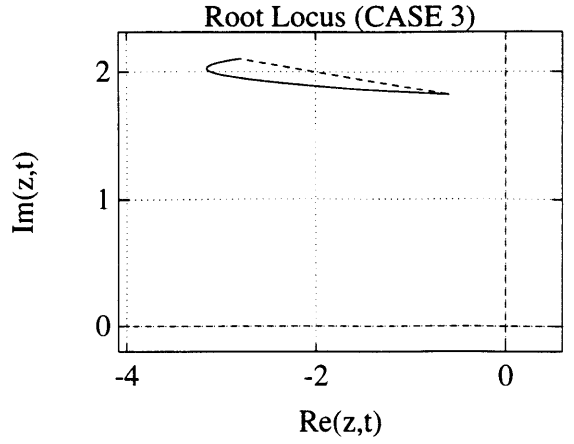
Root Locus (CASE 3)
Im(z,t)
Re(z,t)
2
1
0
-4
-2
0

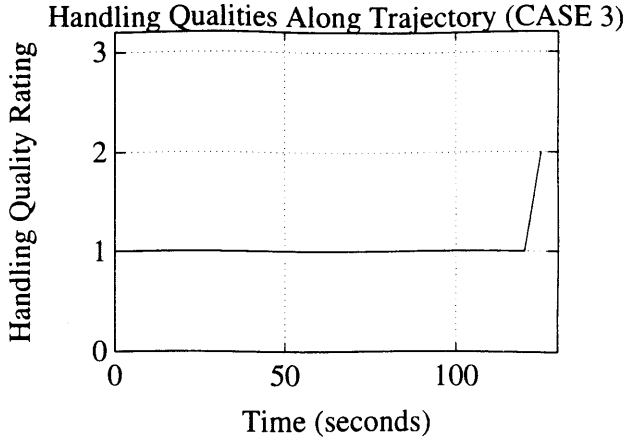
Handling Qualities Along Trajectory (CASE 3)
Handling Quality Rating
Time (seconds)
3
2
1
0
0
50
100

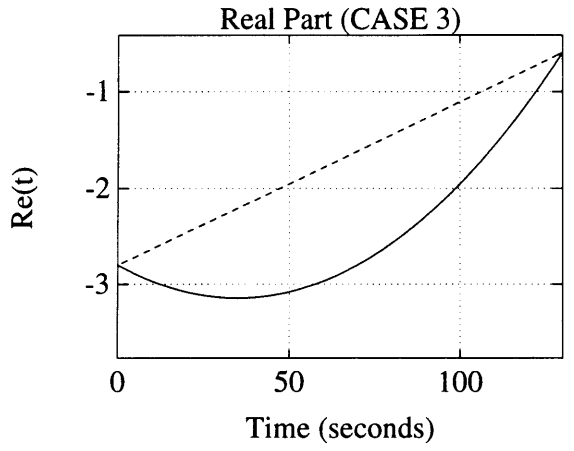
Real Part (CASE 3)
Re(t)
Time (seconds)
-1
-2
-3
0
50
100

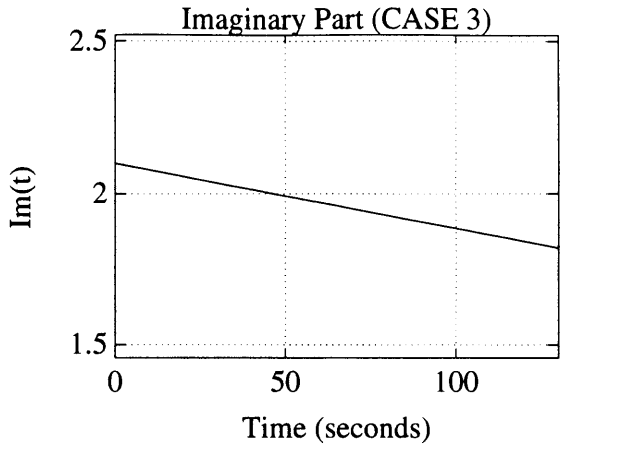
Imaginary Part (CASE 3)
Im(t)
Time (seconds)
2.5
2
1.5
0
50
100

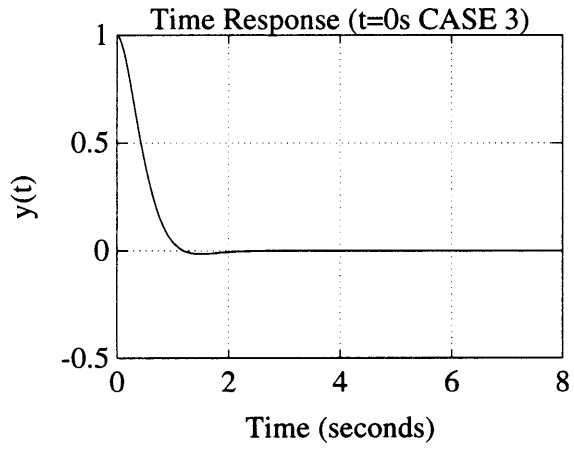
Time Response (t=0s CASE 3)
y(t)
Time (seconds)
1
0.5
0
-0.5
0
2
4
6
8

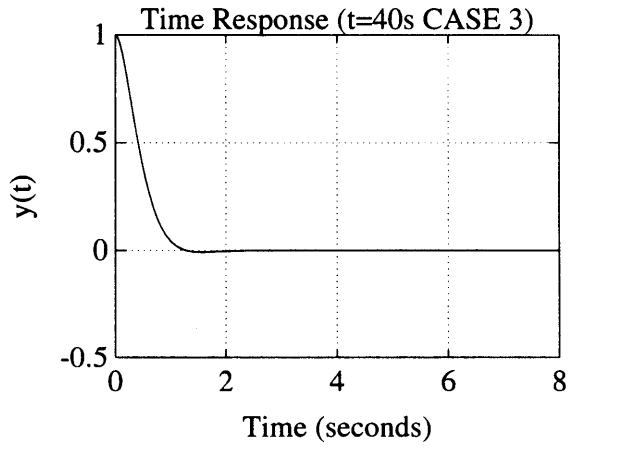
Time Response (t=40s CASE 3)
y(t)
Time (seconds)
1
0.5
0
-0.5
0
2
4
6
8

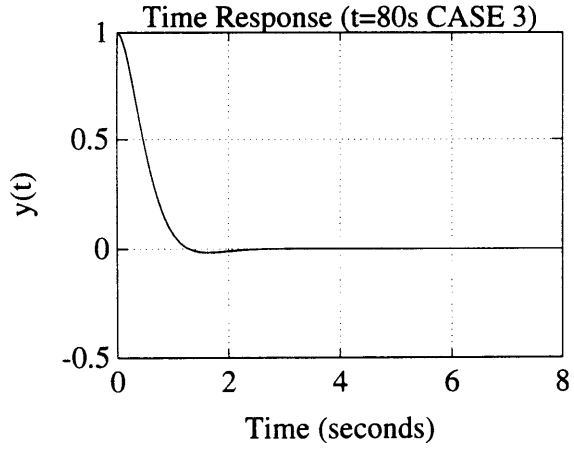
Time Response (t=80s CASE 3)
y(t)
Time (seconds)
1
0.5
0
-0.5
0
2
4
6
8

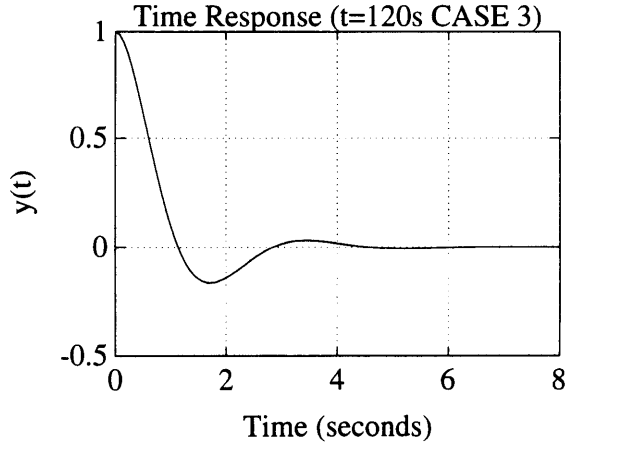
Time Response (t=120s CASE 3)
y(t)
Time (seconds)
1
0.5
0
-0.5
0
2
4
6
8

Trajectory 2: (see plots on page 104)

The second case corresponds to a curved path of the roots as shown on the root locus plot of figure 8.3. The plot corresponding to the time history of the handling qualities shows that this particular trajectory yields worst handling qualities than the previous one. The aircraft only has level 1 rating for the first 45 seconds. After that it has level 2 and even level 3 ratings (between 75 seconds and 115 seconds). The time response at t = 80 s exhibits the very low damping of the system responsible for the level 3 rating at that point. Although the time responses at t = 0 s, 40 s and 120 s yield the same rating as in case 1, the handling qualities are clearly not as good as in the first case because of the poor damping of the system along this trajectory.

Trajectory 3: (see plots on page 105)

The third case corresponds to a different curved path of the short period roots which is shown on the roots locus plot of figure 8.3. The time history of the handling qualities shows that the aircraft has level 1 rating for nearly the entire flight. It only gets a level 2 rating after 125 seconds into the trajectory. At the four different points in time, the responses of the system are fast and well damped justifying the level 1 handling qualities of the aircraft along most of this trajectory. Of the three, this is certainly the trajectory that exhibits the best handling qualities from the desired initial point to the final point.

8.4 HANDLING QUALITY INFORMATION DISPLAY

In order to inform the pilot of the evolution of the handling qualities of the aircraft and alert him of critical sections in the trajectory, it may be desirable to present stability and handling quality information in the form of a display in the cockpit. It is assumed that all of the trajectory and vehicle information is known, or can be determined, prior to the flight phase.

The flight crew could, therefore, be presented with the immediate past, present and future handling quality levels of the aircraft.

A possible display is one that would be in the form of a moving window. This display would use bar graphs to present stability and handling quality information in the neighborhood of a particular time along the trajectory. The height of the bar reflects the level of handling qualities. If the bar has no height, the aircraft is unstable. Handling quality information is displayed every 5 seconds for up to 30 seconds into the immediate future and 10 seconds of the immediate past. The display is updated continuously as the vehicle flies along the trajectory.

This display is presented on page 108 at four different points in time for the second case of variable flight conditions described in the previous section.

DISPLAY t = 10 s

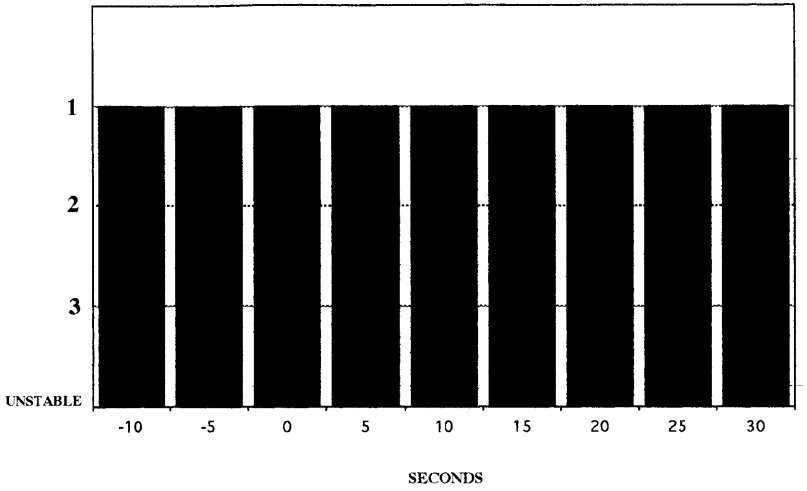

DISPLAY t = 40 s

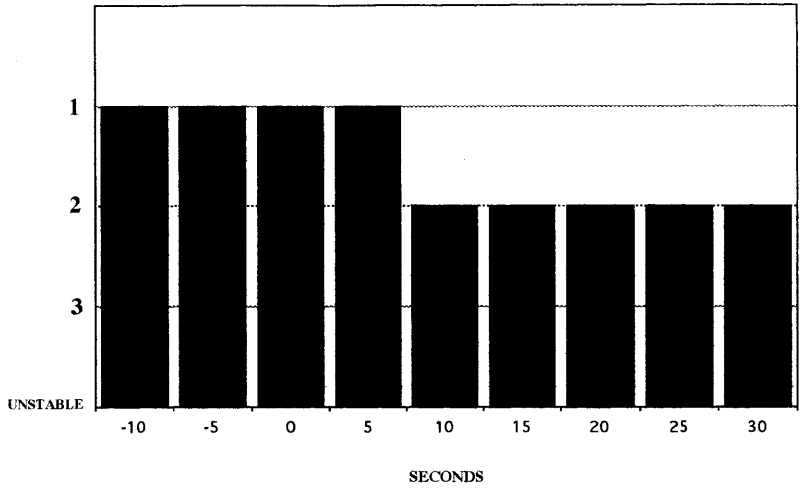

DISPLAY t = 70 s

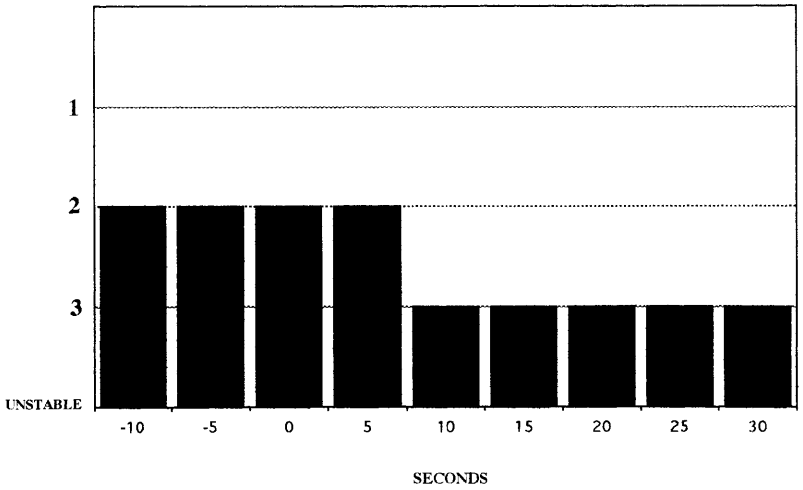

DISPLAY t = 100 s

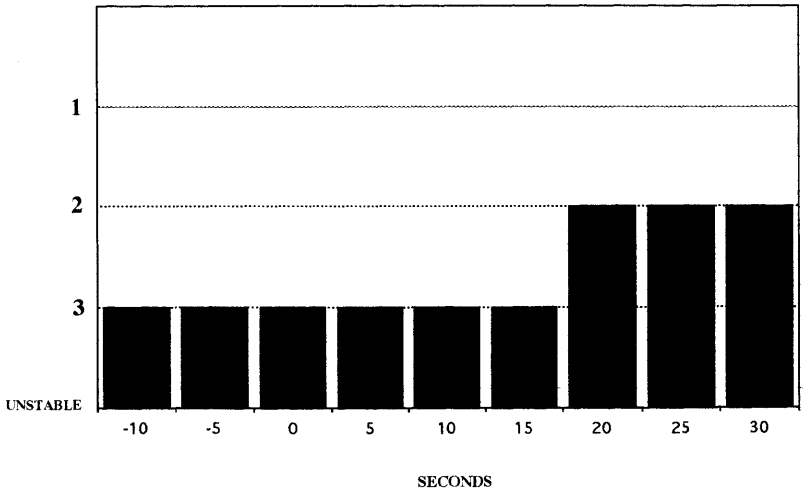

CHAPTER 9

Conclusions and Recommendations

9.1 CONCLUSIONS

The objectives of this work were to use results of the Generalized Multiple Scales (GMS) theory to study several issues related to the dynamics of high speed aircraft along prescribed atmospheric trajectories .

The reentry dynamics of the Generic Hypersonic Aerodynamic Model Example (GHAME) vehicle were examined along a Space Shuttle optimal trajectory. Asymptotic approximate solutions to fourth order models of the longitudinal and lateral directional dynamics of the aircraft were derived using the GMS method. The simple form of these solutions allowed a complete analytical sensitivity analysis to first and second order variations in vehicle stability derivatives over portions of the reentry. It appeared that the lateral directional dynamics were by far most sensitive to first and second order variations in the directional derivative N_V and dihedral term L_V along the trajectory. The longitudinal dynamics proved to be most sensitive to the lift velocity derivative L_V/V_0 and the speed stability term M_V. Having identified large sensitivity to parameter variations as a source of potential problems in controlling flight vehicles, an optimal control, incorporating sensitivity considerations through state augmentation, was designed and applied to the longitudinal dynamics of the GHAME vehicle. This approach proved to be very effective in reducing the systems sensitivity to first order variations in the lift velocity term L_V/V_0.

The dynamics of the SR-71 along a prescribed trajectory were also studied using results from the GMS theory. Stability issues were raised and applied to the aircraft when flown from supersonic to subsonic speeds.

Extended handling quality criteria, for vehicles with large flight envelopes, were defined based on the analytical forms of GMS asymptotic approximations to the solutions of linear time varying systems. Unlike classical criteria, based on the analysis of the dynamic equation of motion at constant flight conditions, these extended criteria specify handling qualities in terms of variable system response. For vehicles flying through continuously varying flight conditions, these extended handling quality criteria are believed to give a more accurate description of the actual performance of the aircraft. Applications to a generic aircraft flying form a level 1 to a level 2 flight condition were presented to illustrate how the path and speed of the characteristic roots can influence the handling qualities. Finally, an approach to presenting stability and handling quality information to the pilot in the cockpit was discussed.

9.2 RECOMMENDATIONS FOR FUTURE WORK

The following is suggested as guidelines for future work in the field of dynamics and control of high speed aircraft using the Generalized Multiple Scales theory:

- Refinement of the previous work by including the "slow" part of the GMS asymptotic approximations.
- Study of vehicle dynamics near turning points using GMS theory.
- Generalization of the optimal control approach for reducing aircraft sensitivity to parameter variations. This could consist of designing control laws that would simultaneously reduce sensitivity to variations in all of the stability derivatives. The control law could also be defined to include second order considerations.

- Definition of extended handling quality criteria that would be closer to existing criteria and validation on real flight test data.

Bibliography

[1] Bowers, A. H. and K. W. Iliff, *A Generic Hypersonic Aerodynamic Model Example (GHAME) for Computer Simulation*, NASA Ames Research Center, Dryden Flight Research Facility. Edwards California. August 5,1988.

[2] Mc Ruer, Ashkensas, and Graham, *Aircraft Dynamics and Automatic Control*, Princeton, New Jersey, 1973.

[3] Etkin, B., *Dynamics of Atmospheric Flight*, John Wiley & Sons, Inc., New York. 1972.

[4] Etkin, B., *Dynamics of Fight: Stability and Control*, 2nd edition. John Wiley & Sons, Inc., New York. 1982.

[5] Ramnath, R. V., Class Notes, *Advanced Flight Dynamics and Control*, MIT course 16.17. Spring 1990.

[6] Ramnath, R. V.,Sandri, G., *A Generalized Multiple Scales Approach to a Class of Linear Differential Equations, Journal of Mathematical Analysis and Application, Vol. 28, 1969.*

[7] Ramnath, R. V. and Sinha P., *Dynamics of the Space Shuttle During Entry Into Earth's Atmosphere*, AIAA Journal, 13, No. 3:337-342, 1975.

[8] Ramnath, R. V. and Radovsky, S., *Sensitivity Analysis of Variable Systems*, Proc. JACC. Denver, 1978.

[9] Cooper, G. and Harper, R., *The Use of Pilot Ratings in Evaluation of Aircraft Handling Qualities*, NASA TN D-5153, April, 1969.

[10] *Military Specification: Flying Qualities of Piloted Airplanes*, MIL-F-87585C, November 5,1980.

[11] Chalk Charles R., *Additional Flight Evaluations of Various Longitudinal Handling Qualities in a Variable-Stability Jet Fighter*, WADC Technical Report 57-719, July 1958.

[12] Bihrle William, *A Handling Qualities Theory for Precise Flight Path Control*, Technical Report AFFDL-TR-65-198, Ohio, June, 1966.

[13] Holleman Euclid C., *Rational for Proposed Flying-Qualities Specifications*, NASA TM X-2101, NASA Flight Research Center.

[14] Lockheed Aircraft Company, *Handling Qualities of the SR-71*, Report no SP-508,)ct 1964.

[15] Araki John, *Reentry Dynamics and Handling Qualities of a Generic Hypersonic Aircraft*, MIT Thesis, 1991.